

CONFIDENTIAL

Copy 436  
RM L52G14a



NACA

# RESEARCH MEMORANDUM

A PRESSURE-DISTRIBUTION INVESTIGATION  
OF A FINENESS-RATIO-12.2 PARABOLIC BODY OF  
REVOLUTION (NACA RM-10) AT  $M = 1.59$  AND  
ANGLES OF ATTACK UP TO  $36^\circ$

By Morton Cooper, John P. Gapcynski, and Lowell E. Hase

Langley Aeronautical Laboratory  
Langley Field, Va.

CLASSIFIED DOCUMENT

This material contains information affecting the National Defense of the United States within the meaning of the espionage laws, Title 18, U.S.C., Secs. 793 and 794, the transmission or revelation of which in any manner to an unauthorized person is prohibited by law.

NATIONAL ADVISORY COMMITTEE  
FOR AERONAUTICS

WASHINGTON

October 30, 1952

CLASSIFICATION CHANGED TO UNCLASSIFIED  
AUTHORITY: NACA RESEARCH ABSTRACT NO. 118  
EFFECTIVE DATE: JULY 26, 1957  
WHL

CONFIDENTIAL

## NATIONAL ADVISORY COMMITTEE FOR AERONAUTICS

## RESEARCH MEMORANDUM

A PRESSURE-DISTRIBUTION INVESTIGATION  
OF A FINENESS-RATIO-12.2 PARABOLIC BODY OF  
REVOLUTION (NACA RM-10) AT  $M = 1.59$  AND  
ANGLES OF ATTACK UP TO  $36^\circ$

By Morton Cooper, John P. Gapcynski, and Lowell E. Hasel

## SUMMARY

A pressure-distribution investigation of a parabolic body of revolution with a fineness ratio of 12.2 has been undertaken in the Langley 4- by 4-foot supersonic tunnel at a Mach number of 1.59 and a Reynolds number of  $3.6 \times 10^6$ , based on the body length, for angles of attack from  $0^\circ$  to  $36^\circ$ . In the low-incidence range up to  $9^\circ$ , a comparison of these data with other experimental data on the same configuration indicates the absence of any significant Reynolds number effects on the pressures (except at the base) in the range from  $3.6 \times 10^6$  to  $29 \times 10^6$ . At an angle of attack of  $0^\circ$ , the pressures were well-predicted by potential (slender-body) theory. In the low-incidence range, similar agreement existed with the pressures on the windward side. On the leeward side, however, the pressures were affected by cross-flow separation, the discrepancies between experiment and theory appeared rearward first, perhaps at about  $5^\circ$ , and progressed forward as the angle of attack was increased. At the higher angles, the cross-flow separation became asymmetrical; the leeward pressures at corresponding radial locations were considerably different. These asymmetries were very pronounced over most of the body for angles of attack of about  $16^\circ$  and higher but were observed for much lower angles at rearward body locations.

With the exception of those stations near the base, the addition of artificial roughness along the sides of the body had no effect on the forebody pressures at angles of attack of  $8^\circ$  or less. At  $12^\circ$  and near the base at  $8^\circ$ , the addition of artificial roughness along the sides of the body appeared to cause "cross-flow transition" and hence delay separation of the flow over the body. This same trend was indicated ahead of the maximum thickness section at  $16^\circ$ , while no consistent effect of roughness was noted rearward of this point on the body.

In the low-incidence range, the normal-force coefficient of the body was underestimated and the axial force predicted reasonably well by potential (slender-body) theory. The center of pressure was rearward of either the potential value or the results obtained from the viscous-cross-flow theory. Although the viscous-cross-flow estimate did improve the agreement with the experimental data in the low-incidence range, perhaps up to  $10^\circ$ , discrepancies of considerable magnitude were found at higher angles.

## INTRODUCTION

In recent years, the accurate prediction of the flow about slender bodies of revolution has become increasingly important in the design of high-speed missiles and aircraft. For the case of the supersonic missile where maneuverability is at a premium, the flow characteristics and the ability to predict these characteristics are required for angles of attack much larger than the customary low-speed low-incidence range. This problem of the flow over inclined slender bodies has been vigorously studied both theoretically and experimentally of late.

Theoretically, the problem of the inviscid flow about slender bodies of revolution at supersonic speeds has been investigated both by linear and nonlinear methods. Among the basic approaches are the linear solutions of references 1 to 3, the higher-order solutions of references 4 to 6, and the nonlinear solutions by the method of characteristics as presented in references 7 to 10. It has been accepted that any inviscid solution about a general body of revolution must inherently be limited to small incidences because of the importance of viscosity in determining the characteristics at large yaw. In order to allow for these viscous effects, Allen (ref. 11) and Van Dyke (ref. 5) introduce, on physical grounds, an approximate cross-flow concept which improves the experimental-theoretical agreement. A fundamental discussion of the viscous cross flow about an infinitely long yawed circular cylinder, presented in reference 12, might be taken somewhat as a justification for the viscous work of references 5 and 11.

Experimentally, detailed force and pressure-distribution measurements have been determined for a reasonably wide range of Mach numbers and body shapes (see refs. 13 to 16, for example). One of the basic bodies tested has been a fineness-ratio-12.2 parabolic body of revolution designated as the NACA RM-10. This body has been extensively tested both in flight (for example, refs. 17 and 18) and in supersonic tunnels (refs. 15, 16, 19, and 20) to study the detailed characteristics over a slender body at supersonic speeds. The present paper further considers the flow over this body by presenting an analysis of the pressures at a Mach number of 1.59 and a Reynolds number of  $3.6 \times 10^6$  for an angle-of-

attack range from  $0^\circ$  to  $36^\circ$ . The data are presented in terms of pressures, local section coefficients, and over-all body coefficients, and are compared with slender-body theory (refs. 3 and 21) and the cross-flow theories (refs. 5 and 11). For the incidence range below  $15^\circ$ , the experimental data of the present investigation overlap the data of reference 15 (Reynolds number of approximately  $30 \times 10^6$ ) and reference 20 (Reynolds numbers of  $8.6 \times 10^6$  and  $17.4 \times 10^6$ ) and hence, the investigations are supplementary with regards to Reynolds number effects.

## SYMBOLS

## Free-stream conditions:

$\rho$	mass density of air
$V$	airspeed
$a$	speed of sound in air
$M$	Mach number, $V/a$
$q$	dynamic pressure, $\frac{1}{2} \rho V^2$
$p$	static pressure

## Body geometry:

$S$	cross-sectional area
$L$	length of body of revolution
$R$	radius of body of revolution
$x$	distance from apex of body of revolution measured along axis of symmetry
$\alpha$	angle of attack of axis of symmetry
$\phi$	body polar angle measured counterclockwise in plane perpendicular to axis of body when facing upstream ( $\phi = 0^\circ$ on bottom of body in plane of angle of attack)

## Pressure data:

$p_l$  local static pressure

$P$  pressure coefficient,  $\frac{p_l - p}{q}$

$c_n$  section normal-force coefficient

$$\frac{1}{2} \int_0^{2\pi} P \cos \phi \, d\phi = \frac{\text{Section normal force}}{2qR}$$

$c_c$  section axial-force coefficient,

$$\frac{1}{2} \frac{dR}{dx} \int_0^{2\pi} P \, d\phi = \frac{\text{Section axial force}}{2qR}$$

$c_y$  section side-force coefficient,

$$\frac{1}{2} \int_0^{2\pi} P \sin \phi \, d\phi = \frac{\text{Section side force}}{2qR}$$

$C_N$  body normal-force coefficient,

$$\frac{2L}{\pi R_{\max}} \int_0^1 c_n \left( \frac{R}{R_{\max}} \right) d \left( \frac{x}{L} \right) = \frac{\text{Body normal force}}{qS_{\max}}$$

$C_C$  body pressure axial-force coefficient,

$$\frac{2L}{\pi R_{\max}} \int_0^1 c_c \left( \frac{R}{R_{\max}} \right) d \left( \frac{x}{L} \right) = \frac{\text{Body axial force}}{qS_{\max}}$$

$C_Y$  body side-force coefficient,

$$\frac{2L}{\pi R_{\max}} \int_0^1 c_y \left( \frac{R}{R_{\max}} \right) d \left( \frac{x}{L} \right) = \frac{\text{Body side force}}{qS_{\max}}$$

$C_m$  body pitching-moment coefficient due to normal forces about apex of body,

$$- \frac{2L}{\pi R_{\max}} \int_0^1 c_n \left( \frac{R}{R_{\max}} \right) \left( \frac{x}{L} \right) d \left( \frac{x}{L} \right) = \frac{\text{Body pitching moment}}{qS_{\max} L}$$

$C_n$  body yawing-moment coefficient due to side forces about apex of body,

$$- \frac{2L}{\pi R_{\max}} \int_0^1 c_y \left( \frac{R}{R_{\max}} \right) \left( \frac{x}{L} \right) d \left( \frac{x}{L} \right) = \frac{\text{Body yawing moment}}{qS_{\max} L}$$

$C_L$  body lift coefficient,  $C_N \cos \alpha - C_C \sin \alpha = \frac{\text{Body lift force}}{qS_{\max}}$

$C_D$  body pressure-drag coefficient,  
 $C_N \sin \alpha + C_C \cos \alpha = \frac{\text{Body drag forces}}{qS_{\max}}$

Subscripts:

max maximum

## APPARATUS

### Tunnel

The Langley 4- by 4-foot supersonic tunnel is a rectangular, closed-throat, single-return wind tunnel designed for a nominal Mach number range from 1.2 to 2.2. The test-section Mach number is varied by deflecting horizontal flexible walls against a series of fixed interchangeable templates which have been designed to produce uniform flow in the test section. For the present investigation, the nozzle walls were set for a test-section Mach number of 1.59. For this Mach number, the test section has a width of 4.5 feet and a height of 4.4 feet. A detailed description of the tunnel, together with calibration data of the test section at this Mach number, is presented in reference 22.

## MODEL

The test model (fig. 1(a)) was a parabolic body of revolution machined from steel to the coordinates given by the equation in figure 1(a). Measurements of the body diameters made at 1-inch intervals along the entire body length indicated that the maximum deviation from the specified diameter at any station was less than 0.009 inch. The base of the model was cut off bluntly 42.05 inches from the apex; the fineness ratio was thereby reduced from 15 to 12.2. The model contained four axial rows of 0.020-inch static-pressure orifices (approximately 32 orifices per row) spaced  $90^\circ$  apart radially, four base-pressure orifices, and one total-pressure orifice at the apex. In order to install the total-pressure orifice, the nose was cut off at a diameter of approximately 0.040 inch. This total-pressure orifice was used in conjunction with another investigation (ref. 23) employing this same model.

### Installation

The model (fig. 1(a)) was sting-supported in the tunnel on a straight (fig. 1(b)) and a  $38^\circ$  bent (fig. 1(c)) sting. Both stings were the same for a distance of 18.5 inches from the base of the model, the bend taking place rearward of this point. The ratio of the sting diameter, at the model base, to the model base diameter was 0.6. The bent sting was used to increase the attainable incidence range of the model from  $0^\circ$  to  $16^\circ$  up to a range from  $14^\circ$  to  $36^\circ$ ; in both cases, the incidence was varied in a horizontal plane. A schematic arrangement of the model mounted in the Langley 4- by 4-foot supersonic tunnel is shown in figure 2 for extreme angle positions of both stings; a photograph of the model mounted in the tunnel on each sting is shown in figure 3.

### TESTS AND CORRECTIONS

#### Tests

The data were obtained for a range of incidence angles from  $0^\circ$  to  $36^\circ$  at a Mach number of 1.59 and a Reynolds number of  $3.6 \times 10^6$ . In order to define accurately the radial pressure distributions at a given axial station, the model was rotated in fixed increments about its own axis to provide a much more detailed orifice coverage. The tests, on both the straight and bent stings, were conducted by varying the angle of attack for a fixed radial index position. Then, after shutting down the tunnel to re-index the model radially, the tests were repeated through the angle-of-attack range. For the straight-sting configuration, six indexing positions were used. Since the high-angle bent-sting tests were not a part of the original program, there was unfortunately insufficient time for such detailed indexing. Hence, only four radial indexing positions were used for these latter tests.

The tests were conducted with the model in a smooth and polished condition over the entire incidence range and with artificial roughness for angles of attack up to  $16.10^\circ$ . For the artificial-roughness tests,  $\frac{1}{4}$ -inch-wide strips of No. 60 carborundum were located at each of the following positions during separate tests: a complete ring at maximum diameter ( $\frac{x}{L} = 0.614$ ), a complete ring 7 inches from the base ( $\frac{x}{L} = 0.834$ ), axial strips (located at radial positions of  $90^\circ$  and  $270^\circ$ ) extending the full length of the body, and axial strips extending from the maximum thickness station to the model base.



The tunnel stagnation conditions were: pressure, 0.25 atmosphere; temperature,  $110^{\circ}$  F; and a dewpoint, approximately  $-35^{\circ}$  F. For these test conditions, the calibration data of the test section (ref. 22) indicate that the effects of condensation on the flow are probably negligible.

### Corrections

Since the gradients of the measured Mach number, flow angle, and pressure are small in the vicinity of the model, no corrections for these effects have, in general, been applied. In the low-incidence range, the effects of the tunnel static-pressure gradient on the individual static-orifice readings have been discussed in reference 24. Though the magnitude of the free-stream static-pressure gradient is small (see fig. 6, ref. 22), the superposition of the free-stream static pressures and the measured pressures on the test body of the present investigation did improve, somewhat, the agreement between experiment and theory (see fig. 8, ref. 24).

The influence of tunnel air-stream angularity on the angle of attack of the model is exceedingly small at low incidences; a specific illustration presented in reference 23 shows that the air-stream angularity changes the local angle at the nose by about  $0.08^{\circ}$ .

Angular corrections due to aerodynamic loads and model droop (caused by the weight of the model) have been applied to the angle of attack and radial position as discussed in reference 23. The maximum magnitude of the combined incidence-angle corrections was less than  $0.28^{\circ}$ . For these tests (unlike those reported in ref. 23), a special jacking rig (fig. 3(a)) eliminated the need for droop corrections at zero incidence.

A series of tests were made in an attempt to establish the effect of the sting on base pressures. These tests were made by using both the force model described in reference 24 and the pressure model of the present investigation. The results indicated that, at zero incidence, the base-pressure coefficient of the present configuration is too positive by an amount of the order of 0.03. Since this amount will undoubtedly change in some unknown manner with angle of attack and change the base pressures accordingly, there is no specific discussion of the magnitude of base pressures in the present paper. The effect of the sting on the pressures in the separated flow region near the base of the body is not known.



## PRESENTATION OF RESULTS

## Basic Pressures

The basic pressure data obtained on the parabolic body of revolution for angles of attack from  $0^\circ$  to  $36^\circ$  are presented in figure 4 as a function of radial angle for 12 representative stations along the body. Since the geometry of the body at incidence is symmetrical with respect to the  $0^\circ$ - $180^\circ$  axis, a folded horizontal scale has been used; the flagged symbols on this figure, as on all succeeding figures, designate data between  $180^\circ$  and  $360^\circ$ . The use of the folded scale provides a convenient manner to condense the data and, hence, better establish the experimental trends, as well as providing a simple means for considering flow symmetry conditions.

The basic data have also been presented as a function of body position ( $x/L$ ) in figure 5 for the complete incidence range for three radial positions. Theoretical curves (refs. 3 and 21) have been added to these figures for the lower incidence angles. In addition, the experimental data for angles of attack of  $20^\circ$  and  $36^\circ$  have been presented for three model positions each (the model locations specify the distance of the model apex from the wall; see fig. 2) to illustrate the influence of tunnel conditions on the flow. In each case the experimental curve has been faired through the data used in succeeding figures.

The data presented in figures 4 and 5 together with other data obtained during these tests (most of which is not explicitly used in the present paper) are presented in tables I to VI. The test conditions for the pressure data presented in these six tables are:

Table	Angle-of-attack range, deg	Transition strips	Sting configuration
I	0 to 16.1	None	Straight
II	14 to 36	None	$38^\circ$ bent
III	4 to 16.1	Axial	Straight
IV	4 to 16.1	One-half axial	Straight
V	4 to 16.1	Radial, $\frac{x}{L} = 0.614$	Straight
VI	4 to 16.1	Radial, $\frac{x}{L} = 0.834$	Straight

The data of figures 4 and 5 have been compared with similar data from reference 15 and with theory (refs. 3 and 21) in figures 6 and 7 for angles of attack of  $0^\circ$  and  $6^\circ$ , respectively. The primary purpose of the comparison of the present data with that reported in reference 15

is to establish the importance of Reynolds number on this particular configuration and in addition evaluate, if possible, the magnitude of the effects of tunnel disturbances on the experimental results. A more comprehensive comparison of the basic pressures with theory is presented in figure 8 for angles of attack of  $4.00^\circ$ ,  $8.05^\circ$ , and  $12.05^\circ$ ; a comparison of the incremental pressure coefficients (defined as the pressure coefficient at incidence minus the zero-incidence value) with theory is shown in figure 9.

An attempt was made to evaluate differences in flow conditions associated with changing the sting configuration. Hence, the results of one overlap test condition for both stings at an angle of attack of about  $16^\circ$  have been compared in figure 10.

A series of additional tests were made to investigate the effects of artificial roughness added at various discrete locations on the body. The data for a representative phase of these tests are summarized in figure 11.

#### Aerodynamic Coefficients

The section normal-force, axial-force, and side-force (resulting from asymmetrical separation on the leeward side of the body) coefficients were obtained from integration of the pressure distributions and are presented in figure 12. The lift and drag coefficients have been obtained by resolving the normal- and axial-force coefficients along the appropriate axes. In all cases, the contribution of skin friction is neglected inasmuch as the coefficients have been obtained from pressure measurements. These experimental coefficients have been compared with inviscid theory (refs. 3, 21, 25, and 26) and with calculations based on the viscous-cross-flow concepts discussed in references 5 and 11. In calculating the cross-flow section coefficients, the ideas of reference 5 were followed in that it was assumed that a viscous-cross-force contribution to the lift existed when the theoretical radial pressure distributions indicated an unfavorable pressure gradient. The values of the section drag coefficient of a circular cylinder for cross-flow Mach numbers in excess of 0.4 were obtained from the results presented in reference 11. No effect of finite cylinder length was taken into consideration. Since the results of the cross-flow concept depend upon the cross-flow Reynolds numbers, the magnitudes of these values are presented in figure 13 for several representative incidence angles.

The data of figure 12 have been plotted in terms of normal-force, axial-force, and side-force loading distributions in figures 14 to 16. These data have been integrated to yield over-all body coefficients which are shown in figure 17 as a function of angle of attack. Two sets of pitching-moment coefficients have been presented; one set represents

the pitching moment of the normal forces, as is customary in pressure investigations, and the second set presents the pitching moment of the normal and axial forces. Since the effect of the axial forces is small, only two points are shown. The centers of pressure of the normal forces have been specified in terms of fraction of the body length behind the apex. Centers of pressure are shown for these data only for angles of attack of  $8^\circ$  and higher. Below  $8^\circ$ , precision limitations on the reduction of the data introduced excessive scatter so that significant trends were masked. An indication of the center-of-pressure locations in the low angle range can be judged from the experimental data of reference 16 which are shown in figure 17 to supplement the present data.

## DISCUSSION

### Asymmetrical Pressures

The most striking feature indicated by the basic data (fig. 4) is the asymmetrical distribution of pressures (with respect to the plane of incidence) over the leeward side of the body for the higher angles of attack. The extent and magnitude of the asymmetrical flow regions corresponding to these pressures are functions of angle of attack and station along the body. Over the forward half of the body these regions occur initially at an angle of attack of about  $16^\circ$ , and with increasing incidence broaden rapidly to extend over the entire leeward side of the body by angles of attack of about  $28^\circ$ . Farther rearward, these asymmetries occur at progressively lower angles of attack and extend over larger regions of the body as the base is approached. Though the data of the last two stations (0.951 and 0.999) indicate, quite consistently, these regions extending around the body radially for angles of attack as low as  $2^\circ$  or  $4^\circ$ , it should be noted that the magnitude of the differences in pressures at corresponding radial position on opposing sides for these angles is small and approaches the experimental accuracy (a value of  $\pm 0.01$  in pressure coefficient). Furthermore these data may be affected by the presence of the sting.<sup>1</sup> Although the absence of experimental data at some critical radial locations together with the absence of visual flow studies precludes a more tangible discussion of the limits of these asymmetrical flow boundaries, it is clearly evident that the occurrence of this phenomenon is qualitatively significant, and for practical configurations may be of prime importance in the evaluation of the characteristics of lifting surfaces located in these flow regions.

---

<sup>1</sup>Though the influence of the sting on the results remains, in essence, unknown, it can be concluded from figure 10 that the change in sting configuration from straight to bent had no significant effect, at least for angles of attack of about  $16^\circ$ .

The nature of these asymmetrical flows is further evident in figures 5 and 9. For example, on the side of the body  $\phi = 90^\circ, 270^\circ$ , (figs. 5(b) and 9(b)) and leeward  $90^\circ \leq \phi \leq 270^\circ$ , (figs. 5(c), 9(c), and 9(d)), the axial distribution of pressures at corresponding radial positions is erratic, being considerably different at an angle of attack of  $36^\circ$  than at  $12^\circ$  or  $20^\circ$ . It is to be noted that the asymmetries of the flow are not, at least up to an angle of attack of  $25.5^\circ$ , associated with a detached shock at the nose of the model. The value,  $25.5^\circ$ , for shock detachment has been conservatively estimated on the basis of shock detachment for an unyawed cone whose semiapex angle is equal to the sum of the present semiapex angle and the angle of attack for shock detachment.

Since the flow over the leeward side of the body at these high incidences is not relatively stable, slight tunnel gradients appear to have a measurable effect on these data. This is evident in figures 5(b) and 5(c) where the leeward pressures change with model location in the tunnel; whereas on the windward side (fig. 5(a)), however, there are no measurable effects of model location. These results, showing the effects of model position, may be indicative of difficulties to be anticipated in correlating, quantitatively, high-angle investigations in various facilities.

Asymmetrical flow conditions have been previously noted in reference 13 from visual-flow studies at high angles and in reference 27 where erratic rolling oscillations were measured on a body-tail combination. These oscillations (reported in ref. 13 and in a paper of limited circulation) were traced to unsteady fluctuations of the leeward vortices which, under certain conditions, were discharged aperiodically from each side of the body. Although there was no regularity in the discharge of the vortices, (when such a discharge did occur), the time interval between reversals from side to side of the aperiodically discharged vortices was noted to be of the order of seconds. Thus a pressure measuring system such as the present (where lag is of the order of minutes) would be expected to indicate a mean value corresponding to symmetrical flow during such a discharge. The "one-sidedness" of the data for the discrete angles of attack presented indicates that switching or reversals of the vortices was not a prime occurrence at these angles. However, for those angles of attack where the side-force coefficients become zero, that is, the angles where the coefficients reverse sign (for example, fig. 12(e), station 0.714,  $\alpha \approx 31^\circ$ ), it is indicated that a rapid switching of the vortex pattern is taking place locally.

Whether this one-sidedness is materially influenced by the tunnel gradients or model conditions is not definitely known. From the results of figure 5, however, it is evident that traversing the model in the tunnel and hence varying the gradients modifies rather than changes the character of the pressure distributions. Furthermore, it is to be noted

that, for the present tests, two sets of data were recorded for each test condition with an elapsed time of from 3 to 5 minutes between points. Since no significant differences were indicated by the two sets of data, the present results are taken to represent a mean value for an unsymmetrical flow. It might also be of interest to note that, because of the test procedure, some question arises as to whether or not the vortex pattern at a specific angle of attack would be the same for each index position. The data shown in figure 4 indicate that the pattern repeated, that is, the vortex nearest the body, appeared on the same side for each index position. The reason for this is not known since it would seem that the disposition of the vortices would be unpredictable and that the vortex pattern might assume the reverse position during the course of the tests unless slight tunnel gradients were of significance in causing the repeatability of the flow.

A discussion of the mechanism of flow over bodies of revolution at high angles of attack has been presented in reference 13. The analogy to impulsive flow over a circular cylinder is pointed out and attention is directed to the results presented in reference 28. In reference 28, the development of flow over a circular cylinder is presented from the initial occurrence of the symmetrical vortex over the leeward side (as found in ref. 13) to the breakdown of the asymmetrical vortex formation.

#### Comparison of Experimental and Theoretical Pressures

Inasmuch as the present model has become practically a standard test vehicle, considerable work has already been reported comparing the experimental and theoretical characteristics of the body. Results are presented in reference 15 for a Mach number range from 1.49 to 1.98 (including a Mach number of 1.59 and a Reynolds number of  $29 \times 10^6$ ) for Reynolds numbers from  $28 \times 10^6$  to  $31 \times 10^6$ , and in reference 20 for Mach numbers of 1.52 and 1.98 at Reynolds numbers of  $8.6 \times 10^6$  and  $17.4 \times 10^6$ . Hence, the results of the present comparisons at a Mach number of 1.59 and a Reynolds number of  $3.6 \times 10^6$  serve primarily to supplement the previously published results insofar as Reynolds number is concerned.

The experimental-theoretical comparison of the pressure distributions at an angle of attack of  $0^\circ$  (fig. 6) clearly indicates the absence of any marked Reynolds number effects on the forebody pressure distribution in the Reynolds number range from  $3.6 \times 10^6$  to  $29 \times 10^6$ . Those discrepancies which do exist are small and are probably not Reynolds number effects. The absence of such effects on the forebody pressures has been noted also in reference 20 for this body for a Reynolds number range of  $8.6 \times 10^6$  to  $30 \times 10^6$ . In order to consider further the effects of boundary layer on the forebody pressures, the present model was tested

with an extremely thick turbulent boundary layer (ref. 24) artificially induced at the nose. Even for this extreme case, no effects on the forebody pressures were evident, the indication, perhaps, being the absence of Reynolds numbers effects even far beyond the presently established  $30 \times 10^6$  value. Though the forebody pressures are unaffected by a change in boundary layer from laminar (Reynolds number of  $3.6 \times 10^6$ ) to primarily turbulent (Reynolds number of  $29 \times 10^6$ ), there is a marked decrease (fig. 6) in base pressure accompanying this Reynolds number change. This effect of Reynolds number on the base pressure of this configuration has been studied in detail in reference 29 and the results presented therein substantiate the data of figure 6.

The same generalization concerning the absence of Reynolds number effects on the pressures for an angle of attack of  $0^\circ$  applies to the forebody pressures at an angle of attack of  $6^\circ$  (fig. 7) for the same Reynolds number range of  $3.6 \times 10^6$  to  $29 \times 10^6$ . For this comparison, the data from the Langley 4- by 4-foot supersonic tunnel have been obtained either from the station nearest that specified (which is a Lewis 8- by 6-foot tunnel station) or an average value of data from two stations, one on each side of the indicated station. The agreement between the two sets of data is good; and though the slight discrepancies at the last station (0.951) might be attributed to differences in cross-flow separation and hence a Reynolds number effect, it is to be noted that discrepancies of the same magnitude occur at the foremost station (0.083) where separation effects are hardly the cause. As has been previously established, in general, in references 15 and 20, the agreement between the experimental and theoretical pressures (figs. 5 and 8) in the low-incidence range up to say an angle of attack of  $4^\circ$  or  $5^\circ$  is relatively good, with viscous effects confined to about the rear 10 percent of the body on the leeward side. Further increases in angle of attack progressively cause a deterioration in the agreement between experiment and theory, where, as has been shown many times before and is evident in figures 5 and 8, the leeward side is affected first and the most. At about  $12^\circ$  (figs. 5 and 8), most of the leeward side is affected by the cross-flow separation, the separation being so predominant as to render inviscid theory practically valueless in predicting the flow. On the windward side, the experimental pressures appear, in general, to be slightly more positive than predicted by theory in the range of angles of attack of  $12^\circ$  and higher. The incremental pressures due to angle of attack (fig. 9) reflect the previously mentioned flow characteristics.

It is quite evident from these data and considerable other similar data that the use of any inviscid theory whether linearized or not, is inherently limited in scope and that further attempts to improve the quality of the predictions, at least over the rear of an inclined body at high angles of attack, should be directed towards improved viscous considerations.

### Artificial Roughness

Several simple and relatively crude exploratory tests were made to study the effect of various types and locations of transition strips on the pressures. The results are plotted in figure 11 for six axial body stations. With the exception of those stations near the base, which are probably affected by the sting, no effect of axial transition strips was noted at an angle of attack of  $8^\circ$ . At  $12^\circ$  and near the base at  $8^\circ$ , however, the addition of axial transition strips appeared to cause "cross-flow transition" and hence delay separation over the body. This same trend is indicated forward of the maximum thickness section for an angle of attack of  $16^\circ$ . Rearward of this section, no consistent effects were observed. The data showing the effects of a radial transition strip at the maximum thickness section were too limited in scope to indicate any definite trends. There was a marked increase in base pressure with the addition of axial transition strips, a change which is opposite to that previously shown (fig. 6) for  $0^\circ$ . This reversed effect is, however, qualitatively similar to results established in conjunction with the tests reported in references 24 and 29.

### Section Coefficients

The integrated section coefficients presented in figure 12 reflect, in general, the pressure-distribution characteristics indicated in the preceding figures. At the foremost stations, the normal-force coefficients in the low-incidence range are accurately predicted by inviscid theory, thereby substantiating the results previously established in reference 19. The absence of any significant cross-flow separation is clearly implied by the comparison of the normal-force coefficients up to  $12^\circ$  for station 0.024. At stations closer towards the maximum thickness, the agreement between the data and slender-body theory becomes progressively worse, the discrepancy being the inability of the theory to predict the increase in slope with angle of attack. Aft of the maximum-thickness section, a hump in the normal-force curve occurs between  $8^\circ$  and  $12^\circ$  at station 0.618 and at lower angles rearward. This hump seems to be associated with the beginning of separation of the cross flow over the body. The addition of axial transition strips resulted in a decrease in normal-force coefficient at an angle of attack of  $12^\circ$ , an effect which would tend to smooth out the abruptness of the hump. The presence of the hump limits the agreement between experiment and inviscid theory to angles of about  $4^\circ$  or less at the rearmost stations. The prediction based on the cross-flow assumption of reference 5, while qualitatively improving the agreement over the mid and rear sections of the body, is hardly adequate locally for angles of attack in excess of about  $8^\circ$ .



A similar type of agreement between the axial-force coefficients and the inviscid theory is shown, as has been previously established in reference 19, the largest discrepancies being evidenced at the foremost stations. Such an effect is somewhat unusual in view of the previously established deficiencies of the theory for the rearward stations.

The side-force coefficients are presented for illustrative purposes only to establish the magnitudes. The primary influence of these asymmetrical flows will be manifested when a lifting surface is located in these regions.

### Body Coefficients

A comparison of the experimental lift or normal-force coefficient with theory (fig. 17) shows the usual underestimation of lift predicted by inviscid theory with the general improvement of the estimate by the application of the cross-flow concept of reference 13. However, even this approximation appears entirely inadequate for angles of attack much in excess of  $8^\circ$ . The absence of any significant Reynolds number effects on the normal force, axial force (excluding base pressure), and pitching-moment coefficient in the Reynolds number range from  $3.6 \times 10^6$  to  $29 \times 10^6$  is indicated by the close agreement between the data of the Lewis 8- by 6-foot tunnel and the Langley 4- by 4-foot tunnel. The experimental center of pressure is considerably aft of the value predicted by the cross-flow separation; the slender-body theoretical location is -0.7. As was the case for the section coefficients, the axial-force prediction was relatively good in the low angle-of-attack range.

### CONCLUDING REMARKS

A pressure-distribution investigation of a parabolic body of revolution with a fineness ratio of 12.2 has been undertaken in the Langley 4- by 4-foot supersonic tunnel at a Mach number of 1.59 and a Reynolds number of  $3.6 \times 10^6$ , based on the body length, for angles of attack from  $0^\circ$  to  $36^\circ$ . In the low-incidence range, up to  $9^\circ$ , a comparison of these data with other experimental data on the same configuration indicated the absence of any significant Reynolds number effects on the pressures (except at the base) in the range from  $3.6 \times 10^6$  to  $29 \times 10^6$ . At an angle of attack of  $0^\circ$ , the pressures were well-predicted by potential (slender-body) theory. In the low-incidence range, similar agreement existed with the pressures on the windward side. On the leeward side, however, the pressures were affected by cross-flow separation; the discrepancies between experiment and theory appeared rearward

first, perhaps at about  $5^\circ$ , and progressed forward as the angle of attack was increased. At the higher angles, the cross-flow separation became asymmetrical; the leeward pressures at corresponding radial locations were considerably different. These asymmetries were very pronounced over most of the body for angles of attack about  $16^\circ$  and higher but were observed for much lower angles at rearward body locations. The data at the higher angles where the asymmetries occurred were affected by tunnel gradients in that differences, solely in the leeward pressures, existed when the model was tested in different tunnel locations. These differences are probably of secondary importance in that they appear to modify rather than cause the asymmetries.

With the exception of those stations near the base, the addition of artificial roughness along the sides of the body had no effect on the forebody pressures at angles of attack of  $8^\circ$  or less. At  $12^\circ$  and near the base at  $8^\circ$ , the addition of artificial roughness along the sides of the body appeared to cause "cross-flow transition" and hence delay separation of the flow over the body. This same trend was indicated ahead of the maximum thickness section at  $16^\circ$  while no consistent effect of roughness was noted rearward of this point on the body.

In the low-incidence range, the normal-force coefficient of the body was underestimated and the chord force predicted reasonably well by potential (slender-body) theory. The center of pressure was considerably rearward of either the potential theory or the results obtained from the viscous-cross-flow theory. Though the cross-flow estimate did improve the agreement with the experimental data in the low-incidence range, perhaps up to  $10^\circ$ , discrepancies of considerable magnitude were found at higher angles.

Langley Aeronautical Laboratory  
National Advisory Committee for Aeronautics  
Langley Field, Va.

## REFERENCES

1. Von Kármán, Theodor, and Moore, Norton B.: Resistance of Slender Bodies Moving With Supersonic Velocities With Special Reference to Projectiles. Trans. A.S.M.E., vol. 54, no. 23, Dec. 15, 1932, pp. 303-310.
2. Tsien, Hsue-Shen: Supersonic Flow Over an Inclined Body of Revolution. Jour. Aero. Sci., vol. 5, no. 12, Oct. 1938, pp. 480-483.
3. Lighthill, M. J.: Supersonic Flow Past Bodies of Revolution. R. & M. No. 2003, British A.R.C., 1945.
4. Lighthill, M. J.: Supersonic Flow Past Slender Pointed Bodies of Revolution at Yaw. Quarterly Jour. Mech. and Appl. Math., vol 1, pt. 1, Mar. 1948, pp. 76-89.
5. Van Dyke, Milton D: First- and Second-Order Theory of Supersonic Flow Past Bodies of Revolution. Jour. Aero. Sci., vol. 18, no. 3, Mar. 1951, pp. 161-178.
6. Broderick, J. B.: Supersonic Flow Round Pointed Bodies of Revolution. Quarterly Jour. Mech. and Appl. Math., vol. II, pt. 1, Mar. 1949, pp. 98-120.
7. Ferrari, C.: Determination of the Pressure Exerted on Solid Bodies of Revolution With Pointed Noses Placed Obliquely in a Stream of Compressible Fluid at Supersonic Velocity. R.T.P. Translation no. 1105, British Ministry of Aircraft Production. (From Atti R. Accad. Sci. Torino, vol. 72, Nov.-Dec. 1936, pp. 140-163.)
8. Sauer, Robert: Supersonic Flow About Projectile Heads of Arbitrary Shape at Small Incidence. R.T.P. Translation No. 1573, British Ministry of Aircraft Production. (From Luftfahrtforschung, vol. 19, no. 4, May 1942, pp. 148-152.)
9. Ferri, Antonio: The Method of Characteristics for the Determination of Supersonic Flow Over Bodies of Revolution at Small Angles of Attack. NACA Rep. 1044, 1951. (Supersedes NACA TN 1809.)
10. Ferri, Antonio: Application of the Method of Characteristics to Supersonic Rotational Flow. NACA Rep. 841, 1946. (Supersedes NACA TN 1135.)
11. Allen, H. Julian: Estimation of the Forces and Moments Acting on Inclined Bodies of Revolution of High Fineness Ratio. NACA RM A9I26, 1949.

12. Jones, Robert T.: Effects of Sweep-Back on Boundary Layer and Separation. NACA Rep. 884, 1947. (Supersedes NACA TN 1402.)
13. Allen, H. Julian, and Perkins, Edward W.: Characteristics of Flow Over Inclined Bodies of Revolution. NACA RM A50L07, 1951.
14. Brown, C. S., and Luther, M. L.: Experimental Studies of Forces, Pressure Distributions and Viscous Effects on Long Inclined Bodies of Revolution at Mach 2.96. NAVORD Rep. 1651, Proceedings of the Bureau of Ordnance Symposium on Aeroballistics, Nov. 16-17, 1950, pp. 57-73.
15. Luidens, Roger W., and Simon, Paul C.: Aerodynamic Characteristics of NACA RM-10 Missile in 8- by 6-Foot Supersonic Wind Tunnel at Mach Numbers From 1.49 to 1.98. I - Presentation and Analysis of Pressure Measurements (Stabilizing Fins Removed). NACA RM E50D10, 1950.
16. Esenwein, Fred T., Obery, Leonard J., and Schueller, Carl F.: Aerodynamic Characteristics of NACA RM-10 Missile in 8- by 6-Foot Supersonic Wind Tunnel at Mach Numbers From 1.49 to 1.98. II - Presentation and Analysis of Force Measurements. NACA RM E50D28, 1950.
17. Rumsey, Charles B. and Lopper, J. Dan: Average Skin-Friction Coefficients From Boundary-Layer Measurements in Flight on a Parabolic Body of Revolution (NACA RM-10) at Supersonic Speeds and at Large Reynolds Numbers. NACA RM L51B12, 1951.
18. Chauvin, Leo T., and deMoraes, Carlos A.: Correlation of Supersonic Convective Heat-Transfer Coefficients From Measurements of the Skin Temperature of a Parabolic Body of Revolution (NACA RM-10). NACA RM L51A18, 1951.
19. Luidens, Roger W., and Simon, Paul C.: Aerodynamic Characteristics of NACA RM-10 Missile in 8- by 6-Foot Supersonic Wind Tunnel at Mach Numbers From 1.49 to 1.98. III - Analysis of Force Distribution at Angle of Attack (Stabilizing Fins Removed). NACA RM E50I19, 1950.
20. Perkins, Edward W., Gowen, Forrest E., and Jorgensen, Leland H.: Aerodynamic Characteristics of the NACA RM-10 Research Missile in the Ames 1- by 3-Foot Supersonic Wind Tunnel No. 2 - Pressure and Force Measurements at Mach Numbers of 1.52 and 1.98. NACA RM A51G13, 1951.

21. Allen, H. Julian: Pressure Distribution and Some Effects of Viscosity on Slender Inclined Bodies of Revolution. NACA TN 2044, 1950.
22. Cooper, Morton, Smith, Norman F., and Kainer, Julian H.: A Pressure-Distribution Investigation of a Supersonic Aircraft Fuselage and Calibration of the Mach Number 1.59 Nozzle of the Langley 4- by 4-Foot Supersonic Tunnel. NACA RM L9E27a, 1949.
23. Cooper, Morton, and Webster, Robert A.: The Use of an Uncalibrated Cone for Determination of Flow Angles and Mach Numbers at Supersonic Speeds. NACA TN 2190, 1951.
24. Hasel, Lowell E., Sinclair, Archibald R., and Hamilton, Clyde W.: Preliminary Investigation of the Drag Characteristics of the NACA RM-10 Missile at Mach Numbers of 1.40 and 1.59 in the Langley 4- by 4-Foot Supersonic Tunnel. NACA RM L52A14, 1952.
25. Staff of the Computing Section, Center of Analysis (Under Direction of Zdeněk Kopal): Tables of Supersonic Flow Around Cones. Tech. Rep. No. 1, M.I.T., 1947.
26. Staff of the Computing Section, Center of Analysis (Under Direction of Zdeněk Kopal): Tables of Supersonic Flow Around Yawing Cones. Tech. Rep. No. 3, M.I.T., 1947.
27. Mead, Merrill H.: Observations of Unsteady Flow Phenomena for an Inclined Body Fitted With Stabilizing Fins. NACA RM A51K05, 1952.
28. Schwabe, M.: Pressure Distribution in Nonuniform Two-Dimensional Flow. NACA TM 1039, 1943.
29. Czarnecki, K. R., and Marte, Jack E.: Skin-Friction Drag and Boundary-Layer Transition on a Parabolic Body of Revolution (NACA RM-10) at a Mach Number of 1.6 in the Langley 4- by 4-Foot Supersonic Pressure Tunnel. NACA RM L52C24, 1952.

TABLE I.- PRESSURE COEFFICIENT DATA FOR PARABOLIC BODY  
OF REVOLUTION (RM-10) MOUNTED ON STRAIGHT STING

NO TRANSITION STRIPS

(a)  $\alpha = 0$

Station, $x/L$	Radial angle, $\phi$ , deg			
	90	180	270	360
0.024	0.057	0.063	0.065	0.069
.048	.048	.063	.061	.057
.071	.042	.055	.048	.063
.095	.044	.052	.044	.055
.119	.042	.044	.042	.044
.143	.036	.038	.038	.040
.167	.032	.038	.036	.040
.190	.028	.036	.030	.036
.214	.026	.032	.030	-----
.238	.014	-----	.022	.016
.262	.012	.016	.010	.012
.285	.010	.012	.010	.008
.333	0	.008	.006	.004
.381	-.004	.002	.006	-.006
.428	-.008	0	0	-.008
.476	-.016	-.012	-.010	-.014
.523	-.016	-.016	-.012	-.014
.571	-.024	-.016	-.020	-.010
.618	-.036	-.032	-.026	-.032
.666	-----	-.036	-.032	-.032
.714	-.040	-.036	-.040	-.044
.761	-.044	-----	-.040	-.048
.785	-.044	-.040	-.032	-.044
.809	-.040	-.032	-.032	-.044
.832	-.048	-.040	-.036	-.044
.856	-.048	-.038	-.038	-.040
.880	-.040	-.036	-.032	-.040
.904	-.030	-.032	-.032	-.044
.928	-.022	-.016	-.030	-.030
.951	-.018	-.016	-.024	-.024
.975	-.016	-.016	-.018	-.020
.999	-.012	-.012	-----	-.020
1.000	-.012	-.012	-.008	-.018

NACA

TABLE I.- PRESSURE COEFFICIENT DATA FOR PARABOLIC BODY  
OF REVOLUTION (RM-10) MOUNTED ON STRAIGHT STING

NO TRANSITION STRIPS - Continued

(b)  $\alpha = 1.00$

Station, x/L	Radial angle, $\phi$ , deg																			
	13.8	28.8	43.8	73.8	88.8	103.8	118.8	133.8	163.8	178.8	193.8	208.8	223.8	253.8	268.8	283.8	298.8	313.8	343.8	358.8
0.024	0.074	0.068	-----	0.062	0.058	0.056	0.054	0.054	0.056	0.056	0.058	0.054	0.076	0.064	0.066	0.070	0.068	0.098	0.072	0.070
0.048	0.068	0.060	-----	0.062	0.058	0.056	0.062	0.054	0.044	0.048	0.048	0.044	0.052	0.054	0.048	0.060	0.060	0.066	0.066	0.064
0.071	0.056	0.050	0.054	0.056	0.052	0.050	0.048	0.050	0.040	0.040	0.042	0.036	0.042	0.042	0.048	0.050	0.058	0.064	0.056	0.052
0.095	0.056	0.052	0.054	0.052	0.050	0.046	0.044	0.044	0.038	0.034	0.038	0.036	0.042	0.044	0.044	0.048	0.048	0.054	-----	0.052
0.119	0.056	0.054	0.054	0.048	0.044	0.042	0.040	0.040	0.034	0.032	0.034	0.028	0.038	0.036	0.036	0.042	0.042	0.046	-----	0.042
0.143	0.048	0.046	0.046	0.040	0.040	0.038	0.032	0.034	0.030	0.028	0.030	0.024	0.030	0.036	0.036	0.040	0.038	0.044	-----	0.040
0.167	0.048	0.042	0.044	0.040	0.036	0.036	0.030	0.034	0.028	0.028	0.026	0.024	0.030	0.034	0.036	0.040	0.038	0.044	0.046	0.040
0.190	0.044	0.038	0.040	0.038	0.034	0.032	0.028	0.030	0.024	0.024	0.024	0.020	0.028	0.032	0.032	0.036	0.032	0.038	0.038	0.038
0.214	0.042	0.036	0.040	0.030	0.030	0.030	0.024	0.028	0.020	0.022	0.024	0.016	0.022	-----	-----	-----	-----	0.038	0.030	0.026
0.238	0.032	0.024	0.028	0.022	0.018	0.018	0.014	0.018	0.014	0.012	0.014	0.008	0.016	0.018	0.014	0.022	0.016	0.024	0.020	0.020
0.262	0.026	0.018	0.024	0.020	0.016	0.018	0.010	0.014	0.008	0.010	0.010	0.006	0.014	0.016	0.014	0.020	0.012	0.020	0.014	0.014
0.285	0.022	0.016	0.020	0.014	0.012	0.014	0.008	0.010	0.006	0.008	0.008	0.006	0.008	0.010	0.006	0.012	0.008	0.012	0.012	0.008
0.330	0.016	0.008	0.008	0.004	0.004	0.002	0.002	0.004	0.002	0.004	0.006	0	0.008	0.010	0.006	0.008	0.004	0.008	0.006	0.002
0.381	0.008	0.002	0.006	0	0	0	0.002	0	0	0	0.002	0	0.006	0.006	0	0.008	0.004	0.008	0.006	0
0.428	0.004	0.004	0	0.002	0.004	0.002	0.008	0.002	0.004	0.004	0.002	0.008	0.002	0.002	0.002	0.002	0.004	0.002	0.002	0.002
0.476	0.004	0.012	0.008	0.012	0.014	0.014	0.008	0.018	0.018	0.018	0.016	0.020	0.014	0.014	0.016	0.006	0.012	0.004	0.010	0.010
0.523	0.004	0.012	0.006	0.016	0.016	0.016	0.020	0.018	0.016	0.016	0.014	0.018	0.014	0.006	0.008	0.008	0.006	0.006	0.010	0.008
0.571	0.012	0.020	0.016	0.022	0.024	0.024	0.028	0.022	0.022	0.024	0.022	0.028	0.024	0.016	0.016	0.016	0.012	0.024	0.018	0.018
0.618	0.020	0.032	0.024	0.034	0.032	0.032	0.036	0.030	0.032	0.032	0.032	0.036	0.030	0.030	0.034	0.024	0.030	0.024	0.028	0.028
0.666	-----	-----	-----	0.036	0.034	0.034	0.042	0.036	0.036	0.036	0.038	0.042	0.038	0.032	0.032	0.034	0.036	0.032	0.028	0.028
0.714	0.032	0.004	0.036	0.040	0.040	0.038	0.042	0.036	0.040	0.040	0.038	0.040	0.038	0.038	0.038	0.028	0.036	0.038	0.042	0.040
0.761	0.038	0.046	0.038	0.042	0.040	0.038	0.044	0.036	0.038	0.038	0.034	0.040	0.032	0.032	0.036	0.030	0.040	0.040	0.046	0.044
0.785	0.038	0.048	0.038	0.042	0.040	0.038	0.044	0.036	0.038	0.036	0.034	0.036	0.030	0.034	0.038	0.032	0.040	0.036	0.038	0.040
0.809	0.040	0.042	0.040	0.036	0.040	0.034	0.034	0.032	0.038	0.036	0.034	0.036	0.030	0.034	0.040	0.032	0.040	0.036	0.042	0.040
0.832	0.042	0.048	0.044	0.044	0.044	0.040	0.044	0.038	0.038	0.036	0.036	0.040	0.034	0.034	0.040	0.032	0.040	0.036	0.042	0.044
0.856	0.044	0.048	0.046	0.048	0.046	0.042	0.044	0.038	0.038	0.036	0.036	0.040	0.034	0.034	0.040	0.032	0.042	0.036	0.042	0.044
0.880	0.040	0.046	0.044	0.042	0.044	0.040	0.042	0.036	0.036	0.036	0.036	0.038	0.034	0.034	0.040	0.032	0.040	0.036	0.042	0.042
0.904	0.038	0.042	0.040	0.040	0.036	0.038	0.040	0.034	0.036	0.032	0.030	0.034	0.032	0.034	0.038	0.032	0.038	0.034	0.040	0.040
0.928	0.036	0.036	0.036	0.028	0.028	0.026	0.028	0.024	0.030	0.032	0.028	0.032	0.030	0.030	0.038	0.032	0.038	0.034	0.034	0.040
0.951	0.036	0.036	0.036	0.034	0.030	0.030	0.034	0.026	0.030	0.028	0.028	0.032	0.030	0.034	0.038	0.034	0.040	0.036	0.030	0.040
0.975	0.036	0.036	0.036	0.034	0.030	0.030	0.034	0.026	0.030	0.028	0.028	0.032	0.030	0.034	0.038	0.034	0.040	0.036	0.036	0.040
0.999	0.042	0.042	0.044	0.044	0.048	0.046	0.048	0.048	0.042	0.042	0.042	0.042	0.042	0.042	0.048	0.040	0.044	0.040	0.042	0.048
1.000	0.042	0.046	0.046	0.046	0.050	0.046	0.050	0.048	0.042	0.042	0.042	0.048	0.048	0.046	0.044	0.046	0.042	0.040	0.042	0.048

NACA



TABLE I.- PRESSURE COEFFICIENT DATA FOR PARABOLIC BODY  
OF REVOLUTION (RM-10) MOUNTED ON STRAIGHT STING

NO TRANSITION STRIPS - Continued

(c)  $\alpha = 2.00$

Station, x/L	Radial angle, $\phi$ , deg															
	7	22	37	52	67	82	97	112	127	142	157	172	187	202	217	232
0.024	0.078	0.080	0.072	0.068	0.060	0.060	0.052	0.052	0.048	0.048	0.046	0.048	0.048	0.048	0.048	0.066
0.048	0.070	0.076	0.068	0.064	0.058	0.058	0.052	0.052	0.048	0.048	0.046	0.048	0.048	0.048	0.048	0.066
0.071	0.060	0.064	0.056	0.056	0.048	0.048	0.042	0.044	0.044	0.044	0.040	0.038	0.032	0.032	0.030	0.034
0.095	0.056	0.062	0.058	0.054	0.048	0.048	0.042	0.044	0.044	0.044	0.040	0.038	0.032	0.032	0.030	0.034
0.119	0.054	0.062	0.058	0.054	0.048	0.048	0.042	0.044	0.044	0.044	0.040	0.038	0.032	0.032	0.030	0.034
0.143	0.048	0.056	0.052	0.048	0.042	0.042	0.038	0.038	0.038	0.038	0.036	0.032	0.026	0.026	0.024	0.028
0.167	0.044	0.052	0.048	0.044	0.040	0.036	0.032	0.032	0.032	0.032	0.030	0.026	0.020	0.020	0.016	0.020
0.190	0.042	0.050	0.044	0.040	0.036	0.034	0.032	0.032	0.032	0.032	0.030	0.026	0.020	0.020	0.016	0.020
0.214	0.040	0.046	0.040	0.036	0.034	0.032	0.028	0.028	0.028	0.028	0.026	0.022	0.018	0.018	0.012	0.020
0.238	0.030	0.036	0.030	0.024	0.020	0.016	0.012	0.012	0.012	0.010	0.010	0.006	0.008	0.008	0.008	0.010
0.262	0.024	0.030	0.026	0.022	0.018	0.014	0.012	0.012	0.012	0.008	0.008	0.002	0.004	0.004	0.002	0.008
0.285	0.016	0.026	0.020	0.020	0.012	0.012	0.008	0.008	0.008	0.004	0.004	0.002	0.002	0.002	0.006	0.006
0.308	0.012	0.020	0.010	0.006	0.002	0.002	0.000	0.000	0.000	0.000	0.000	0.000	0.000	0.000	0.000	0.000
0.331	0.004	0.012	0.004	0.000	0.000	0.000	0.000	0.000	0.000	0.000	0.000	0.000	0.000	0.000	0.000	0.000
0.354	0.000	0.000	0.000	0.000	0.000	0.000	0.000	0.000	0.000	0.000	0.000	0.000	0.000	0.000	0.000	0.000
0.377	0.000	0.000	0.000	0.000	0.000	0.000	0.000	0.000	0.000	0.000	0.000	0.000	0.000	0.000	0.000	0.000
0.400	0.000	0.000	0.000	0.000	0.000	0.000	0.000	0.000	0.000	0.000	0.000	0.000	0.000	0.000	0.000	0.000
0.423	0.000	0.000	0.000	0.000	0.000	0.000	0.000	0.000	0.000	0.000	0.000	0.000	0.000	0.000	0.000	0.000
0.446	0.000	0.000	0.000	0.000	0.000	0.000	0.000	0.000	0.000	0.000	0.000	0.000	0.000	0.000	0.000	0.000
0.469	0.000	0.000	0.000	0.000	0.000	0.000	0.000	0.000	0.000	0.000	0.000	0.000	0.000	0.000	0.000	0.000
0.492	0.000	0.000	0.000	0.000	0.000	0.000	0.000	0.000	0.000	0.000	0.000	0.000	0.000	0.000	0.000	0.000
0.515	0.000	0.000	0.000	0.000	0.000	0.000	0.000	0.000	0.000	0.000	0.000	0.000	0.000	0.000	0.000	0.000
0.538	0.000	0.000	0.000	0.000	0.000	0.000	0.000	0.000	0.000	0.000	0.000	0.000	0.000	0.000	0.000	0.000
0.561	0.000	0.000	0.000	0.000	0.000	0.000	0.000	0.000	0.000	0.000	0.000	0.000	0.000	0.000	0.000	0.000
0.584	0.000	0.000	0.000	0.000	0.000	0.000	0.000	0.000	0.000	0.000	0.000	0.000	0.000	0.000	0.000	0.000
0.607	0.000	0.000	0.000	0.000	0.000	0.000	0.000	0.000	0.000	0.000	0.000	0.000	0.000	0.000	0.000	0.000
0.630	0.000	0.000	0.000	0.000	0.000	0.000	0.000	0.000	0.000	0.000	0.000	0.000	0.000	0.000	0.000	0.000
0.653	0.000	0.000	0.000	0.000	0.000	0.000	0.000	0.000	0.000	0.000	0.000	0.000	0.000	0.000	0.000	0.000
0.676	0.000	0.000	0.000	0.000	0.000	0.000	0.000	0.000	0.000	0.000	0.000	0.000	0.000	0.000	0.000	0.000
0.699	0.000	0.000	0.000	0.000	0.000	0.000	0.000	0.000	0.000	0.000	0.000	0.000	0.000	0.000	0.000	0.000
0.722	0.000	0.000	0.000	0.000	0.000	0.000	0.000	0.000	0.000	0.000	0.000	0.000	0.000	0.000	0.000	0.000
0.745	0.000	0.000	0.000	0.000	0.000	0.000	0.000	0.000	0.000	0.000	0.000	0.000	0.000	0.000	0.000	0.000
0.768	0.000	0.000	0.000	0.000	0.000	0.000	0.000	0.000	0.000	0.000	0.000	0.000	0.000	0.000	0.000	0.000
0.791	0.000	0.000	0.000	0.000	0.000	0.000	0.000	0.000	0.000	0.000	0.000	0.000	0.000	0.000	0.000	0.000
0.814	0.000	0.000	0.000	0.000	0.000	0.000	0.000	0.000	0.000	0.000	0.000	0.000	0.000	0.000	0.000	0.000
0.837	0.000	0.000	0.000	0.000	0.000	0.000	0.000	0.000	0.000	0.000	0.000	0.000	0.000	0.000	0.000	0.000
0.860	0.000	0.000	0.000	0.000	0.000	0.000	0.000	0.000	0.000	0.000	0.000	0.000	0.000	0.000	0.000	0.000
0.883	0.000	0.000	0.000	0.000	0.000	0.000	0.000	0.000	0.000	0.000	0.000	0.000	0.000	0.000	0.000	0.000
0.906	0.000	0.000	0.000	0.000	0.000	0.000	0.000	0.000	0.000	0.000	0.000	0.000	0.000	0.000	0.000	0.000
0.929	0.000	0.000	0.000	0.000	0.000	0.000	0.000	0.000	0.000	0.000	0.000	0.000	0.000	0.000	0.000	0.000
0.952	0.000	0.000	0.000	0.000	0.000	0.000	0.000	0.000	0.000	0.000	0.000	0.000	0.000	0.000	0.000	0.000
0.975	0.000	0.000	0.000	0.000	0.000	0.000	0.000	0.000	0.000	0.000	0.000	0.000	0.000	0.000	0.000	0.000
0.998	0.000	0.000	0.000	0.000	0.000	0.000	0.000	0.000	0.000	0.000	0.000	0.000	0.000	0.000	0.000	0.000
1.000	0.000	0.000	0.000	0.000	0.000	0.000	0.000	0.000	0.000	0.000	0.000	0.000	0.000	0.000	0.000	0.000

NACA

TABLE I.- PRESSURE COEFFICIENT DATA FOR PARABOLIC BODY  
OF REVOLUTION (RM-10) MOUNTED ON STRAIGHT STING

NO TRANSITION STRIPS - Continued

(a)  $\alpha = 3.00$

Station, x/L	Radial angle, $\phi$ , deg																					
	9.7	24.7	39.7	54.7	84.7	99.7	114.7	129.7	144.7	174.7	189.7	204.7	219.7	234.7	264.7	279.7	294.7	309.7	324.7	354.7		
0.024	0.086	0.088	0.074	-----	0.054	0.050	0.044	0.044	0.040	0.040	0.042	0.042	0.044	0.056	0.056	0.066	0.074	0.080	0.100	0.088		
0.048	0.078	0.084	0.072	-----	0.054	0.050	0.044	0.042	0.040	0.032	0.032	0.034	0.032	0.036	0.048	0.054	0.064	0.070	0.076	0.082		
0.071	0.068	0.072	0.060	0.050	0.050	0.046	0.040	0.040	0.034	0.024	0.024	0.024	0.026	0.028	0.038	0.042	0.052	0.058	0.064	0.072		
0.095	0.066	0.068	0.060	0.048	0.042	0.040	0.034	0.030	0.028	0.020	0.020	0.020	0.020	0.022	0.026	0.032	0.044	0.048	0.056	-----		
0.119	0.060	0.068	-----	0.048	0.042	0.036	0.032	0.028	0.016	0.014	0.016	0.016	0.016	0.016	0.026	0.034	0.044	0.048	0.052	-----		
0.143	0.056	0.062	-----	0.044	0.034	0.030	0.026	0.022	0.016	0.014	0.014	0.014	0.012	0.016	0.026	0.034	0.042	0.048	0.052	0.066		
0.167	0.052	0.060	0.050	0.040	0.032	0.026	0.024	0.020	0.016	0.012	0.012	0.012	0.012	0.012	0.022	0.028	0.036	0.040	0.046	0.052		
0.190	0.052	0.056	0.044	0.034	0.026	0.022	0.016	0.016	0.012	0.010	0.010	0.010	0.008	0.012	0.008	0.012	0.024	0.020	0.026	0.040		
0.214	0.046	0.052	0.042	0.032	0.022	0.018	0.016	0.008	0.012	0.010	0.002	0.002	0.004	0.002	0.006	0.006	0.020	0.020	0.024	0.032		
0.238	0.042	0.042	0.030	0.020	0.012	0.008	0.006	0.004	0.004	0.002	0.002	0.002	0.002	0.002	0.006	0.010	0.020	0.018	0.016	0.020		
0.262	0.034	0.036	0.024	0.016	0.010	0.006	0.004	0.002	0.002	0.002	0.000	0.000	0.000	0.000	0.008	0.002	0.016	0.008	0.012	0.020		
0.285	0.026	0.028	0.016	0.012	0.008	0.002	0.002	0.002	0.002	0.002	0.000	0.000	0.000	0.000	0.002	0.002	0.008	0.004	0.004	0.008		
0.333	0.020	0.022	0.008	0.000	0.002	0.006	0.008	0.008	0.008	0.006	0.006	0.004	0.004	0.006	0.006	0.004	0.008	0.008	0.008	0.012		
0.381	0.012	0.020	0.004	-----	0.002	0.008	0.010	0.010	0.012	0.012	0.012	0.012	0.014	0.012	0.012	0.004	0.008	0.012	0.012	0.020		
0.428	0.010	0.012	0.000	0.008	0.012	0.012	0.012	0.014	0.012	0.014	0.012	0.012	0.014	0.012	0.012	0.008	0.000	0.004	0.004	0.008		
0.476	0.004	0.002	0.014	0.018	0.024	0.024	0.024	0.024	0.024	0.024	0.022	0.022	0.024	0.026	0.024	0.020	0.010	0.014	0.014	0.004		
0.523	0.004	0.000	0.014	0.018	0.024	0.024	0.024	0.024	0.024	0.020	0.015	0.020	0.020	0.024	0.014	0.012	0.000	0.008	0.014	0.006		
0.571	0.014	0.012	0.024	0.028	0.030	0.034	0.032	0.032	0.028	0.030	0.026	0.026	0.032	0.034	0.024	0.022	0.000	0.018	0.036	0.012		
0.618	0.026	0.022	0.036	0.040	0.042	0.040	0.038	0.036	0.036	0.036	0.034	0.036	0.036	0.034	0.042	0.042	0.032	0.036	0.036	0.024		
0.666	0.032	0.030	0.044	0.044	0.042	0.040	0.038	0.038	0.040	0.040	0.038	0.038	0.036	0.034	0.042	0.042	0.036	0.032	0.032	0.024		
0.714	0.040	0.036	0.050	0.050	0.046	0.046	0.044	0.044	0.044	0.040	0.038	0.038	0.042	0.044	0.044	0.044	0.044	0.044	0.050	0.044		
0.761	0.046	0.044	0.054	0.056	0.048	0.046	0.046	0.046	0.040	0.036	0.036	0.036	0.040	0.044	0.040	0.044	0.044	0.050	0.052	0.050		
0.785	0.046	0.044	0.056	0.058	0.048	0.046	0.046	0.046	0.040	0.036	0.030	0.028	0.032	0.038	0.044	0.046	0.040	0.048	0.048	0.044		
0.809	0.046	0.044	0.050	0.048	0.042	0.046	0.038	0.036	0.034	0.032	0.030	0.028	0.032	0.040	0.044	0.046	0.040	0.048	0.048	0.046		
0.832	0.046	0.048	0.056	0.056	0.054	0.048	0.048	0.046	0.038	0.032	0.030	0.028	0.036	0.040	0.044	0.046	0.044	0.052	0.052	0.052		
0.856	0.050	0.052	0.060	0.058	0.054	0.050	0.048	0.046	0.038	0.032	0.030	0.028	0.032	0.038	0.044	0.046	0.042	0.052	0.052	0.052		
0.880	0.048	0.052	0.056	0.056	0.050	0.050	0.046	0.044	0.038	0.030	0.028	0.026	0.032	0.038	0.044	0.046	0.042	0.052	0.052	0.052		
0.904	0.046	0.048	0.056	0.056	0.048	0.048	0.046	0.038	0.026	0.026	0.026	0.026	0.028	0.036	0.042	0.046	0.042	0.050	0.050	0.052		
0.928	0.044	0.046	0.050	0.048	0.036	0.038	0.038	0.026	0.018	0.018	0.018	0.020	0.024	0.032	0.042	0.046	0.040	0.050	0.052	0.052		
0.951	0.048	0.046	0.048	0.048	0.040	0.038	0.028	0.026	0.020	0.022	0.020	0.022	0.028	0.032	0.046	0.048	0.044	0.054	0.052	0.048		
0.975	0.048	0.046	0.048	0.044	0.044	0.042	0.038	0.028	0.020	0.018	0.020	0.022	0.028	0.032	0.050	0.050	0.044	0.052	0.056	0.048		
0.999	0.099	0.100	0.100	0.104	0.105	0.107	0.088	0.080	0.080	0.088	0.088	0.088	0.088	0.088	0.107	0.105	0.096	0.099	0.100	0.088		
1.000	0.099	0.116	0.119	0.120	0.125	0.129	0.124	0.127	0.126	0.117	0.117	0.118	0.119	0.124	0.123	0.117	0.096	0.117	0.122	0.092		
																						NACA

NACA

TABLE I.- PRESSURE COEFFICIENT DATA FOR PARABOLIC BODY  
OF REVOLUTION (RM-10) MOUNTED ON STRAIGHT STING

NO TRANSITION STRIPS - Continued

(e)  $\alpha = 4.00$

Station, x/L	Radial angle, $\phi$ , deg															
	11	26	41	56	71	86	101	116	131	146	161	176	191	206	221	236
0.024	0.096	0.092	0.080	-----	0.060	0.054	0.046	0.040	0.038	0.032	0.034	0.038	0.036	0.034	0.040	0.046
0.048	0.090	0.090	0.076	-----	0.056	0.052	0.044	0.036	0.034	0.032	0.030	0.024	0.028	0.026	0.026	0.028
0.071	0.078	0.080	0.068	0.064	0.050	0.048	0.040	0.034	0.034	0.028	0.028	0.020	0.020	0.018	0.018	0.022
0.095	0.074	0.076	0.064	0.060	0.046	0.042	0.036	0.026	0.026	0.020	0.022	0.020	0.020	0.016	0.014	0.016
0.119	0.070	0.070	0.060	0.056	0.040	0.032	0.024	0.016	0.016	0.012	0.012	0.012	0.012	0.010	0.008	0.010
0.143	0.066	0.070	0.060	0.056	0.040	0.032	0.022	0.012	0.014	0.012	0.012	0.012	0.010	0.008	0.004	0.010
0.167	0.062	0.066	0.054	0.052	0.036	0.030	0.022	0.014	0.014	0.010	0.008	0.008	0.008	0.004	0.004	0.008
0.190	0.062	0.060	0.048	0.044	0.028	0.020	0.012	0.006	0.006	0.008	0.008	0.008	0.008	0.008	0.006	0.006
0.214	0.056	0.056	0.046	0.044	0.028	0.020	0.012	0.006	0.006	0.008	0.008	0.008	0.008	0.008	0.006	0.006
0.238	0.048	0.048	0.034	0.030	0.016	0.008	0.006	0.006	0.006	0.006	0.006	0.006	0.006	0.006	0.006	0.006
0.262	0.042	0.042	0.028	0.028	0.012	0.006	0.006	0.006	0.006	0.006	0.006	0.006	0.006	0.006	0.006	0.006
0.285	0.032	0.032	0.020	0.020	0.008	0.004	0.004	0.004	0.004	0.004	0.004	0.004	0.004	0.004	0.004	0.004
0.333	0.026	0.024	0.012	0.012	0.006	0.006	0.006	0.006	0.006	0.006	0.006	0.006	0.006	0.006	0.006	0.006
0.381	0.018	0.018	0.006	0.006	0.006	0.006	0.006	0.006	0.006	0.006	0.006	0.006	0.006	0.006	0.006	0.006
0.428	0.016	0.012	0.006	0.006	0.006	0.006	0.006	0.006	0.006	0.006	0.006	0.006	0.006	0.006	0.006	0.006
0.476	0.002	0.002	0.002	0.002	0.002	0.002	0.002	0.002	0.002	0.002	0.002	0.002	0.002	0.002	0.002	0.002
0.523	0.002	0.002	0.002	0.002	0.002	0.002	0.002	0.002	0.002	0.002	0.002	0.002	0.002	0.002	0.002	0.002
0.571	0.010	0.012	0.022	0.020	0.030	0.036	0.036	0.036	0.036	0.032	0.032	0.032	0.032	0.032	0.032	0.032
0.618	0.022	0.022	0.036	0.032	0.044	0.048	0.048	0.046	0.046	0.040	0.038	0.032	0.032	0.032	0.032	0.032
0.666	0.030	0.030	0.044	0.038	0.054	0.054	0.054	0.054	0.054	0.044	0.040	0.032	0.032	0.032	0.032	0.032
0.714	0.038	0.038	0.052	0.046	0.068	0.068	0.068	0.068	0.068	0.058	0.054	0.046	0.046	0.046	0.046	0.046
0.761	0.046	0.046	0.068	0.060	0.084	0.084	0.084	0.084	0.084	0.074	0.070	0.062	0.062	0.062	0.062	0.062
0.809	0.046	0.048	0.072	0.064	0.096	0.096	0.096	0.096	0.096	0.086	0.082	0.074	0.074	0.074	0.074	0.074
0.856	0.050	0.054	0.080	0.072	0.104	0.104	0.104	0.104	0.104	0.094	0.090	0.082	0.082	0.082	0.082	0.082
0.880	0.050	0.056	0.084	0.076	0.108	0.108	0.108	0.108	0.108	0.098	0.094	0.086	0.086	0.086	0.086	0.086
0.904	0.048	0.052	0.088	0.080	0.112	0.112	0.112	0.112	0.112	0.102	0.098	0.090	0.090	0.090	0.090	0.090
0.928	0.048	0.052	0.092	0.084	0.116	0.116	0.116	0.116	0.116	0.106	0.102	0.094	0.094	0.094	0.094	0.094
0.951	0.050	0.052	0.096	0.088	0.120	0.120	0.120	0.120	0.120	0.110	0.106	0.098	0.098	0.098	0.098	0.098
0.975	0.050	0.052	0.096	0.088	0.120	0.120	0.120	0.120	0.120	0.110	0.106	0.098	0.098	0.098	0.098	0.098
0.999	0.050	0.052	0.096	0.088	0.120	0.120	0.120	0.120	0.120	0.110	0.106	0.098	0.098	0.098	0.098	0.098
1.000	0.050	0.052	0.096	0.088	0.120	0.120	0.120	0.120	0.120	0.110	0.106	0.098	0.098	0.098	0.098	0.098

NACA

TABLE I.- PRESSURE COEFFICIENT DATA FOR PARABOLIC BODY OF REVOLUTION (RM-10) MOUNTED ON STRAIGHT STING

NO TRANSITION STRIPS - Continued

$$(f) \quad \alpha = 6.05$$

Station, x/L	Radial angle, $\phi$ , deg																			
	12.3	27.3	42.3	57.3	87.3	102.3	117.3	132.3	147.3	177.3	192.3	207.3	222.3	237.3	267.3	282.3	297.3	312.3	327.3	357.3
0.024	0.117	0.109	0.088	-----	0.042	0.026	0.024	0.022	0.020	0.024	0.020	0.024	0.026	0.028	0.042	0.093	0.078	0.097	0.115	0.127
0.048	0.109	0.105	0.088	-----	0.040	0.026	0.022	0.020	0.018	0.012	0.010	0.016	0.008	0.012	0.026	0.042	0.062	0.080	0.096	0.121
0.071	0.099	0.093	0.078	0.060	0.034	0.022	0.020	0.016	0.014	0.008	0.006	0.010	0.006	0.008	0.028	0.042	0.064	0.082	0.096	0.109
0.095	0.094	0.089	0.076	0.056	0.026	0.014	0.012	0.008	0.008	0.008	0.008	0.008	0.006	0.008	0.020	0.030	0.054	0.074	0.088	0.109
0.119	0.088	0.087	-----	0.04	0.024	0.006	0.006	0.002	0.004	0.004	0.004	0.004	0	0	0.008	0.020	0.042	0.060	0.076	-----
0.143	0.084	0.081	-----	0.048	0.014	0.004	0.002	0	0.002	0.002	0.002	0	0	0.002	0.008	0.020	0.040	0.058	0.074	-----
0.167	0.080	0.077	0.064	0.044	0.010	0.002	0	0.004	0	0	0.002	0	0.004	0.004	0.004	0.018	0.040	0.058	0.074	0.097
0.190	0.078	0.069	0.056	0.036	0.006	0.004	0.004	0.004	0.004	0.004	0.004	0.002	0.004	0.004	0.004	0.012	0.032	0.046	0.064	0.086
0.214	0.074	0.069	0.054	0.034	0.002	0.008	0.006	0.008	0.004	0.004	0.006	0.002	0.008	0.008	0.012	0.004	0.012	0.028	0.044	0.070
0.238	0.064	0.057	0.042	0.024	0.006	0.014	0.012	0.008	0.012	0.006	0.008	0.008	0.012	0.016	0.012	0.010	0.010	0.026	0.040	0.064
0.262	0.056	0.051	0.036	0.018	0.012	0.018	0.016	0.018	0.010	0.008	0.010	0.012	0.016	0.016	0.010	0.004	0.010	0.024	0.036	0.050
0.285	0.048	0.041	0.028	0.012	0.014	0.020	0.016	0.018	0.010	0.010	0.010	0.010	0.014	0.016	0.010	0.004	0.010	0.028	0.040	0.050
0.333	0.042	0.034	0.024	0.002	0.024	0.030	0.024	0.026	0.022	0.012	0.010	0.014	0.018	0.020	0.016	0.012	0.002	0.016	0.028	0.050
0.381	0.032	0.024	0.012	0.004	0.030	0.034	0.028	0.028	0.024	0.008	0.010	0.020	0.024	0.028	0.026	0.020	0.010	0.008	0.020	0.040
0.428	0.024	0.018	0.004	0.012	0.032	0.034	0.030	0.032	0.030	0.012	0.018	0.026	0.034	0.032	0.032	0.026	0.016	0.004	0.012	0.032
0.476	0.010	0.002	0.012	0.024	0.044	0.044	0.038	0.042	0.040	0.024	0.026	0.034	0.038	0.046	0.046	0.042	0.028	0.012	0	0.016
0.523	0.010	0.004	0.012	0.024	0.046	0.052	0.042	0.042	0.042	0.016	0.018	0.022	0.038	0.040	0.034	0.030	0.022	0.010	0.006	0.010
0.571	0.006	0.012	0.024	0.038	0.056	0.058	0.050	0.042	0.040	0.008	0.028	0.026	0.042	0.042	0.046	0.042	0.030	0.022	0.000	0.002
0.618																				

TABLE I.- PRESSURE COEFFICIENT DATA FOR PARABOLIC BODY  
OF REVOLUTION (RM-10) MOUNTED ON STRAIGHT STING

NO TRANSITION STRIPS - Continued

(g)  $\alpha = 8.05$

Station, $x/L$	Radial angle, $\phi$ , deg													
	13	28	43	58	88	103	118	133	148	178	193	208	223	238
0.024	0.146	0.122	0.097	0.024	0.024	0.010	0.004	0.008	0.012	0.022	0.012	0.008	0.008	0.012
0.048	0.138	0.122	0.097	0.026	0.018	0.006	0.004	0.006	0.010	0.010	0.004	0.002	0.002	0.002
0.071	0.128	0.109	0.086	0.060	0.018	0.006	0.012	0.008	0.004	0.008	0.006	0.004	0.006	0.006
0.095	0.120	0.103	0.082	0.052	0.006	0.006	0.012	0.010	0.004	0.002	0.004	0.010	0.012	0.012
0.119	0.112	0.099	0.082	0.052	0.006	0.008	0.012	0.016	0.010	0.002	0.004	0.012	0.014	0.018
0.143	0.112	0.096	0.082	0.048	0.002	0.018	0.020	0.018	0.014	0.010	0.004	0.016	0.016	0.010
0.167	0.104	0.092	0.068	0.040	0.010	0.022	0.024	0.018	0.018	0.010	0.002	0.018	0.018	0.010
0.190	0.100	0.084	0.060	0.036	0.012	0.026	0.026	0.022	0.018	0.004	0.002	0.020	0.022	0.020
0.214	0.098	0.080	0.058	0.036	0.014	0.026	0.026	0.022	0.024	0.008	0.004	0.026	0.030	0.034
0.238	0.088	0.070	0.048	0.024	0.024	0.034	0.036	0.032	0.028	0.008	0.006	0.026	0.030	0.030
0.262	0.080	0.064	0.042	0.018	0.030	0.036	0.036	0.032	0.028	0.008	0.006	0.026	0.030	0.030
0.285	0.072	0.054	0.032	0.012	0.034	0.038	0.040	0.038	0.034	0.012	0.010	0.020	0.034	0.032
0.308	0.064	0.044	0.020	0.006	0.042	0.046	0.048	0.044	0.032	0.010	0.014	0.024	0.042	0.044
0.331	0.052	0.036	0.012	0.006	0.050	0.054	0.058	0.054	0.028	0.018	0.020	0.024	0.042	0.052
0.354	0.042	0.026	0.002	0.016	0.054	0.058	0.062	0.056	0.032	0.018	0.020	0.032	0.048	0.052
0.377	0.028	0.010	0.012	0.028	0.066	0.066	0.066	0.062	0.032	0.018	0.020	0.032	0.048	0.052
0.400	0.026	0.008	0.016	0.032	0.070	0.066	0.062	0.058	0.032	0.024	0.024	0.036	0.050	0.060
0.423	0.010	0.008	0.028	0.044	0.078	0.074	0.068	0.064	0.032	0.024	0.032	0.036	0.050	0.060
0.446	0.004	0.022	0.044	0.060	0.086	0.082	0.076	0.072	0.044	0.036	0.036	0.040	0.058	0.064
0.469	0.016	0.032	0.064	0.076	0.090	0.082	0.076	0.072	0.048	0.042	0.038	0.044	0.062	0.062
0.492	0.024	0.044	0.084	0.080	0.090	0.082	0.076	0.072	0.052	0.046	0.042	0.048	0.062	0.062
0.515	0.040	0.054	0.097	0.080	0.086	0.082	0.076	0.072	0.056	0.050	0.046	0.052	0.062	0.062
0.538	0.040	0.060	0.076	0.080	0.086	0.082	0.076	0.072	0.056	0.050	0.046	0.052	0.062	0.062
0.561	0.042	0.056	0.068	0.078	0.086	0.082	0.076	0.072	0.056	0.050	0.046	0.052	0.062	0.062
0.584	0.044	0.060	0.076	0.084	0.086	0.082	0.076	0.072	0.056	0.050	0.046	0.052	0.062	0.062
0.607	0.046	0.064	0.076	0.084	0.086	0.082	0.076	0.072	0.056	0.050	0.046	0.052	0.062	0.062
0.630	0.046	0.064	0.076	0.084	0.086	0.082	0.076	0.072	0.056	0.050	0.046	0.052	0.062	0.062
0.653	0.046	0.064	0.076	0.084	0.086	0.082	0.076	0.072	0.056	0.050	0.046	0.052	0.062	0.062
0.676	0.046	0.064	0.076	0.084	0.086	0.082	0.076	0.072	0.056	0.050	0.046	0.052	0.062	0.062
0.699	0.046	0.064	0.076	0.084	0.086	0.082	0.076	0.072	0.056	0.050	0.046	0.052	0.062	0.062
0.722	0.046	0.064	0.076	0.084	0.086	0.082	0.076	0.072	0.056	0.050	0.046	0.052	0.062	0.062
0.745	0.046	0.064	0.076	0.084	0.086	0.082	0.076	0.072	0.056	0.050	0.046	0.052	0.062	0.062
0.768	0.046	0.064	0.076	0.084	0.086	0.082	0.076	0.072	0.056	0.050	0.046	0.052	0.062	0.062
0.791	0.046	0.064	0.076	0.084	0.086	0.082	0.076	0.072	0.056	0.050	0.046	0.052	0.062	0.062
0.814	0.046	0.064	0.076	0.084	0.086	0.082	0.076	0.072	0.056	0.050	0.046	0.052	0.062	0.062
0.837	0.046	0.064	0.076	0.084	0.086	0.082	0.076	0.072	0.056	0.050	0.046	0.052	0.062	0.062
0.860	0.046	0.064	0.076	0.084	0.086	0.082	0.076	0.072	0.056	0.050	0.046	0.052	0.062	0.062
0.883	0.046	0.064	0.076	0.084	0.086	0.082	0.076	0.072	0.056	0.050	0.046	0.052	0.062	0.062
0.906	0.046	0.064	0.076	0.084	0.086	0.082	0.076	0.072	0.056	0.050	0.046	0.052	0.062	0.062
0.929	0.046	0.064	0.076	0.084	0.086	0.082	0.076	0.072	0.056	0.050	0.046	0.052	0.062	0.062
0.952	0.046	0.064	0.076	0.084	0.086	0.082	0.076	0.072	0.056	0.050	0.046	0.052	0.062	0.062
0.975	0.046	0.064	0.076	0.084	0.086	0.082	0.076	0.072	0.056	0.050	0.046	0.052	0.062	0.062
0.998	0.046	0.064	0.076	0.084	0.086	0.082	0.076	0.072	0.056	0.050	0.046	0.052	0.062	0.062
1.000	0.046	0.064	0.076	0.084	0.086	0.082	0.076	0.072	0.056	0.050	0.046	0.052	0.062	0.062

NACA

TABLE I.- PRESSURE COEFFICIENT DATA FOR PARABOLIC BODY  
OF REVOLUTION (RM-10) MOUNTED ON STRAIGHT STING

NO TRANSITION STRIPS - Continued

(h)  $\alpha = 10.05$

Station, x/L	Radial angle, $\phi$ , deg															
	13.4	28.4	43.4	58.4	73.4	88.4	103.4	118.4	133.4	148.4	163.4	178.4	193.4	208.4	223.4	238.4
0.024	0.172	0.144	0.107	0.066	0.026	0.006	-0.010	-0.014	-0.006	-0.004	0.002	0.016	0.002	-0.006	-0.008	-0.006
0.048	0.166	0.144	0.107	0.066	0.026	0.006	-0.014	-0.018	-0.012	-0.010	0.006	0	-0.012	-0.016	-0.016	-0.024
0.071	0.152	0.132	0.094	0.056	0.012	0.008	-0.022	-0.024	-0.016	-0.016	0.012	0.002	-0.014	-0.018	-0.022	-0.028
0.095	0.144	0.124	0.090	0.032	0.010	0.014	-0.030	-0.030	-0.024	-0.022	0.018	0.002	0.006	-0.022	-0.024	-0.028
0.119	0.138	0.124	0.090	0.032	0.012	0.018	-0.034	-0.034	-0.028	-0.024	0.020	0.002	0.012	-0.028	-0.032	-0.032
0.143	0.136	0.116	0.088	0.032	0.012	0.024	-0.044	-0.042	-0.036	-0.032	0.024	0.008	0.014	-0.035	-0.034	-0.038
0.167	0.124	0.112	0.078	0.038	0.004	0.034	-0.046	-0.042	-0.036	-0.036	0.024	0.008	0.010	-0.035	-0.036	-0.038
0.190	0.124	0.102	0.068	0.028	0.012	0.036	-0.046	-0.042	-0.036	-0.036	0.022	0.012	0.008	-0.035	-0.038	-0.038
0.214	0.120	0.102	0.068	0.030	0.012	0.040	-0.050	-0.046	-0.040	-0.038	0.016	0.008	0.010	-0.035	-0.040	-0.042
0.238	0.108	0.088	0.052	0.016	0.024	0.050	-0.058	-0.050	-0.046	-0.044	0.018	0.012	0.014	-0.042	-0.046	-0.048
0.262	0.102	0.080	0.046	0.008	0.030	0.052	-0.058	-0.054	-0.048	-0.044	0.020	0.014	0.018	-0.042	-0.048	-0.048
0.285	0.092	0.072	0.038	0.002	0.038	0.060	-0.062	-0.058	-0.052	-0.048	0.024	0.016	0.020	-0.040	-0.048	-0.048
0.309	0.084	0.062	0.028	0.006	0.044	0.064	-0.062	-0.058	-0.052	-0.048	0.024	0.016	0.020	-0.040	-0.048	-0.048
0.333	0.072	0.052	0.016	0.016	0.056	0.074	-0.070	-0.064	-0.062	-0.060	0.028	0.018	0.028	-0.048	-0.052	-0.052
0.357	0.060	0.038	0.004	0.026	0.062	0.074	-0.068	-0.070	-0.064	-0.060	0.024	0.024	0.034	-0.050	-0.056	-0.056
0.381	0.048	0.022	0.016	0.040	0.072	0.084	-0.078	-0.074	-0.072	-0.070	0.040	0.024	0.034	-0.054	-0.056	-0.056
0.405	0.038	0.016	0.030	0.060	0.088	0.098	-0.082	-0.074	-0.074	-0.070	0.046	0.030	0.048	-0.054	-0.056	-0.056
0.429	0.024	0.016	0.030	0.060	0.088	0.098	-0.090	-0.082	-0.088	-0.088	0.058	0.036	0.056	-0.082	-0.082	-0.082
0.453	0.008	0.008	0.016	0.074	0.095	0.098	-0.090	-0.082	-0.088	-0.088	0.068	0.040	0.056	-0.090	-0.092	-0.092
0.477	0.008	0.008	0.016	0.074	0.095	0.098	-0.090	-0.082	-0.088	-0.088	0.068	0.040	0.056	-0.090	-0.092	-0.092
0.501	0.008	0.008	0.016	0.074	0.095	0.098	-0.090	-0.082	-0.088	-0.088	0.068	0.040	0.056	-0.090	-0.092	-0.092
0.525	0.008	0.008	0.016	0.074	0.095	0.098	-0.090	-0.082	-0.088	-0.088	0.068	0.040	0.056	-0.090	-0.092	-0.092
0.549	0.008	0.008	0.016	0.074	0.095	0.098	-0.090	-0.082	-0.088	-0.088	0.068	0.040	0.056	-0.090	-0.092	-0.092
0.573	0.008	0.008	0.016	0.074	0.095	0.098	-0.090	-0.082	-0.088	-0.088	0.068	0.040	0.056	-0.090	-0.092	-0.092
0.597	0.008	0.008	0.016	0.074	0.095	0.098	-0.090	-0.082	-0.088	-0.088	0.068	0.040	0.056	-0.090	-0.092	-0.092
0.621	0.008	0.008	0.016	0.074	0.095	0.098	-0.090	-0.082	-0.088	-0.088	0.068	0.040	0.056	-0.090	-0.092	-0.092
0.645	0.008	0.008	0.016	0.074	0.095	0.098	-0.090	-0.082	-0.088	-0.088	0.068	0.040	0.056	-0.090	-0.092	-0.092
0.669	0.008	0.008	0.016	0.074	0.095	0.098	-0.090	-0.082	-0.088	-0.088	0.068	0.040	0.056	-0.090	-0.092	-0.092
0.693	0.008	0.008	0.016	0.074	0.095	0.098	-0.090	-0.082	-0.088	-0.088	0.068	0.040	0.056	-0.090	-0.092	-0.092
0.717	0.008	0.008	0.016	0.074	0.095	0.098	-0.090	-0.082	-0.088	-0.088	0.068	0.040	0.056	-0.090	-0.092	-0.092
0.741	0.008	0.008	0.016	0.074	0.095	0.098	-0.090	-0.082	-0.088	-0.088	0.068	0.040	0.056	-0.090	-0.092	-0.092
0.765	0.008	0.008	0.016	0.074	0.095	0.098	-0.090	-0.082	-0.088	-0.088	0.068	0.040	0.056	-0.090	-0.092	-0.092
0.789	0.008	0.008	0.016	0.074	0.095	0.098	-0.090	-0.082	-0.088	-0.088	0.068	0.040	0.056	-0.090	-0.092	-0.092
0.813	0.008	0.008	0.016	0.074	0.095	0.098	-0.090	-0.082	-0.088	-0.088	0.068	0.040	0.056	-0.090	-0.092	-0.092
0.837	0.008	0.008	0.016	0.074	0.095	0.098	-0.090	-0.082	-0.088	-0.088	0.068	0.040	0.056	-0.090	-0.092	-0.092
0.861	0.008	0.008	0.016	0.074	0.095	0.098	-0.090	-0.082	-0.088	-0.088	0.068	0.040	0.056	-0.090	-0.092	-0.092
0.885	0.008	0.008	0.016	0.074	0.095	0.098	-0.090	-0.082	-0.088	-0.088	0.068	0.040	0.056	-0.090	-0.092	-0.092
0.909	0.008	0.008	0.016	0.074	0.095	0.098	-0.090	-0.082	-0.088	-0.088	0.068	0.040	0.056	-0.090	-0.092	-0.092
0.933	0.008	0.008	0.016	0.074	0.095	0.098	-0.090	-0.082	-0.088	-0.088	0.068	0.040	0.056	-0.090	-0.092	-0.092
0.957	0.008	0.008	0.016	0.074	0.095	0.098	-0.090	-0.082	-0.088	-0.088	0.068	0.040	0.056	-0.090	-0.092	-0.092
0.981	0.008	0.008	0.016	0.074	0.095	0.098	-0.090	-0.082	-0.088	-0.088	0.068	0.040	0.056	-0.090	-0.092	-0.092
1.000	0.008	0.008	0.016	0.074	0.095	0.098	-0.090	-0.082	-0.088	-0.088	0.068	0.040	0.056	-0.090	-0.092	-0.092

NACA

TABLE I.- PRESSURE COEFFICIENT DATA FOR PARABOLIC BODY  
OF REVOLUTION (RM-10) MOUNTED ON STRAIGHT STING

NO TRANSITION STRIPS - Continued

(1)  $\alpha = 12.05$

Station, x/L	Radial angle, $\phi$ , deg																			
	13.7	28.7	43.7	58.7	88.7	103.7	118.7	133.7	148.7	178.7	193.7	208.7	223.7	238.7	268.7	283.7	298.7	313.7	328.7	358.7
0.024	0.197	0.164	0.115	-----	-0.022	-0.008	-0.036	-0.028	-0.026	0.004	-0.014	-0.024	-0.028	-0.034	-0.028	-0.008	0.058	0.117	0.164	0.219
0.048	0.191	0.164	0.119	-----	-0.026	-0.046	-0.038	-0.032	-0.028	-0.008	-0.034	-0.038	-0.036	-0.042	-0.040	-0.008	0.042	0.097	0.150	0.209
0.071	0.181	0.150	0.103	0.048	-0.036	-0.052	-0.040	-0.034	-0.036	-0.010	-0.040	-0.040	-0.042	-0.048	-0.034	-0.002	0.054	0.109	0.158	0.193
0.095	0.173	0.146	0.103	0.048	-0.038	-0.056	-0.040	-0.040	-0.040	0.004	0.022	0.048	0.044	0.050	0.050	0.016	0.034	0.090	0.140	0.185
0.119	0.165	0.142	-----	0.046	-0.050	-0.064	-0.050	-0.046	-0.044	0.006	0.028	0.050	0.050	0.052	0.062	0.032	0.022	0.078	0.128	0.177
0.143	0.157	0.132	-----	0.036	-0.058	-0.072	-0.058	-0.054	-0.050	0.016	0.036	0.056	0.052	0.056	0.062	0.036	0.014	0.070	0.120	0.161
0.167	0.151	0.126	0.084	0.032	-0.064	-0.074	-0.058	-0.058	-0.054	0.016	0.032	0.058	0.054	0.058	0.062	0.040	0.006	0.060	0.110	0.157
0.190	0.149	0.120	0.082	0.026	-0.064	-0.074	-0.062	-0.058	-0.054	0.012	0.032	0.062	-0.058	0.060	-----	-----	-----	-----	-----	0.153
0.214	0.145	0.118	0.076	0.020	-0.068	-0.078	-0.066	-0.064	-0.066	0.018	0.032	0.066	-0.064	0.066	-0.078	0.056	0.012	0.040	0.092	0.141
0.238	0.133	0.102	0.064	0.008	-0.078	-0.080	-0.070	-0.066	-0.068	0.022	0.040	0.066	0.064	0.066	-0.076	0.058	0.010	0.040	0.090	0.135
0.262	0.127	0.098	0.056	0.004	-0.084	-0.080	-0.074	-0.070	-0.076	0.022	0.036	0.070	0.062	0.064	0.074	0.058	0.018	0.036	0.084	0.129
0.285	0.117	0.086	0.044	0.008	-0.088	-0.080	-0.074	-0.070	-0.080	0.022	0.036	0.086	0.074	0.076	0.084	0.066	0.024	0.028	0.076	0.117
0.309	0.109	0.078	0.036	0.012	-0.088	-0.080	-0.078	-0.082	-0.090	0.032	0.052	0.086	0.080	0.082	0.090	0.086	0.052	0.002	0.048	0.088
0.333	0.096	0.062	0.020	0.008	-0.096	-0.084	-0.078	-0.082	-0.090	0.032	0.052	0.090	0.086	0.084	0.090	0.097	0.068	0.020	0.028	0.074
0.357	0.078	0.050	0.010	0.008	-0.096	-0.084	-0.078	-0.082	-0.090	0.032	0.052	0.090	0.086	0.084	0.090	0.097	0.068	0.020	0.028	0.074
0.381	0.064	0.034	0.008	0.008	-0.094	-0.084	-0.078	-0.082	-0.090	0.040	0.064	0.098	0.086	0.084	0.090	0.097	0.068	0.020	0.028	0.074
0.405	0.048	0.028	0.016	0.008	-0.101	-0.090	-0.086	-0.084	-0.090	0.040	0.064	0.098	0.086	0.084	0.090	0.097	0.068	0.020	0.028	0.074
0.429	0.038	0.028	0.016	0.008	-0.101	-0.090	-0.086	-0.084	-0.090	0.040	0.064	0.098	0.086	0.084	0.090	0.097	0.068	0.020	0.028	0.074
0.453	0.028	0.010	0.008	0.008	-0.101	-0.090	-0.086	-0.084	-0.090	0.040	0.064	0.098	0.086	0.084	0.090	0.097	0.068	0.020	0.028	0.074
0.477	0.028	0.010	0.008	0.008	-0.101	-0.090	-0.086	-0.084	-0.090	0.040	0.064	0.098	0.086	0.084	0.090	0.097	0.068	0.020	0.028	0.074
0.501	0.022	0.010	0.008	0.008	-0.101	-0.090	-0.086	-0.084	-0.090	0.040	0.064	0.098	0.086	0.084	0.090	0.097	0.068	0.020	0.028	0.074
0.525	0.022	0.010	0.008	0.008	-0.101	-0.090	-0.086	-0.084	-0.090	0.040	0.064	0.098	0.086	0.084	0.090	0.097	0.068	0.020	0.028	0.074
0.549	0.022	0.010	0.008	0.008	-0.101	-0.090	-0.086	-0.084	-0.090	0.040	0.064	0.098	0.086	0.084	0.090	0.097	0.068	0.020	0.028	0.074
0.573	0.022	0.010	0.008	0.008	-0.101	-0.090	-0.086	-0.084	-0.090	0.040	0.064	0.098	0.086	0.084	0.090	0.097	0.068	0.020	0.028	0.074
0.597	0.022	0.010	0.008	0.008	-0.101	-0.090	-0.086	-0.084	-0.090	0.040	0.064	0.098	0.086	0.084	0.090	0.097	0.068	0.020	0.028	0.074
0.621	0.022	0.010	0.008	0.008	-0.101	-0.090	-0.086	-0.084	-0.090	0.040	0.064	0.098	0.086	0.084	0.090	0.097	0.068	0.020	0.028	0.074
0.645	0.022	0.010	0.008	0.008	-0.101	-0.090	-0.086	-0.084	-0.090	0.040	0.064	0.098	0.086	0.084	0.090	0.097	0.068	0.020	0.028	0.074
0.669	0.022	0.010	0.008	0.008	-0.101	-0.090	-0.086	-0.084	-0.090	0.040	0.064	0.098	0.086	0.084	0.090	0.097	0.068	0.020	0.028	0.074
0.693	0.022	0.010	0.008	0.008	-0.101	-0.090	-0.086	-0.084	-0.090	0.040	0.064	0.098	0.086	0.084	0.090	0.097	0.068	0.020	0.028	0.074
0.717	0.022	0.010	0.008	0.008	-0.101	-0.090	-0.086	-0.084	-0.090	0.040	0.064	0.098	0.086	0.084	0.090	0.097	0.068	0.020	0.028	0.074
0.741	0.022	0.010	0.008	0.008	-0.101	-0.090	-0.086	-0.084	-0.090	0.040	0.064	0.098	0.086	0.084	0.090	0.097	0.068	0.020	0.028	0.074
0.765	0.022	0.010	0.008	0.008	-0.101	-0.090	-0.086	-0.084	-0.090	0.040	0.064	0.098	0.086	0.084	0.090	0.097	0.068	0.020	0.028	0.074
0.789	0.022	0.010	0.008	0.008	-0.101	-0.090	-0.086	-0.084	-0.090	0.040	0.064	0.098	0.086	0.084	0.090	0.097	0.068	0.020	0.028	0.074
0.813	0.022	0.010	0.008	0.008	-0.101	-0.090	-0.086	-0.084	-0.090	0.040	0.064	0.098	0.086	0.084	0.090	0.097	0.068	0.020	0.028	0.074
0.837	0.022	0.010	0.008	0.008	-0.101	-0.090	-0.086	-0.084	-0.090	0.040	0.064	0.098	0.086	0.084	0.090	0.097	0.068	0.020	0.028	0.074
0.861	0.022	0.010	0.008	0.008	-0.101	-0.090	-0.086	-0.084	-0.090	0.040	0.064	0.098	0.086	0.084	0.090	0.097	0.068	0.020	0.028	0.074
0.885	0.022	0.010	0.008	0.008	-0.101	-0.090	-0.086	-0.084	-0.090	0.040	0.064	0.098	0.086	0.084	0.090	0.097	0.068	0.020	0.028	0.074
0.909	0.022	0.010	0.008	0.008	-0.101	-0.090	-0.086	-0.084	-0.090	0.040	0.064	0.098	0.086	0.084	0.090	0.097	0.068	0.020	0.028	0.074
0.933	0.022	0.010	0.008	0.008	-0.101	-0.090	-0.086	-0.084	-0.090	0.040	0.064	0.098	0.086	0.084	0.090	0.097	0.068	0.020	0.028	0.074
0.957	0.022	0.010	0.008	0.008	-0.101	-0.090	-0.086	-0.084	-0.090	0.040	0.064	0.098	0.086	0.084	0.090	0.097	0.068	0.020	0.028	0.074
0.981	0.022	0.010	0.008	0.008	-0.101	-0.090	-0.086	-0.084	-0.090	0.040	0.064	0.098	0.086	0.084	0.090	0.097	0.068	0.020	0.028	0.074
0.999	0.022	0.010	0.008	0.008	-0.101	-0.090	-0.086	-0.084	-0.090	0.040	0.064	0.098	0.086	0.084	0.090	0.097	0.068	0.020	0.028	0.074
1.000	0.022	0.010	0.008	0.008	-0.101	-0.090	-0.086	-0.084	-0.090	0.040	0.064	0.098	0.086	0.084	0.090	0.097	0.068	0.020	0.028	0.074

NACA



TABLE I.- PRESSURE COEFFICIENT DATA FOR PARABOLIC BODY  
OF REVOLUTION (RM-10) MOUNTED ON STRAIGHT STING

NO TRANSITION STRIPS - Continued

(j)  $\alpha = 14.05$

Station, x/L	Radial angle, $\phi$ , deg														
	13.9	28.9	43.9	58.9	88.9	103.9	118.9	133.9	148.9	178.9	193.9	208.9	223.9	238.9	268.9
0.024	0.230	0.188	0.122	-----	-0.046	-0.070	-0.058	-0.050	-0.050	-0.004	-0.036	-0.050	-0.050	-0.056	-0.054
0.048	0.224	0.194	0.130	-----	-0.030	-0.070	-0.058	-0.052	-0.048	-0.014	-0.034	-0.060	-0.054	-0.060	-0.066
0.071	0.214	0.182	0.114	0.048	-0.054	-0.070	-0.058	-0.050	-0.056	-0.008	-0.060	-0.068	-0.058	-0.064	-0.066
0.095	0.210	0.178	0.118	0.048	-0.064	-0.076	-0.062	-0.058	-0.056	0	-0.032	-0.062	-0.060	-0.062	-0.070
0.119	0.196	0.170	-----	0.042	-0.072	-0.086	-0.068	-0.064	-0.068	-0.010	-0.032	-0.072	-0.066	-0.068	-0.082
0.143	0.186	0.158	-----	0.028	-0.082	-0.090	-0.076	-0.074	-0.076	-0.016	-0.050	-0.084	-0.070	-0.076	-0.084
0.167	0.176	0.150	0.092	0.018	-0.086	-0.088	-0.076	-0.076	-0.084	-0.018	-0.060	-0.086	-0.074	-0.080	-0.086
0.190	0.171	0.146	0.084	0.012	-0.090	-0.088	-0.078	-0.080	-0.088	-0.022	-0.062	-0.092	-0.078	-0.080	-0.092
0.214	0.161	0.126	0.064	0.004	-0.094	-0.092	-0.082	-0.080	-0.096	-0.030	-0.064	-0.098	-0.082	-0.084	-----
0.238	0.155	0.122	0.058	-----	-0.102	-0.096	-0.090	-0.086	-0.100	-0.030	-0.072	-0.098	-0.086	-0.088	-0.108
0.262	0.145	0.110	0.032	0.014	-0.108	-0.097	-0.090	-0.090	-0.104	-0.030	-0.064	-0.098	-0.084	-0.086	-0.102
0.285	0.135	0.100	0.040	0.024	-0.110	-0.096	-0.094	-0.090	-0.104	-0.030	-0.076	-0.102	-0.088	-0.096	-0.108
0.333	0.119	0.086	0.022	0.040	-0.114	-0.101	-0.100	-0.100	-0.116	-0.038	-0.078	-0.106	-0.088	-0.096	-0.106
0.381	0.103	0.068	0.006	-----	-0.106	-0.099	-0.098	-0.086	-0.112	-0.038	-0.088	-0.106	-0.088	-0.100	-0.110
0.428	0.084	0.050	0.010	0.064	-0.106	-0.103	-0.110	-0.102	-0.124	-0.050	-0.101	-0.126	-0.106	-0.112	-0.114
0.476	0.080	0.042	0.016	0.068	-0.102	-0.103	-0.110	-0.102	-0.132	-0.056	-0.109	-0.130	-0.108	-0.108	-0.102
0.523	0.062	0.030	0.028	0.080	-0.108	-0.111	-0.110	-0.106	-0.134	-0.060	-0.115	-0.132	-0.116	-0.108	-0.102
0.571	0.040	0.004	0.022	0.100	-0.114	-0.117	-0.114	-0.118	-0.136	-0.072	-0.123	-0.134	-0.130	-0.116	-0.116
0.618	0.026	0.004	-----	0.108	-0.118	-0.123	-0.122	-0.118	-0.132	-0.080	-0.121	-0.130	-0.130	-0.116	-0.110
0.666	0.014	0.020	0.078	0.116	-0.110	-0.115	-0.114	-0.108	-0.116	-0.086	-0.121	-0.126	-0.130	-0.114	-----
0.714	0	0.026	0.080	0.112	-0.106	-0.111	-0.114	-0.110	-0.112	-0.078	-0.111	-0.114	-0.114	-0.100	-0.086
0.761	0.004	0.030	0.082	0.112	-0.096	-0.104	-0.107	-0.108	-0.110	-0.078	-0.105	-0.108	-0.108	-0.096	-0.086
0.809	0.002	0.038	0.080	0.116	-0.096	-0.099	-0.098	-0.096	-0.102	-0.074	-0.103	-0.106	-0.102	-0.094	-0.094
0.832	0.002	0.044	0.090	0.116	-0.098	-0.103	-0.100	-0.104	-0.108	-0.074	-0.101	-0.104	-0.098	-0.094	-0.094
0.856	0.022	0.054	0.094	0.112	-0.094	-0.096	-0.094	-0.100	-0.112	-0.082	-0.105	-0.102	-0.094	-0.090	-0.090
0.880	0.028	0.060	0.094	0.084	-0.086	-0.092	-0.090	-0.092	-0.106	-0.078	-0.096	-0.098	-0.090	-0.084	-0.086
0.904	0.028	0.058	-----	0.084	-0.078	-0.084	-0.084	-0.084	-0.100	-0.078	-0.096	-0.096	-0.086	-0.084	-0.084
0.928	0.028	0.052	0.074	0.076	-0.058	-0.070	-0.072	-0.074	-0.088	-0.070	-0.088	-0.086	-0.082	-0.076	-0.078
0.951	0.030	0.052	0.072	0.072	-0.058	-0.064	-0.074	-0.082	-0.094	-0.080	-0.092	-0.090	-0.084	-0.084	-0.078
0.975	0.032	0.054	0.070	0.068	-0.056	-0.064	-0.074	-0.082	-0.088	-0.080	-0.092	-0.090	-0.082	-0.084	-0.082
0.999	0.084	0.102	-----	0.148	-0.131	-0.115	-0.114	-0.126	-0.136	-----	-----	-----	-----	-0.084	-0.082
1.000	0.174	0.186	0.190	0.194	-0.189	-0.194	-0.186	-0.178	-0.180	-0.175	-0.171	-0.172	-0.176	-0.176	-0.186

NACA

TABLE I.- PRESSURE COEFFICIENT DATA FOR PARABOLIC BODY  
OF REVOLUTION (RM-10) MOUNTED ON STRAIGHT STING

NO TRANSITION STRIPS - Concluded

( $k$ )  $\alpha = 16.10$

Station, x/L	Radial angle, $\phi$ , deg														
	14	29	44	59	74	89	104	119	134	149	164	179	194	209	224
0.024	0.267	0.214	0.135	-----	-0.036	-0.070	-0.088	-0.074	-0.069	-0.068	-0.074	-0.014	-0.048	-0.070	-0.067
0.048	.267	.226	.145	-----	-.028	-.076	-.088	-.074	-.071	-.072	-.084	-.022	-.072	-.084	-.077
0.071	.253	.210	.131	0.048	-.040	-.082	-.092	-.078	-.073	-.076	-.078	-.018	-.072	-.084	-.083
0.095	.243	.198	.121	.036	-.052	-.097	-.099	-.086	-.089	-.084	-.094	-.018	-.060	-.088	-.093
0.119	.227	.190	-----	.028	-.058	-.109	-.103	-.082	-.093	-.099	-.103	-.026	-.080	-.093	-.092
0.143	.221	.182	-----	.024	-.064	-.117	-.107	-.098	-.101	-.110	-.113	-.030	-.096	-.110	-.100
0.167	.203	.172	.097	.040	-.076	-.121	-.107	-.102	-.105	-.110	-.115	-.030	-.088	-.116	-.105
0.190	.205	.164	.089	.006	-.076	-.121	-.107	-.100	-.103	-.112	-.111	-.030	-.088	-.116	-.105
0.214	.195	.158	.081	0	-.080	-.121	-.105	-.100	-.105	-.116	-.113	-.036	-.084	-.118	-.101
0.238	.189	.148	.073	.008	-.092	-.127	-.111	-.110	-.111	-.124	-.119	-.036	-.096	-.116	-.101
0.262	.185	.140	.065	-.016	-.096	-.133	-.111	-.110	-.109	-.124	-.119	-.040	-.096	-.116	-.105
0.285	.173	.126	.056	-.028	-.107	-.133	-.111	-.112	-.113	-.124	-.119	-.040	-.096	-.116	-.105
0.309	.161	.118	.040	-.040	-.115	-.129	-.111	-.114	-.115	-.132	-.127	-.046	-.103	-.126	-.109
0.333	.147	.104	.026	-.048	-.121	-.125	-.111	-.114	-.117	-.136	-.129	-.050	-.113	-.130	-.113
0.357	.131	.086	.012	-.064	-.131	-.125	-.113	-.118	-.113	-.136	-.135	-.062	-.121	-.132	-.117
0.381	.109	.070	-.004	-.078	-.143	-.131	-.127	-.130	-.127	-.148	-.147	-.072	-.129	-.142	-.131
0.405	.097	.054	-.020	-.092	-.151	-.133	-.129	-.132	-.127	-.148	-.143	-.072	-.129	-.146	-.133
0.429	.076	.038	-.032	-.108	-.157	-.133	-.131	-.134	-.123	-.142	-.141	-.078	-.143	-.154	-.145
0.453	.060	.020	-.056	-.124	-.157	-.135	-.135	-.138	-.137	-.152	-.151	-.090	-.149	-.154	-.157
0.477	.044	.002	-----	-.134	-.155	-.135	-.135	-.142	-.149	-.154	-.151	-.094	-.147	-.154	-.157
0.501	.026	-.014	-.083	-.136	-.139	-.125	-.125	-.124	-.133	-.142	-.139	-.086	-.129	-.134	-.139
0.525	.020	-.016	-.083	-.132	-.123	-.109	-.111	-.120	-.133	-.134	-.131	-.070	-.107	-.110	-.117
0.549	.018	-.020	-.087	-.124	-.115	-.105	-.105	-.112	-.127	-.134	-.133	-.074	-.107	-.110	-.113
0.573	.016	-.026	-.081	-.120	-.107	-.096	-.099	-.102	-.117	-.128	-.133	-.082	-.111	-.110	-.111
0.597	.012	-.030	-.085	-.112	-.109	-.101	-.103	-.110	-.133	-.132	-.133	-.086	-.111	-.108	-.105
0.621	.008	-.042	-.091	-.116	-.103	-.094	-.096	-.106	-.125	-.124	-.127	-.086	-.103	-.102	-.099
0.645	.004	-.046	-.091	-.112	-.103	-.094	-.096	-.100	-.113	-.112	-.113	-.080	-.096	-.094	-.091
0.669	.000	-.044	-.091	-.110	-.103	-.090	-.082	-.086	-.093	-.092	-.096	-.074	-.088	-.084	-.081
0.693	.000	-.042	-.091	-.110	-.099	-.078	-.080	-.082	-.091	-.092	-.092	-.080	-.088	-.084	-.077
0.717	.000	-.040	-.091	-.110	-.096	-.076	-.078	-.078	-.082	-.088	-.088	-.072	-.088	-.084	-.076
0.741	.000	-.038	-.093	-.108	-.092	-.074	-.076	-.076	-.081	-.088	-.088	-.072	-.088	-.084	-.076
0.765	.000	-.036	-.093	-.106	-.092	-.072	-.074	-.074	-.077	-.084	-.084	-.072	-.088	-.084	-.076
0.789	.000	-.034	-.093	-.104	-.090	-.070	-.072	-.072	-.075	-.082	-.082	-.072	-.088	-.084	-.076
0.813	.000	-.032	-.093	-.102	-.088	-.068	-.070	-.070	-.073	-.080	-.080	-.072	-.088	-.084	-.076
0.837	.000	-.030	-.093	-.100	-.086	-.066	-.068	-.066	-.069	-.076	-.076	-.072	-.088	-.084	-.076
0.861	.000	-.028	-.093	-.098	-.084	-.062	-.064	-.062	-.065	-.072	-.072	-.072	-.088	-.084	-.076
0.885	.000	-.026	-.093	-.096	-.080	-.060	-.062	-.060	-.063	-.070	-.070	-.072	-.088	-.084	-.076
0.909	.000	-.024	-.093	-.094	-.078	-.058	-.060	-.058	-.061	-.070	-.070	-.072	-.088	-.084	-.076
0.933	.000	-.022	-.093	-.092	-.076	-.056	-.058	-.056	-.059	-.070	-.070	-.072	-.088	-.084	-.076
0.957	.000	-.020	-.093	-.090	-.074	-.054	-.056	-.054	-.057	-.070	-.070	-.072	-.088	-.084	-.076
0.981	.000	-.018	-.093	-.088	-.072	-.052	-.054	-.052	-.055	-.070	-.070	-.072	-.088	-.084	-.076
1.000	.000	-.016	-.093	-.086	-.070	-.050	-.052	-.050	-.053	-.070	-.070	-.072	-.088	-.084	-.076

NACA

TABLE II.- PRESSURE COEFFICIENT DATA FOR PARABOLIC BODY

OF REVOLUTION (RM-10) MOUNTED ON BENT STRING

NO TRANSITION STRIPS

(a)  $\alpha = 14.00$ 

Station, x/L	Radial angle, $\phi$ , deg													
	42.7	57.7	72.7	87.7	132.7	147.7	162.7	177.7	222.7	237.7	252.7	267.7	312.7	327.7
0.024	0.125	0.054	-0.014	-0.056	-0.046	-0.048	-0.050	-0.016	-0.046	-0.054	-0.066	-0.062	0.123	0.189
0.048	.137	.064	.006	.054	.038	.040	.048	.004	.054	.060	.070	.070	.111	.175
0.071	.123	.048	.020	.066	.052	.054	.062	.008	.060	.066	.074	.076	.123	.187
0.095	.113	.040	.030	.074	.062	.058	.066	.008	.062	.066	.074	.078	.105	.167
0.119	.109	.032	.034	.080	.066	.068	.078	.014	.070	.074	.078	.086	.088	.155
0.143	.101	.028	.038	.086	.074	.078	.086	.020	.074	.078	.082	.088	.082	.147
0.167	.093	.022	.046	.090	.074	.078	.086	.016	.074	.078	.082	.088	.082	.143
0.190	.088	.020	.046	.088	.078	.082	.086	.016	.076	.078	.082	.086	.072	.133
0.214	.084	.012	.054	.096	.078	.084	.086	.016	.076	.078	.082	.086	.072	.133
0.238	.068	0	.066	.102	.082	.093	.090	.024	.078	.082	.082	.086	.052	.113
0.262	.060	.010	.072	.104	.082	.088	.088	.024	.078	.082	.082	.086	.048	.110
0.285	.052	.018	.078	.106	.082	.088	.088	.024	.082	.086	.086	.088	.036	.097
0.333	.034	.032	.090	.112	.088	.107	.102	.030	.086	.093	.094	.108	.026	.084
0.381	.024	.040	.096	.110	.092	.115	.108	.038	.086	.095	.097	.110	.010	.072
0.428	.012	.056	.110	.112	.095	.115	.108	.040	.090	.099	.100	.108	0	.058
0.476	.008	.074	.122	.118	.099	.121	.114	.052	.102	.109	.106	.112	.032	.040
0.523	.000	.099	.134	.112	.099	.121	.118	.060	.105	.109	.106	.108	.040	.014
0.571	.036	.099	.134	.112	.099	.121	.118	.060	.105	.109	.106	.108	.040	.014
0.618	.054	.113	.134	.114	.115	.131	.130	.076	.123	.115	.118	.114	.068	.016
0.666	.068	.121	.128	.110	.119	.131	.126	.076	.127	.107	.110	.108	.070	.018
0.714	.076	.117	.116	.104	.115	.107	.118	.044	.127	.107	.108	.102	.076	.032
0.761	.078	.115	.106	.096	.115	.119	.114	.076	.121	.105	.102	.102	.080	.034
0.785	.080	.113	.102	.096	.115	.119	.114	.076	.121	.105	.102	.102	.080	.034
0.809	.076	.105	.094	.088	.103	.107	.104	.072	.119	.103	.102	.108	.084	.040
0.832	.078	.105	.094	.088	.111	.115	.112	.084	.102	.103	.108	.108	.093	.048
0.856	.088	.101	.090	.086	.103	.107	.106	.084	.111	.103	.108	.108	.099	.060
0.880	.088	.097	.088	.086	.097	.101	.102	.080	.103	.103	.104	.108	.105	.068
0.904	.084	.086	.080	.078	.086	.090	.088	.076	.099	.099	.098	.102	.103	.072
0.928	.078	.080	.074	.070	.074	.080	.070	.062	.090	.095	.095	.096	.103	.072
0.951	.076	.072	.070	.066	.074	.080	.080	.074	.086	.090	.089	.086	.105	.076
0.975	.072	.072	.070	.066	.074	.080	.078	.076	.088	.090	.089	.092	.097	.076
0.999	.135	.153	.154	.142	.115	.123	.118	.114	.088	.090	.089	.092	.143	.117
1.000	.199	.201	.200	.198	.184	.189	.190	.190	.088	.090	.089	.092	.197	.201

NACA

TABLE II.- PRESSURE COEFFICIENT DATA FOR PARABOLIC BODY  
OF REVOLUTION (RM-10) MOUNTED ON BENT STRING

NO TRANSITION STRIPS - Continued

(b)  $\alpha = 16.00$

Station, x/L	Radial angle, $\phi$ , deg															
	43	58	73	88	133	148	163	178	223	238	253	268	313	328	343	358
0.024	0.130	0.044	-0.038	-0.096	-0.074	-0.074	-0.078	-0.036	-0.074	-0.078	-0.090	-0.103	0.130	0.213	0.270	0.294
0.048	.148	.062	-.022	-.092	-.064	-.066	-.074	-.016	-.082	-.082	-.092	-.109	.112	.197	.256	.287
0.071	.128	.040	-.042	-.109	-.080	-.082	-.088	-.024	-.090	-.086	-.100	-.115	.130	.207	.260	---
0.095	.122	.036	-.048	-.117	-.090	-.084	-.096	-.024	-.088	-.086	-.096	-.115	.110	.191	.244	---
.119	.116	.030	-.054	-.117	-.094	-.095	-.104	-.028	-.092	-.090	-.098	-.119	.102	.181	.232	.257
.143	.116	.032	-.052	-.117	-.098	-.103	-.112	-.028	-.098	-.095	-.100	-.125	.090	.171	.224	.247
.167	.106	.020	-.064	-.121	-.102	-.107	-.114	-.028	-.102	-.101	-.104	-.131	.086	.167	.220	.243
.190	.100	.020	-.062	-.125	-.098	-.115	-.116	-.034	-.102	-.099	-.100	-.123	.078	.155	.206	.231
.214	.092	.006	-.074	-.129	-.102	-.115	-.116	-.030	-.098	-.095	-.096	-.123	---	---	---	---
.238	.082	0	-.080	-.131	-.102	-.121	-.120	-.036	-.098	-.101	-.100	-.125	.056	.137	.186	.209
.262	.072	-.010	-.086	-.131	---	---	---	---	-.102	-.107	-.108	-.133	.052	.131	.182	.205
.285	.064	-.020	-.096	-.135	-.110	-.123	-.122	-.040	-.108	-.111	-.112	-.139	.044	.121	.170	.193
.309	.044	-.036	-.112	-.141	-.116	-.127	-.128	-.052	-.114	-.119	-.120	-.141	.022	.101	.150	.175
.333	.028	-.052	-.118	-.135	-.118	-.135	-.132	-.052	-.114	-.117	-.120	-.133	.008	.088	.138	.161
.381	.018	-.064	-.128	-.133	-.114	-.135	-.136	-.060	-.114	-.119	-.120	-.131	-.008	.068	.122	.145
.428	-.006	-.082	-.142	-.135	-.118	-.139	-.148	-.070	-.130	-.127	-.124	-.135	-.024	.052	.104	.125
.476	---	---	---	---	-.118	-.139	-.140	-.066	-.136	-.125	-.124	-.131	-.028	.046	.096	.117
.523	---	---	---	---	-.122	-.143	-.146	-.076	---	---	---	---	-.036	.038	.082	.103
.571	.036	.107	.146	.127	.136	-.147	-.148	-.088	-.150	-.135	-.132	-.139	.068	0	.050	.072
.618	.092	.121	-.150	.129	-.136	-.147	-.146	-.094	-.146	-.131	-.132	-.135	-.076	-.010	.034	.050
.666	.068	.131	-.148	.127	-.138	-.147	-.146	-.094	-.136	-.127	-.124	-.131	-.082	-.020	.020	.038
.714	.084	.137	-.134	.125	-.133	-.119	-.132	-.066	-.128	-.119	-.116	-.125	-.088	-.028	.014	.032
.761	-.088	.137	-.126	.117	---	---	---	---	-.126	-.115	-.115	-.123	-.088	-.030	.010	.026
.785	-.088	.131	-.118	.113	-.130	-.133	-.130	-.092	-.126	-.115	-.114	-.125	-.092	-.032	.008	.026
.809	-.086	.125	-.110	.103	-.118	-.121	-.118	-.084	-.124	-.115	-.116	-.123	-.092	-.032	.008	.026
.832	-.092	.123	-.106	.101	-.122	-.123	-.124	-.094	-.112	-.115	-.116	-.125	-.094	-.036	.002	.018
.856	-.100	.117	-.102	.097	-.114	-.117	-.116	-.092	-.118	-.115	-.116	-.125	-.102	-.050	-.010	.008
.880	-.100	.107	-.094	.094	-.106	-.109	-.110	-.092	-.112	-.109	-.112	-.117	-.108	-.058	-.020	.006
.904	-.094	.097	-.086	.084	-.094	-.095	-.098	-.084	-.106	-.103	-.106	-.111	-.108	-.064	-.026	.010
.928	-.088	.088	-.078	.078	-.074	-.078	-.080	-.072	-.102	-.101	-.104	-.109	-.104	-.064	-.026	.010
.951	-.088	.082	-.076	.072	-.088	-.090	-.088	-.086	-.098	-.093	-.090	-.107	-.114	-.074	-.042	.026
.975	-.084	.080	-.072	.070	-.086	-.090	-.092	-.094	-.098	-.099	-.096	-.103	-.104	-.074	-.044	.026
.999	-.140	.157	-.158	.147	-.130	-.139	-.132	-.131	---	---	---	---	-.148	-.115	-.084	.070
1.000	-.204	-.205	-.202	-.203	-.190	-.193	-.194	-.195	---	---	---	---	-.208	-.205	-.200	-.193

NACA

TABLE II.- PRESSURE COEFFICIENT DATA FOR PARABOLIC BODY  
OF REVOLUTION (RM-10) MOUNTED ON BENT STING

NO TRANSITION STRIPS - Continued

(c)  $\alpha = 20.00$

Station, x/L	Radial angle, $\phi$ , deg															
	43.4	58.4	73.4	88.4	133.4	148.4	163.4	178.4	223.4	238.4	253.4	268.4	313.4	328.4	343.4	358.4
0.024	0.161	0.036	-0.078	-0.152	-0.121	-0.138	-0.139	-0.062	-0.119	-0.134	-0.141	-0.158	0.163	0.274	0.352	0.381
0.048	.179	.056	-.062	-.148	-.113	-.122	-.131	-.034	-.129	-.136	-.145	-.166	.139	.254	.336	.373
0.071	.159	.036	-.078	-.168	-.131	-.142	-.153	-.042	-.135	-.146	-.151	-.170	.165	.270	.342	-----
0.095	.155	.032	-.086	-.168	-.139	-.158	-.161	-.040	-.131	-.142	-.147	-.172	.143	.250	.326	-----
0.119	.151	.028	-.090	-.170	-.143	-.162	-.169	-.042	-.139	-.146	-.149	-.174	.131	.238	.312	.337
0.143	.151	.028	-.088	-.170	-.145	-.164	-.171	-.044	-.147	-.154	-.153	-.178	.119	.230	.302	.327
0.167	.137	.016	-.099	-.176	-.151	-.170	-.177	-.046	-.147	-.158	-.155	-.175	.115	.222	.298	.325
0.190	.133	.012	-.099	-.172	-.147	-.174	-.177	-.054	-.145	-.152	-.153	-.176	.103	.210	.282	.311
0.214	.123	.002	-.115	-.176	-.151	-.174	-.177	-.046	-.139	-.150	-.149	-.170	-----	-----	-----	-----
0.238	.113	.006	-.121	-.172	-.151	-.180	-.181	-.056	-.143	-.154	-.153	-.174	.084	.188	.259	.290
0.262	.103	-.014	-.129	-.168	-.151	-.182	-.181	-.064	-.147	-.158	-.161	-.182	.076	.180	.255	.284
0.285	.090	-.028	-.139	-.168	-.153	-.184	-.185	-.070	-.151	-.162	-.163	-.182	.068	.172	.243	.272
0.333	.072	-.046	-.155	-.168	-.153	-.186	-.185	-.074	-.155	-.170	-.169	-.182	.048	.148	.219	.248
0.381	.052	-.062	-.169	-.160	-.155	-.186	-.185	-.074	-.159	-.166	-.167	-.176	.036	.136	.207	.236
0.428	.040	-.076	-.179	-.160	-.153	-.186	-.183	-.074	-.163	-.166	-.167	-.170	.016	.116	.187	.216
0.476	.016	-.096	-.191	-.162	-.163	-.194	-.187	-.082	-.185	-.170	-.171	-.176	-.004	.096	.167	.192
0.523	-----	-----	-----	-----	-.161	-.186	-.179	-.088	-.187	-.170	-.171	-.176	-.012	.088	.159	.184
0.571	.016	-.128	-.191	-.152	-.171	-.186	-.185	-.090	-----	-----	-----	-----	-.020	.076	.143	.166
0.618	.080	-.148	-.185	-.152	-.179	-.190	-.185	-.112	-.185	-.174	-.181	-.194	.056	.036	.105	.132
0.666	.060	-.164	-.175	-.144	-.185	-.188	-.179	-.114	-.177	-.170	-.179	-.190	.068	.026	.088	.112
0.714	.078	-.174	-.167	-.138	-.175	-.162	-.165	-.066	-.169	-.162	-.169	-.182	.080	.008	.070	.094
0.761	.084	-.172	-.151	-.124	-.175	-----	-----	-----	-.161	-.154	-.157	-.174	.092	.004	.058	.080
0.785	.088	-.172	-.143	-.118	-.153	-.168	-.155	-.122	-.159	-.148	-.153	-.170	.092	.006	.054	.076
0.809	.086	-.164	-.135	-.108	-.141	-.154	-.141	-.122	-.155	-.144	-.153	-.170	.094	.012	.048	.072
0.832	.096	-.160	-.129	-.104	-.145	-.154	-.145	-.138	-.149	-.144	-.153	-.174	.099	.018	.040	.064
0.856	.103	-.156	-.121	-.098	-.137	-.150	-.139	-.142	-.153	-.142	-.155	-.170	.109	.028	.026	.052
0.880	.107	-.144	-.115	-.092	-.129	-.142	-.133	-.142	-.147	-.136	-.153	-.174	.119	.044	.014	.036
0.904	.107	-.132	-.105	-.082	-.117	-.128	-.121	-.138	-.137	-.126	-.139	-.162	.123	.050	.004	.030
0.928	.107	-.124	-.099	-.076	-.097	-.110	-.101	-.126	-.127	-.126	-.139	-.174	.119	.052	0	.024
0.951	.103	-.116	-.095	-.072	-.107	-.118	-.107	-.134	-.121	-.118	-.131	-.146	.125	.064	-.016	.008
0.975	.099	-.100	-.086	-.066	-.101	-.116	-.113	-.148	-.121	-.118	-.129	-.150	.119	.062	-.014	.008
0.999	.139	-.172	-.171	-.152	-.147	-.154	-.147	-.176	-----	-----	-----	-----	.159	.104	-.062	-.040
1.000	.219	-.222	-.225	-.226	-.211	-.210	-.213	-.218	-----	-----	-----	-----	.221	.222	-.221	-.218

NACA

TABLE II.- PRESSURE COEFFICIENT DATA FOR PARABOLIC BODY  
OF REVOLUTION (RM-10) MOUNTED ON BENT STRING

NO TRANSITION STRIPS - Continued

(a)  $\alpha = 24.00$

Station, x/L	Radial angle, $\phi$ , deg															
	43.7	58.7	73.7	88.7	133.7	148.7	163.7	178.7	223.7	238.7	253.7	268.7	313.7	328.7	343.7	358.7
0.024	0.208	0.092	-0.095	-0.211	-0.178	-0.198	-0.202	-0.084	-0.164	-0.174	-0.186	-0.215	0.210	0.349	0.452	0.487
0.048	.222	.068	-.079	-.209	-.178	-.180	-.188	-.056	-.187	-.186	-.196	-.231	.178	.321	.426	.470
0.071	.202	.048	-.097	-.225	-.194	-.206	-.214	-.062	-.184	-.192	-.198	-.231	.214	.345	.440	-----
0.095	.200	.044	-.099	-.223	-.198	-.218	-.222	-.060	-.184	-.194	-.198	-.235	.186	.321	.418	-----
0.119	.192	.042	-.105	-.227	-.202	-.224	-.230	-.062	-.188	-.194	-.198	-.235	.178	.313	.408	.436
0.143	.192	.044	-.103	-.227	-.206	-.230	-.234	-.074	-.198	-.198	-.202	-.239	.162	.302	.394	.424
0.167	.182	.030	-.111	-.229	-.206	-.234	-.236	-.074	-.198	-.198	-.202	-.239	.162	.296	.392	.422
0.190	.180	.028	-.113	-.227	-.201	-.238	-.240	-.076	-.194	-.196	-.202	-.237	.146	.282	.377	.406
0.214	.164	.012	-.127	-.223	-.201	-.234	-.238	-.072	-.194	-.194	-.198	-.235	-----	-----	-----	-----
0.238	.158	.010	-.135	-.219	-.201	-.238	-.242	-.078	-.198	-.198	-.202	-.237	.128	.258	.353	.386
0.262	.148	.004	-.143	-.215	-----	-----	-----	-----	-.198	-.200	-.206	-.243	.118	.250	.345	.376
0.285	.128	.020	-.159	-.211	-.210	-.240	-.240	-.088	-.200	-.202	-.206	-.235	.108	.236	.329	.360
0.309	.112	.036	-.172	-.209	-.210	-.242	-.238	-.092	-.210	-.202	-.210	-.235	.088	.214	.307	.338
0.333	.088	.052	-.186	-.199	-.216	-.244	-.240	-.099	-.214	-.198	-.204	-.231	.072	.196	.291	.322
0.357	.076	.068	-.200	-.195	-.214	-.244	-.240	-.103	-.214	-.194	-.202	-.231	.056	.180	.268	.298
0.381	.076	.068	-.200	-.195	-.214	-.244	-.240	-.103	-.214	-.194	-.202	-.231	.056	.180	.268	.298
0.405	.052	.088	-.216	-.195	-.224	-.254	-.240	-.117	-.224	-.194	-.212	-.239	.032	.156	.244	.275
0.429	-----	-----	-----	-----	-.224	-.248	-.238	-.127	-.218	-.194	-.210	-.237	.024	.148	.236	.267
0.453	.014	.122	-.240	-.187	-.234	-.254	-.240	-.131	-----	-----	-----	-----	.014	.132	.218	.243
0.477	.008	.142	-.250	-.181	-.238	-.258	-.236	-.151	-.214	-.182	-.204	-.239	-.024	.090	.176	.205
0.501	.032	.162	-.238	-.171	-.238	-.258	-.238	-.159	-.206	-.174	-.198	-.237	.036	.076	.159	.185
0.525	.050	.180	-.224	-.161	-.230	-.234	-.220	-.137	-.194	-.158	-.182	-.231	.050	.060	.139	.167
0.549	.064	.190	-.202	-.143	-----	-----	-----	-----	-.178	-.150	-.172	-.227	.066	.044	.123	.151
0.573	.072	.198	-.194	-.135	-.210	-.242	-.220	-.177	-.174	-.144	-.170	-.223	.068	.042	.119	.145
0.597	.072	.198	-.184	-.125	-.198	-.226	-.202	-.171	-.170	-.142	-.163	-.221	.072	.036	.113	.139
0.621	.082	.206	-.180	-.123	-.202	-.234	-.206	-.187	-.162	-.138	-.165	-.221	.082	.028	.099	.129
0.645	.098	.216	-.176	-.119	-.196	-.226	-.202	-.187	-.166	-.142	-.165	-.219	.092	.012	.083	.111
0.669	.108	.214	-.168	-.117	-.184	-.214	-.194	-.187	-.160	-.142	-.161	-.211	.108	-.002	.071	.097
0.693	.116	.206	-.155	-.111	-.182	-.198	-.180	-.181	-.158	-.138	-.157	-.211	.114	-.012	.059	.084
0.717	.122	.188	-.147	-.111	-.148	-.168	-.153	-.165	-.154	-.138	-.149	-.183	.112	-.014	.050	.076
0.741	.124	.168	-.135	-.111	-.146	-.174	-.161	-.175	-.150	-.138	-.139	-.159	.122	-.028	.034	.060
0.765	.124	.148	-.127	-.111	-.142	-.164	-.161	-.187	-.154	-.150	-.139	-.155	.124	-.030	.032	.058
0.789	.168	.212	-.200	-.191	-.178	-.194	-.182	-.207	-----	-----	-----	-----	.164	-.080	-.022	.002
1.000	-.244	-.254	-.250	-.253	-.238	-.242	-.238	-.237	-----	-----	-----	-----	-.250	-.260	-.244	-.247

NACA

TABLE II.- PRESSURE COEFFICIENT DATA FOR PARABOLIC BODY  
OF REVOLUTION (RM-10) MOUNTED ON BENT STRING

NO TRANSITION STRIPS - Continued

(e)  $\alpha = 28.00$

Station, x/L	Radial angle, $\phi$ , deg											
	43.9	58.9	73.9	88.9	133.9	148.9	163.9	178.9	223.9	238.9	253.9	268.9
0.024	0.265	0.078	-0.092	-0.245	-0.234	-0.258	-0.256	-0.111	-0.212	-0.216	-0.269	-0.235
0.048	.277	.096	-.074	.233	-.226	-.240	-.240	-.092	-.230	-.226	-.240	-.247
0.071	.261	.078	-.088	.247	-.240	-.263	-.263	-.096	-.232	-.232	-.240	-.249
0.095	.252	.070	-.096	.251	-.248	-.281	-.285	-.099	-.232	-.228	-.236	-.261
0.119	.244	.066	-.100	-.253	-.252	-.291	-.287	-.107	-.236	-.228	-.236	-.263
0.143	.250	.066	-.096	-.253	-.256	-.297	-.297	-.107	-.240	-.228	-.236	-.263
0.167	.236	.058	-.106	-.259	-.256	-.301	-.297	-.111	-.240	-.224	-.230	-.269
0.190	.232	.058	-.100	-.259	-.252	-.299	-.295	-.111	-.236	-.224	-.230	-.269
0.214	.220	.042	-.120	-.271	-.250	-.299	-.293	-.115	-.240	-.220	-.228	-.271
0.238	.216	.040	-.128	-.275	-.256	-.307	-.297	-.119	-.244	-.218	-.228	-.275
0.262	.196	.024	-.136	-.283	-----	-----	-----	-----	-.244	-.212	-.224	-.271
0.285	.176	.006	-.152	-.291	-.265	-.309	-.299	-.129	-.250	-.208	-.220	-.263
0.309	.164	-.010	-.164	-.291	-.263	-.315	-.301	-.135	-.256	-.210	-.222	-.267
0.331	.144	-.024	-.176	-.283	-.273	-.323	-.309	-.149	-.248	-.200	-.214	-.257
0.353	.124	-.040	-.192	-.283	-.269	-.323	-.311	-.155	-.248	-.192	-.212	-.249
0.376	.100	-.062	-.208	-.279	-.277	-.331	-.315	-.163	-.250	-.192	-.214	-.247
0.400	-----	-----	-----	-----	-.277	-.337	-.317	-.169	-.244	-.180	-.204	-.239
0.424	.060	.094	-.232	-.267	-.279	-.337	-.317	-.167	-----	-----	-----	-----
0.448	.032	.114	-.250	-.265	-.281	-.339	-.325	-.183	-.236	-.176	-.200	-.241
0.472	.014	.134	-.265	-.255	-.281	-.359	-.319	-.185	-.228	-.176	-.190	-.231
0.496	-.006	.150	-.277	-.245	-.267	-.285	-.309	-.153	-.216	-.176	-.182	-.219
0.520	-.016	.166	-.281	-.233	-----	-----	-----	-----	-.210	-.182	-.180	-.207
0.544	-.028	.174	-.277	-.223	-.248	-.287	-.289	-.193	-.210	-.188	-.180	-.203
0.568	-.040	.184	-.256	-.211	-.228	-.288	-.265	-.189	-.212	-.200	-.184	-.201
0.592	-.056	.198	-.234	-.203	-.232	-.296	-.269	-.201	-.208	-.212	-.192	-.201
0.616	-.070	.206	-.214	-.193	-.218	-.244	-.256	-.199	-.218	-.228	-.200	-.201
0.640	-.088	.202	-.194	-.183	-.204	-.228	-.240	-.199	-.218	-.240	-.216	-.197
0.664	-.092	.186	-.171	-.171	-.192	-.212	-.224	-.195	-.218	-.261	-.228	-.191
0.688	-.108	.162	-.156	-.163	-.164	-.186	-.192	-.177	-.218	-.281	-.236	-.187
0.712	-.124	.140	-.140	-.155	-.168	-.198	-.198	-.191	-.216	-.285	-.240	-.181
0.736	-.140	.128	-.141	-.141	-.160	-.202	-.196	-.195	-.220	-.305	-.261	-.181
0.760	-.160	.112	-.128	-.207	-.200	-.246	-.230	-.215	-----	-----	-----	-----
0.784	-.176	.100	-.128	-.212	-.200	-.246	-.230	-.215	-----	-----	-----	-----
0.808	-.192	.088	-.128	-.212	-.200	-.246	-.230	-.215	-----	-----	-----	-----
0.832	-.208	.076	-.128	-.212	-.200	-.246	-.230	-.215	-----	-----	-----	-----
0.856	-.224	.064	-.128	-.212	-.200	-.246	-.230	-.215	-----	-----	-----	-----
0.880	-.240	.052	-.128	-.212	-.200	-.246	-.230	-.215	-----	-----	-----	-----
0.904	-.256	.040	-.128	-.212	-.200	-.246	-.230	-.215	-----	-----	-----	-----
0.928	-.272	.028	-.128	-.212	-.200	-.246	-.230	-.215	-----	-----	-----	-----
0.952	-.288	.016	-.128	-.212	-.200	-.246	-.230	-.215	-----	-----	-----	-----
0.976	-.304	.004	-.128	-.212	-.200	-.246	-.230	-.215	-----	-----	-----	-----
0.999	-.320	-.008	-.128	-.212	-.200	-.246	-.230	-.215	-----	-----	-----	-----
1.000	-.336	-.024	-.128	-.212	-.200	-.246	-.230	-.215	-----	-----	-----	-----

NACA



TABLE II.- PRESSURE COEFFICIENT DATA FOR PARABOLIC BODY  
OF REVOLUTION (RM-10) MOUNTED ON BENT STING

NO TRANSITION STRIPS - Continued

(f)  $\alpha = 32.00$

Station, x/L	Radial angle, $\phi$ , deg													
	44.1	59.1	74.1	89.1	134.1	149.1	164.1	179.1	224.1	239.1	254.1	269.1	314.1	329.1
0.024	0.321	0.109	-0.087	-0.251	-0.277	-0.302	-0.307	-0.173	-0.240	-0.237	-0.258	-0.237	0.337	0.531
0.048	0.311	0.133	-0.063	-0.231	-0.269	-0.275	-0.283	-0.159	-0.254	-0.251	-0.270	-0.245	0.301	0.499
0.071	0.317	0.107	-0.083	-0.249	-0.289	-0.302	-0.313	-0.157	-0.261	-0.257	-0.274	-0.249	0.341	0.523
0.095	0.309	0.105	-0.087	-0.255	-0.301	-0.316	-0.323	-0.167	-0.265	-0.253	-0.266	-0.261	0.307	0.523
0.119	0.305	0.097	-0.091	-0.255	-0.303	-0.322	-0.325	-0.173	-0.265	-0.249	-0.258	-0.257	0.303	0.483
0.143	0.313	0.109	-0.079	-0.249	-0.303	-0.322	-0.313	-0.173	-0.267	-0.249	-0.258	-0.253	0.299	0.481
0.167	0.297	0.095	-0.091	-0.257	-0.301	-0.322	-0.313	-0.173	-0.273	-0.253	-0.262	-0.271	0.291	0.481
0.190	0.299	0.097	-0.089	-0.255	-0.297	-0.318	-0.325	-0.173	-0.273	-0.253	-0.262	-0.271	0.271	0.450
0.214	0.283	0.080	-0.105	-0.271	-0.297	-0.318	-0.319	-0.173	-0.273	-0.249	-0.254	-0.271	0.236	0.418
0.238	0.269	0.070	-0.115	-0.275	-0.301	-0.326	-0.327	-0.175	-0.277	-0.249	-0.254	-0.277	0.228	0.414
0.262	0.252	0.056	-0.125	-0.281	-----	-----	-----	-----	-0.277	-0.249	-0.258	-0.277	0.218	0.402
0.285	0.234	0.040	-0.139	-0.291	-0.297	-0.322	-0.313	-0.175	-0.281	-0.253	-0.260	-0.281	0.200	0.370
0.333	0.220	0.024	-0.153	-0.302	-0.297	-0.324	-0.326	-0.175	-0.281	-0.257	-0.266	-0.289	0.180	0.354
0.381	0.200	0.006	-0.168	-0.310	-0.299	-0.326	-0.327	-0.183	-0.281	-0.257	-0.266	-0.281	0.160	0.330
0.428	0.178	-0.008	-0.178	-0.318	-0.297	-0.322	-0.313	-0.191	-0.289	-0.257	-0.266	-0.281	0.138	0.306
0.476	0.154	-0.028	-0.192	-0.314	-0.297	-0.318	-0.319	-0.195	-0.291	-0.255	-0.274	-0.279	0.130	0.294
0.523	-----	-----	-----	-----	-0.293	-0.318	-0.315	-0.207	-0.285	-0.259	-0.266	-0.273	0.114	0.273
0.571	0.116	-0.058	-0.218	-0.287	-0.283	-0.306	-0.303	-0.207	-----	-----	-----	-----	0.080	0.237
0.618	0.086	-0.082	-0.236	-0.273	-0.283	-0.302	-0.303	-0.229	-0.283	-0.273	-0.274	-0.273	0.068	0.237
0.666	0.066	-0.100	-0.250	-0.257	-0.273	-0.282	-0.287	-0.225	-0.281	-0.278	-0.270	-0.267	0.052	0.221
0.714	0.050	-0.117	-0.260	-0.247	-0.256	-0.241	-0.268	-0.197	-0.277	-0.278	-0.268	-0.263	0.032	0.203
0.761	0.032	-0.133	-0.256	-0.231	-----	-----	-----	-----	-0.273	-0.278	-0.262	-0.257	0.022	0.183
0.785	0.022	-0.141	-0.244	-0.225	-0.240	-0.245	-0.260	-0.241	-0.267	-0.278	-0.254	-0.253	0.026	0.175
0.809	0.024	-0.141	-0.232	-0.209	-0.226	-0.225	-0.240	-0.231	-0.265	-0.278	-0.254	-0.249	0.020	0.169
0.832	0.010	-0.153	-0.224	-0.209	-0.236	-0.233	-0.246	-0.241	-0.256	-0.278	-0.254	-0.249	0.008	0.157
0.856	0.012	-0.169	-0.216	-0.207	-0.228	-0.229	-0.246	-0.241	-0.256	-0.278	-0.254	-0.245	-0.008	0.141
0.880	0.022	-0.175	-0.212	-0.201	-0.224	-0.221	-0.242	-0.241	-0.248	-0.265	-0.242	-0.237	0.024	0.123
0.904	0.028	-0.179	-0.204	-0.193	-0.220	-0.215	-0.238	-0.239	-0.240	-0.265	-0.234	-0.229	0.032	0.107
0.928	0.036	-0.185	-0.202	-0.193	-0.200	-0.197	-0.214	-0.221	-0.228	-0.253	-0.220	-0.215	0.034	0.103
0.951	0.044	-0.185	-0.196	-0.191	-0.212	-0.213	-0.230	-0.237	-0.216	-0.237	-0.206	-0.197	0.056	0.078
0.975	0.062	-0.193	-0.196	-0.191	-0.212	-0.217	-0.234	-0.237	-0.212	-0.231	-0.202	-0.197	0.064	0.070
0.999	0.128	-0.247	-0.242	-0.233	-0.236	-0.241	-0.242	-0.239	-0.212	-----	-----	-----	0.120	0.008
1.000	0.263	-0.267	-0.264	-0.257	-0.252	-0.257	-0.246	-0.241	-----	-----	-----	-----	0.263	-0.269

NACA

TABLE II.- PRESSURE COEFFICIENT DATA FOR PARABOLIC BODY  
OF REVOLUTION (RM-10) MOUNTED ON BENT STRING

NO TRANSITION STRIPS - Concluded

(g)  $\alpha = 36.00$

Station, x/L	Radial angle, $\phi$ , deg															
	44.2	59.2	74.2	89.2	134.2	149.2	164.2	179.2	224.2	239.2	254.2	269.2	314.2	329.2	344.2	359.2
0.024	0.381	0.138	-0.079	-0.256	-0.321	-0.333	-0.339	-0.248	-0.264	-0.240	-0.268	-0.238	0.409	0.633	0.783	0.834
0.048	0.405	0.168	-0.048	-0.232	-0.288	-0.291	-0.295	-0.194	-0.294	-0.277	-0.317	-0.244	0.361	0.589	0.751	0.810
0.071	0.381	0.146	-0.065	-0.248	-0.288	-0.291	-0.287	-0.186	-0.309	-0.313	-0.349	-0.240	0.415	0.623	0.759	0.800
0.095	0.373	0.150	-0.071	-0.250	-0.280	-0.291	-0.279	-0.196	-0.323	-0.331	-0.359	-0.256	0.381	0.593	0.735	---
0.119	0.367	0.136	-0.075	-0.252	-0.276	-0.277	-0.238	-0.228	-0.337	-0.339	-0.363	-0.252	0.369	0.581	0.727	0.769
0.143	0.377	0.146	-0.063	-0.248	-0.274	-0.277	-0.226	-0.252	-0.345	-0.349	-0.365	-0.250	0.361	0.571	0.714	0.757
0.167	0.363	0.134	-0.075	-0.256	-0.274	-0.273	-0.210	-0.267	-0.351	-0.361	-0.379	-0.273	0.359	0.571	0.716	0.761
0.190	0.359	0.134	-0.073	-0.256	-0.270	-0.273	-0.218	-0.285	-0.353	-0.361	-0.371	-0.269	0.333	0.541	0.686	0.741
0.214	0.339	0.114	-0.095	-0.269	-0.270	-0.275	-0.220	-0.283	-0.349	-0.349	-0.371	-0.273	---	---	---	---
0.238	0.331	0.106	-0.099	-0.273	-0.274	-0.289	-0.238	-0.289	-0.349	-0.353	-0.367	-0.281	0.304	0.507	0.654	0.707
0.262	0.319	0.096	-0.107	-0.281	---	---	---	---	-0.345	-0.345	-0.355	-0.287	0.296	0.499	0.646	0.697
0.285	0.296	0.074	-0.121	-0.291	-0.282	-0.301	-0.260	-0.293	-0.337	-0.325	-0.331	-0.293	0.286	0.483	0.624	0.673
0.333	0.280	0.062	-0.135	-0.299	-0.300	-0.325	-0.289	-0.299	-0.325	-0.307	-0.311	-0.305	0.264	0.463	0.603	0.653
0.381	0.260	0.042	-0.147	-0.309	-0.321	-0.361	-0.333	-0.307	-0.304	-0.279	-0.283	-0.309	0.240	0.435	0.575	0.633
0.428	0.240	0.028	-0.161	-0.321	-0.341	-0.371	-0.363	-0.313	-0.290	-0.252	-0.256	-0.289	0.220	0.415	0.553	0.605
0.476	0.214	0.006	-0.178	-0.331	-0.365	-0.389	-0.398	-0.339	-0.276	-0.242	-0.242	-0.250	0.198	0.387	0.525	0.577
0.523	---	---	---	---	-0.377	-0.393	-0.404	-0.361	-0.258	-0.242	-0.238	-0.240	0.190	0.379	0.517	0.569
0.571	0.176	0.024	-0.202	-0.347	-0.377	-0.379	-0.400	-0.373	---	---	---	---	0.176	0.355	0.486	0.535
0.618	0.152	0.046	-0.216	-0.355	-0.365	-0.363	-0.387	-0.385	-0.282	-0.309	-0.287	-0.305	0.144	0.321	0.448	0.495
0.666	0.132	0.058	-0.228	-0.323	-0.337	-0.329	-0.355	-0.379	-0.319	-0.357	-0.333	-0.339	0.132	0.307	0.430	0.475
0.714	0.108	0.080	-0.244	-0.269	-0.304	-0.275	-0.327	-0.317	-0.357	-0.397	-0.387	-0.357	0.114	0.287	0.406	0.449
0.761	0.092	0.096	-0.256	-0.240	---	---	---	---	-0.391	-0.415	-0.422	-0.371	0.092	0.263	0.385	0.425
0.785	0.078	0.106	-0.260	-0.236	-0.278	-0.305	-0.335	-0.381	-0.391	-0.397	-0.412	-0.371	0.086	0.254	0.373	0.415
0.809	0.080	0.104	-0.260	-0.240	-0.262	-0.301	-0.323	-0.367	-0.395	-0.389	-0.400	-0.379	0.080	0.248	0.363	0.405
0.832	0.064	0.114	-0.268	-0.267	-0.286	-0.337	-0.355	-0.393	-0.395	-0.365	-0.373	-0.385	0.070	0.234	0.349	0.391
0.856	0.046	0.130	-0.285	-0.291	-0.298	-0.361	-0.373	-0.403	-0.377	-0.345	-0.349	-0.371	0.054	0.216	0.329	0.367
0.880	0.034	0.138	-0.291	-0.323	-0.319	-0.385	-0.390	-0.401	-0.327	-0.313	-0.319	-0.321	0.036	0.194	0.311	0.351
0.904	0.028	0.144	-0.297	-0.359	-0.345	-0.401	-0.396	-0.399	-0.343	-0.297	-0.301	-0.307	0.024	0.182	0.299	0.337
0.928	0.022	0.152	-0.301	-0.389	-0.341	-0.363	-0.355	-0.347	-0.321	-0.281	-0.283	-0.285	0.024	0.180	0.293	0.335
0.951	0.014	0.154	-0.305	-0.401	-0.363	-0.387	-0.375	-0.365	-0.296	-0.267	-0.258	-0.265	0.002	0.152	0.268	0.311
0.975	0.008	0.176	-0.321	-0.409	-0.383	-0.393	-0.387	-0.373	-0.302	-0.283	-0.274	-0.267	0.010	0.144	0.254	0.295
0.999	0.082	0.232	-0.353	-0.365	-0.369	-0.357	-0.361	-0.363	---	---	---	---	0.072	0.072	0.180	0.216
1.000	0.369	0.359	0.363	0.365	0.365	0.345	0.349	0.361	---	---	---	---	0.373	0.369	0.371	0.373

NACA

NACA

TABLE III.- PRESSURE COEFFICIENT DATA FOR PARABOLIC BODY  
OF REVOLUTION (RM-10) MOUNTED ON STRAIGHT STING

WITH AXIAL TRANSITION STRIPS

(a)  $\alpha = 4.00$

Station, x/L	Radial angle, $\phi$ , deg													
	56	81	131	146	161	171	221	236	251	261	311	326	341	351
0.024	0.062	0.050	0.032	0.032	0.030	0.030	0.034	0.040	0.042	0.046	0.084	0.094	0.098	0.102
0.048	0.062	0.046	0.032	0.032	0.030	0.030	0.026	0.030	0.036	0.033	0.074	0.084	0.090	0.096
0.071	0.054	0.040	0.028	0.026	0.024	0.026	0.018	0.020	0.014	0.026	0.060	0.070	0.090	---
0.095	0.054	0.042	0.026	0.022	0.018	0.018	0.018	0.022	0.024	0.026	0.052	0.064	---	---
0.119	0.050	0.038	0.020	0.016	0.014	0.014	0.014	0.018	0.008	0.022	0.050	0.064	0.066	0.076
0.143	0.046	0.030	0.016	0.010	0.008	0.010	0.010	0.010	0.014	0.010	0.050	0.062	0.066	0.072
0.167	0.038	0.026	0.012	0.010	0.008	0.008	0.008	0.008	0.014	0.012	0.042	0.054	0.058	0.066
0.190	0.038	0.024	0.008	0.006	0.008	0.006	0.008	0.008	0.006	0.008	---	---	---	---
0.214	0.036	0.024	0.008	0.006	0.008	0.006	0.008	0.008	0.006	0.008	---	---	---	0.050
0.238	0.026	0.014	0.002	0.002	0.002	0.002	0.004	0.004	0.006	0.008	---	---	---	0.040
0.262	0.022	0.010	0.002	0.002	0.002	0.002	0.004	0.004	0.008	0.008	---	---	---	0.034
0.285	0.014	0.006	0.006	0.002	0.002	0.002	0.008	0.008	0.002	0.002	---	---	---	0.030
0.309	0.006	0.008	0.012	0.008	0.008	0.004	0.008	0.008	0.010	0.006	---	---	---	0.018
0.333	0.002	0.008	0.012	0.010	0.010	0.010	0.016	0.016	0.014	0.014	---	---	---	0.014
0.357	0.006	0.016	0.016	0.014	0.014	0.010	0.028	0.028	0.034	0.030	---	---	---	0.002
0.381	0.006	0.016	0.028	0.026	0.026	0.022	0.028	0.028	0.034	0.030	---	---	---	0.002
0.405	0.014	0.024	0.026	0.022	0.022	0.018	0.020	0.022	0.026	0.022	---	---	---	0.002
0.429	0.014	0.024	0.026	0.022	0.022	0.018	0.020	0.022	0.026	0.022	---	---	---	0.002
0.453	0.026	0.034	0.032	0.030	0.028	0.024	0.032	0.034	0.038	0.038	---	---	---	0.002
0.477	0.042	0.046	0.038	0.034	0.034	0.032	0.038	0.038	0.042	0.042	---	---	---	0.002
0.501	0.044	0.046	0.038	0.038	0.036	0.032	0.036	0.046	0.050	0.054	---	---	---	0.002
0.525	0.050	0.048	0.044	0.038	0.038	0.034	0.044	0.046	0.048	0.052	---	---	---	0.002
0.549	0.054	0.054	0.044	0.038	0.038	0.034	0.044	0.046	0.048	0.052	---	---	---	0.002
0.573	0.056	0.054	0.042	0.036	0.036	0.032	0.036	0.034	0.040	0.042	---	---	---	0.002
0.597	0.052	0.052	0.032	0.030	0.026	0.022	0.034	0.034	0.040	0.042	---	---	---	0.002
0.621	0.058	0.062	0.040	0.036	0.034	0.030	0.036	0.038	0.042	0.046	---	---	---	0.002
0.645	0.062	0.062	0.040	0.038	0.034	0.030	0.034	0.034	0.042	0.046	---	---	---	0.002
0.669	0.060	0.064	0.038	0.036	0.034	0.030	0.034	0.034	0.042	0.044	---	---	---	0.002
0.693	0.054	0.064	0.032	0.032	0.030	0.028	0.032	0.030	0.038	0.040	---	---	---	0.002
0.717	0.050	0.050	0.020	0.018	0.018	0.018	0.028	0.030	0.036	0.038	---	---	---	0.002
0.741	0.042	0.044	0.020	0.018	0.020	0.018	0.026	0.030	0.034	0.034	---	---	---	0.002
0.765	0.042	0.032	0.020	0.018	0.022	0.020	0.026	0.030	0.034	0.034	---	---	---	0.002
0.789	0.042	0.026	0.020	0.018	0.022	0.020	0.026	0.030	0.034	0.034	---	---	---	0.002
0.813	0.042	0.026	0.020	0.018	0.022	0.020	0.026	0.030	0.034	0.034	---	---	---	0.002
0.837	0.042	0.026	0.020	0.018	0.022	0.020	0.026	0.030	0.034	0.034	---	---	---	0.002
0.861	0.042	0.026	0.020	0.018	0.022	0.020	0.026	0.030	0.034	0.034	---	---	---	0.002
0.885	0.042	0.026	0.020	0.018	0.022	0.020	0.026	0.030	0.034	0.034	---	---	---	0.002
0.909	0.042	0.026	0.020	0.018	0.022	0.020	0.026	0.030	0.034	0.034	---	---	---	0.002
0.933	0.042	0.026	0.020	0.018	0.022	0.020	0.026	0.030	0.034	0.034	---	---	---	0.002
0.957	0.042	0.026	0.020	0.018	0.022	0.020	0.026	0.030	0.034	0.034	---	---	---	0.002
0.975	0.042	0.026	0.020	0.018	0.022	0.020	0.026	0.030	0.034	0.034	---	---	---	0.002
0.999	0.042	0.026	0.020	0.018	0.022	0.020	0.026	0.030	0.034	0.034	---	---	---	0.002
1.000	0.018	0.018	0.020	0.018	0.010	0.016	0.010	0.012	0.014	0.012	---	---	---	0.002

NACA

TABLE III.- PRESSURE COEFFICIENT DATA FOR PARABOLIC BODY  
OF REVOLUTION (RM-10) MOUNTED ON STRAIGHT STING

WITH AXIAL TRANSITION STRIPS - Continued

(b)  $\alpha = 8.05$

Station, $x/L$	Radial angle, $\phi$ , deg									
	58	83	133	148	163	173	223	238	253	263
0.024	0.060	0.024	0.006	0.008	0.010	0.012	0.006	0.006	0.008	0.014
0.048	0.064	0.024	0.004	0.008	0.008	0.014	-.002	-.004	-.008	0.004
0.071	0.052	0.014	-.002	0	0.004	0.008	0.006	-.008	-.024	-.004
0.095	0.052	0.012	-.008	-.006	-.008	0.006	-.008	-.010	-.044	0.103
0.119	0.048	0.016	-.012	-.008	-.002	0.004	-.016	-.020	-.030	0.084
0.143	0.040	0.004	-.020	-.016	-.006	-.002	-.022	-.024	-.030	0.076
0.167	0.034	-.004	-.020	-.016	0.006	-.002	-.020	-.024	-.020	0.064
0.190	0.034	-.004	-.020	-.020	-.008	0	-.016	-.022	-.026	0.050
0.214	0.028	0.004	-.020	-.020	-.004	0.004	-.014	-.022	-.026	0.032
0.238	0.016	0.016	-.024	-.020	-.010	0	-.022	-.032	-.036	0.028
0.262	0.014	-.020	-.028	-.016	-.012	-.004	-.020	-.032	-.028	0.024
0.285	0.006	-.024	-.032	-.020	-.016	-.008	-.020	-.028	-.046	0.020
0.309	-.004	-.036	-.034	-.024	-.020	-.010	-.024	-.032	-.040	0.014
0.333	-.012	-.040	-.034	-.026	-.020	-.012	-.032	-.042	-.046	0.008
0.357	-.022	-.048	-.034	-.028	-.026	-.020	-.034	-.044	-.048	0.004
0.381	-.036	-.056	-.042	-.034	-.032	-.028	-.040	-.052	-.062	0.000
0.405	-.038	-.060	-.040	-.032	-.030	-.022	-.036	-.048	-.060	0.000
0.429	-.052	-.076	-.040	-.034	-.032	-.028	-.040	-.056	-.072	0.000
0.453	-.068	-.084	-.048	-.044	-.042	-.034	-.046	-.058	-.076	0.000
0.477	-.072	-.084	-.048	-.044	-.042	-.036	-.048	-.058	-.084	0.000
0.501	-.088	-.094	-.044	-.040	-.038	-.030	-.036	-.044	-.064	0.000
0.525	-.092	-.092	-.044	-.040	-.038	-.026	-.036	-.042	-.064	0.000
0.549	-.088	-.088	-.036	-.032	-.032	-.026	-.036	-.042	-.064	0.000
0.573	-.094	-.092	-.044	-.040	-.038	-.034	-.040	-.048	-.068	0.000
0.597	-.094	-.092	-.044	-.040	-.038	-.034	-.040	-.048	-.068	0.000
0.621	-.084	-.084	-.032	-.028	-.028	-.026	-.038	-.040	-.062	0.000
0.645	-.072	-.072	-.022	-.016	-.016	-.016	-.036	-.036	-.064	0.000
0.669	-.064	-.060	-.024	-.016	-.016	-.016	-.036	-.036	-.064	0.000
0.693	-.052	-.048	-.024	-.016	-.016	-.016	-.036	-.036	-.064	0.000
0.717	-.048	-.044	-.024	-.016	-.016	-.016	-.036	-.036	-.064	0.000
0.741	-.044	-.040	-.024	-.016	-.016	-.016	-.036	-.036	-.064	0.000
0.765	-.040	-.036	-.024	-.016	-.016	-.016	-.036	-.036	-.064	0.000
0.789	-.036	-.032	-.024	-.016	-.016	-.016	-.036	-.036	-.064	0.000
0.813	-.032	-.028	-.024	-.016	-.016	-.016	-.036	-.036	-.064	0.000
0.837	-.028	-.024	-.024	-.016	-.016	-.016	-.036	-.036	-.064	0.000
0.861	-.024	-.020	-.024	-.016	-.016	-.016	-.036	-.036	-.064	0.000
0.885	-.020	-.016	-.024	-.016	-.016	-.016	-.036	-.036	-.064	0.000
0.909	-.016	-.012	-.024	-.016	-.016	-.016	-.036	-.036	-.064	0.000
0.933	-.012	-.008	-.024	-.016	-.016	-.016	-.036	-.036	-.064	0.000
0.957	-.008	-.004	-.024	-.016	-.016	-.016	-.036	-.036	-.064	0.000
0.981	-.004	0	-.024	-.016	-.016	-.016	-.036	-.036	-.064	0.000
1.000	0	0	-.024	-.016	-.016	-.016	-.036	-.036	-.064	0.000

NACA

TABLE III.- PRESSURE COEFFICIENT DATA FOR PARABOLIC BODY  
OF REVOLUTION (RM-10) MOUNTED ON STRAIGHT STING

WITH AXIAL TRANSITION STRIPS - Continued

(c)  $\alpha = 12.05$

Station, x/L	Radial angle, $\phi$ , deg													
	58.7	83.7	133.7	148.7	163.7	173.7	223.7	238.7	253.7	263.7	313.7	328.7	343.7	353.7
0.024	0.050	-0.022	-0.030	-0.028	-0.030	-0.016	-0.028	-0.034	-0.042	-0.040	0.114	0.168	0.206	0.219
0.048	0.054	-0.022	-0.034	-0.030	-0.036	-0.008	-0.038	-0.042	-0.054	-0.048	0.098	0.152	0.192	0.205
0.071	0.038	-0.038	-0.038	-0.038	-0.040	-0.008	-0.042	-0.046	-0.086	-0.058	0.110	0.158	0.194	0.199
0.095	0.042	-0.032	-0.040	-0.038	-0.040	-0.008	-0.040	-0.054	-0.098	-0.082	0.096	0.142	0.182	0.199
0.119	0.036	-0.028	-0.042	-0.046	-0.032	-0.010	-0.054	-0.060	-0.098	-0.084	0.074	0.124	0.160	0.171
0.143	0.026	-0.036	-0.058	-0.050	-0.036	-0.018	-0.062	-0.060	-0.112	-0.084	0.072	0.122	0.160	0.171
0.167	0.018	-0.044	-0.058	-0.048	-0.036	-0.016	-0.046	-0.072	-0.094	-0.090	0.062	0.112	0.148	0.159
0.190	0.022	-0.044	-0.046	-0.038	-0.034	-0.020	-0.054	-0.078	-0.094	-0.088	0.072	0.112	0.148	0.159
0.214	0.014	-0.054	-0.054	-0.034	-0.032	-0.012	-0.050	-0.078	-0.094	-0.088	0.072	0.112	0.148	0.159
0.238	0.002	-0.064	-0.070	-0.040	-0.038	-0.008	-0.058	-0.082	-0.110	-0.096	0.070	0.112	0.148	0.159
0.262	-0.002	-0.070	-0.074	-0.042	-0.042	-0.008	-0.060	-0.086	-0.114	-0.099	0.070	0.112	0.148	0.159
0.285	-0.014	-0.076	-0.080	-0.042	-0.046	-0.024	-0.064	-0.090	-0.114	-0.111	0.070	0.112	0.148	0.159
0.309	-0.022	-0.080	-0.074	-0.048	-0.048	-0.036	-0.064	-0.090	-0.130	-0.129	0.070	0.112	0.148	0.159
0.333	-0.038	-0.088	-0.062	-0.048	-0.048	-0.042	-0.052	-0.086	-0.130	-0.131	0.070	0.112	0.148	0.159
0.357	-0.050	-0.103	-0.062	-0.038	-0.054	-0.042	-0.048	-0.086	-0.130	-0.131	0.070	0.112	0.148	0.159
0.381	-0.060	-0.107	-0.054	-0.036	-0.054	-0.042	-0.048	-0.086	-0.130	-0.131	0.070	0.112	0.148	0.159
0.405	-0.070	-0.107	-0.062	-0.046	-0.054	-0.044	-0.058	-0.096	-0.136	-0.143	0.070	0.112	0.148	0.159
0.429	-0.088	-0.123	-0.074	-0.048	-0.058	-0.044	-0.082	-0.094	-0.138	-0.147	0.070	0.112	0.148	0.159
0.453	-0.102	-0.131	-0.106	-0.062	-0.066	-0.056	-0.094	-0.102	-0.138	-0.147	0.070	0.112	0.148	0.159
0.477	-0.110	-0.131	-0.106	-0.062	-0.066	-0.056	-0.094	-0.102	-0.138	-0.147	0.070	0.112	0.148	0.159
0.501	-0.122	-0.123	-0.122	-0.068	-0.062	-0.052	-0.106	-0.106	-0.128	-0.129	0.070	0.112	0.148	0.159
0.525	-0.114	-0.109	-0.120	-0.068	-0.058	-0.058	-0.118	-0.106	-0.138	-0.145	0.070	0.112	0.148	0.159
0.549	-0.122	-0.115	-0.126	-0.094	-0.054	-0.048	-0.120	-0.090	-0.118	-0.127	0.070	0.112	0.148	0.159
0.573	-0.110	-0.109	-0.120	-0.102	-0.052	-0.044	-0.118	-0.080	-0.114	-0.105	0.070	0.112	0.148	0.159
0.597	-0.106	-0.101	-0.110	-0.122	-0.052	-0.044	-0.118	-0.074	-0.102	-0.105	0.070	0.112	0.148	0.159
0.621	-0.106	-0.099	-0.118	-0.138	-0.068	-0.038	-0.118	-0.088	-0.098	-0.105	0.070	0.112	0.148	0.159
0.645	-0.100	-0.092	-0.120	-0.138	-0.078	-0.062	-0.120	-0.098	-0.092	-0.098	0.070	0.112	0.148	0.159
0.669	-0.090	-0.080	-0.138	-0.138	-0.084	-0.064	-0.120	-0.098	-0.082	-0.092	0.070	0.112	0.148	0.159
0.693	-0.076	-0.070	-0.116	-0.130	-0.086	-0.060	-0.118	-0.102	-0.074	-0.082	0.070	0.112	0.148	0.159
0.717	-0.068	-0.064	-0.100	-0.112	-0.086	-0.052	-0.108	-0.094	-0.076	-0.076	0.070	0.112	0.148	0.159
0.741	-0.062	-0.056	-0.094	-0.110	-0.100	-0.056	-0.102	-0.088	-0.062	-0.072	0.070	0.112	0.148	0.159
0.765	-0.051	-0.052	-0.082	-0.100	-0.098	-0.072	-0.090	-0.084	-0.062	-0.072	0.070	0.112	0.148	0.159
0.789	-0.058	-0.052	-0.082	-0.100	-0.098	-0.072	-0.090	-0.084	-0.062	-0.072	0.070	0.112	0.148	0.159
0.813	-0.062	-0.070	-0.058	-0.070	-0.058	-0.080	-0.088	-0.078	-0.062	-0.072	0.070	0.112	0.148	0.159
0.837	-0.066	-0.070	-0.050	-0.066	-0.046	-0.068	-0.048	-0.056	-0.040	-0.060	0.070	0.112	0.148	0.159
0.861	-0.066	-0.070	-0.050	-0.066	-0.046	-0.068	-0.048	-0.056	-0.040	-0.060	0.070	0.112	0.148	0.159
0.885	-0.066	-0.070	-0.050	-0.066	-0.046	-0.068	-0.048	-0.056	-0.040	-0.060	0.070	0.112	0.148	0.159
0.909	-0.066	-0.070	-0.050	-0.066	-0.046	-0.068	-0.048	-0.056	-0.040	-0.060	0.070	0.112	0.148	0.159
0.933	-0.066	-0.070	-0.050	-0.066	-0.046	-0.068	-0.048	-0.056	-0.040	-0.060	0.070	0.112	0.148	0.159
0.957	-0.066	-0.070	-0.050	-0.066	-0.046	-0.068	-0.048	-0.056	-0.040	-0.060	0.070	0.112	0.148	0.159
0.981	-0.066	-0.070	-0.050	-0.066	-0.046	-0.068	-0.048	-0.056	-0.040	-0.060	0.070	0.112	0.148	0.159
1.000	-0.066	-0.070	-0.050	-0.066	-0.046	-0.068	-0.048	-0.056	-0.040	-0.060	0.070	0.112	0.148	0.159

NACA

TABLE III.- PRESSURE COEFFICIENT DATA FOR PARABOLIC BODY  
OF REVOLUTION (RM-10) MOUNTED ON STRAIGHT STING

WITH AXIAL TRANSITION STRIPS - Concluded

(a)  $\alpha = 16.10$

Station, x/L	Radial angle, $\phi$ , deg													
	59	84	134	149	164	174	224	239	254	264	314	329	344	354
0.024	0.042	-0.074	-0.070	-0.070	-0.078	-0.050	-0.070	-0.070	-0.088	-0.094	0.136	0.218	0.274	0.294
0.048	0.052	-0.070	-0.076	-0.074	-0.086	-0.034	-0.078	-0.078	-0.136	-0.103	.122	.204	.262	.286
0.071	0.038	-0.084	-0.076	-0.074	-0.078	-0.026	-0.084	-0.082	-0.156	-0.109	.162	.216	.270	-----
0.095	0.034	-0.088	-0.106	-0.086	-0.070	-0.038	-0.064	-0.086	-0.176	-0.133	.122	.196	-----	-----
0.119	0.026	-0.068	-0.110	-0.100	-0.068	-0.040	-0.134	-0.084	-0.150	-0.161	.103	.182	-----	-----
0.143	0.020	-0.074	-0.106	-0.102	-0.086	-0.046	-0.086	-0.132	-0.180	-0.161	.092	.172	.224	.242
0.167	0.006	-0.086	-0.090	-0.090	-0.094	-0.046	-0.082	-0.152	-0.150	-0.169	.086	.166	.218	.240
0.190	0.008	-0.090	-0.090	-0.070	-0.088	-0.046	-0.094	-0.140	-0.138	-0.165	.074	.154	.200	.222
0.214	0.002	-0.107	-0.102	-0.060	-0.088	-0.044	-0.134	-0.142	-0.134	-0.173	-----	-----	-----	-----
0.238	-0.010	-0.117	-0.118	-0.066	-0.102	-0.050	-0.120	-0.144	-0.134	-0.175	-----	.132	-----	.201
0.262	-0.020	-0.125	-0.126	-0.074	-0.097	-0.042	-0.112	-0.138	-0.134	-0.177	-----	.132	-----	.197
0.285	-0.032	-0.129	-0.148	-0.076	-0.090	-0.046	-0.118	-0.132	-0.126	-0.169	-----	.124	-----	.187
0.303	-0.044	-0.129	-0.150	-0.084	-0.074	-0.050	-0.118	-0.132	-0.146	-0.167	-----	.112	-----	.177
0.381	-0.060	-0.121	-0.138	-0.064	-0.064	-0.050	-0.040	-0.130	-0.170	-0.185	-----	.096	-----	.157
0.428	-0.072	-0.131	-0.128	-0.062	-0.078	-0.056	-0.088	-0.140	-0.186	-0.185	-----	.078	-----	.145
0.476	-0.083	-0.131	-0.134	-0.098	-0.114	-0.070	-0.116	-0.138	-0.192	-0.181	-----	.058	-----	.117
0.523	-0.100	-0.129	-0.136	-0.156	-0.122	-0.066	-0.150	-0.132	-0.164	-0.153	-----	.040	-----	.107
0.571	-0.112	-0.129	-0.142	-0.190	-0.122	-0.072	-0.176	-0.126	-0.148	-0.141	-----	.040	-----	.099
0.618	-0.124	-0.125	-0.152	-0.202	-0.146	-0.090	-0.166	-0.114	-0.136	-0.135	-----	.008	-----	.070
0.666	-0.132	-0.123	-0.150	-0.188	-0.162	-0.086	-0.154	-0.118	-0.134	-0.135	-----	.004	-----	.058
0.714	-0.132	-0.113	-0.126	-0.192	-0.182	-0.086	-0.136	-0.102	-0.114	-0.127	-----	.020	-----	.036
0.761	-0.132	-0.099	-0.118	-----	-----	-----	-0.122	-0.078	-0.088	-0.117	-----	.028	-----	.030
0.785	-0.132	-0.092	-0.112	-0.130	-0.194	-0.082	-0.122	-0.084	-0.078	-0.113	-----	.022	-----	.028
0.809	-0.124	-0.082	-0.104	-0.114	-0.174	-0.088	-0.122	-0.100	-0.078	-0.103	-----	.024	-----	.026
0.832	-0.124	-0.082	-0.116	-0.126	-0.176	-0.101	-0.120	-0.100	-----	-0.119	-----	.036	-----	.014
0.856	-0.124	-0.078	-0.116	-0.126	-0.168	-0.105	-0.118	-0.100	-0.070	-0.119	-----	.038	-----	.004
0.880	-0.118	-0.074	-0.112	-0.122	-0.158	-0.101	-0.114	-0.094	-0.070	-0.119	-----	.040	-----	.002
0.904	-0.112	-0.070	-0.104	-0.110	-0.136	-0.094	-0.104	-0.086	-0.070	-0.117	-----	.048	-----	.002
0.928	-0.106	-0.066	-0.088	-0.098	-0.118	-0.080	-0.094	-0.082	-0.066	-0.113	-----	.060	-----	.018
0.951	-0.094	-0.062	-0.086	-0.098	-0.114	-0.082	-0.088	-0.082	-0.064	-0.109	-----	.054	-----	.058
0.975	-0.076	-0.056	-0.078	-0.092	-0.112	-0.088	-0.086	-0.078	-0.062	-0.097	-----	.064	-----	.058
0.999	-0.048	-0.078	-0.054	-0.050	-0.060	-0.090	-----	-----	-----	-----	-----	.056	-----	.068
1.000	-0.052	-0.078	-0.046	-0.038	-0.034	-0.072	-0.038	-0.042	-0.026	-0.054	-----	-----	-----	-----

NACA

TABLE IV.- PRESSURE COEFFICIENT DATA FOR PARABOLIC BODY  
OF REVOLUTION (RM-10) MOUNTED ON STRAIGHT STING

HALF AXIAL TRANSITION STRIPS

(a)  $\alpha = 4.00$

Station, $x/L$	Radial angle, $\phi$ , deg		
	131	221	311
0.024	0.036	0.040	0.086
.048	.038	.034	.078
.071	.032	.022	.076
.095	.026	.022	.064
.119	.022	.016	.056
.143	.016	.014	.056
.167	.016	.012	.052
.190	.008	.008	.046
.214	.008	.008	.046
.238	0	0	-----
.262	0	-.002	-----
.285	-.004	-.002	-----
.333	-.010	-.008	-----
.381	-.012	-.010	-----
.428	-.016	-.016	-----
.476	-.024	-.024	-----
.523	-.026	-.020	-----
.571	-.034	-.032	-----
.618	-.040	-.040	-----
.666	-.040	-.036	-----
.714	-.040	-.040	-----
.761	-.036	-.036	-----
.785	-.036	-.028	-----
.809	-.030	-.028	-----
.832	-.036	-.036	-----
.856	-.038	-.028	-----
.880	-.036	-.030	-----
.904	-.028	-.030	-----
.928	-.016	-.024	-----
.951	-.016	-.024	-----
.975	-.016	-.022	-----
.999	-.020	-----	-----
1.000	-.018	-.010	-----



TABLE IV.- PRESSURE COEFFICIENT DATA FOR PARABOLIC BODY  
OF REVOLUTION (RM-10) MOUNTED ON STRAIGHT STING

HALF AXIAL TRANSITION STRIPS - Continued

(b)  $\alpha = 8.05$

Station, x/L	Radial angle, $\phi$ , deg		
	133	223	313
0.024	0.006	0.006	0.104
.048	.006	0	.086
.071	0	-.006	.090
.095	-.008	-.006	.078
.119	-.010	-.012	.064
.143	-.016	-.014	.064
.167	-.018	-.018	.062
.190	-.020	-.020	.054
.214	-.022	-.022	.054
.238	-.030	-.030	-----
.262	-.030	-.030	-----
.285	-.034	-.030	-----
.333	-.038	-.034	-----
.381	-.046	-.042	-----
.428	-.050	-.042	-----
.476	-.054	-.048	-----
.523	-.048	-.044	-----
.571	-.048	-.050	-----
.618	-.056	-.058	-----
.666	-.056	-.056	-----
.714	-.060	-.062	-----
.761	-.054	-.050	-----
.785	-.054	-.040	-----
.809	-.046	-.040	-----
.832	-.054	-.042	-----
.856	-.058	-.042	-----
.880	-.056	-.042	-----
.904	-.048	-.044	-----
.928	-.038	-.042	-----
.951	-.038	-.048	-----
.975	-.042	-.052	-----
.999	-.046	-----	-----
1.000	-.034	-.024	-----





TABLE IV.- PRESSURE COEFFICIENT DATA FOR PARABOLIC BODY  
OF REVOLUTION (RM-10) MOUNTED ON STRAIGHT STING

HALF AXIAL TRANSITION STRIPS - Continued

(c)  $\alpha = 12.05$

Station, $x/L$	Radial angle, $\phi$ , deg		
	. 133.7	223.7	313.7
0.024	-0.030	-0.032	0.116
.048	-.032	-.038	.098
.071	-.040	-.044	.108
.095	-.040	-.044	.092
.119	-.048	-.052	.080
.143	-.056	-.054	.074
.167	-.060	-.056	.072
.190	-.060	-.060	.064
.214	-.060	-.060	.060
.238	-.068	-.064	-----
.262	-.068	-.064	-----
.285	-.072	-.064	-----
.333	-.072	-.076	-----
.381	-.080	-.078	-----
.428	-.084	-.082	-----
.476	-.086	-.088	-----
.523	-.086	-.092	-----
.571	-.086	-.100	-----
.618	-.103	-.116	-----
.666	-.107	-.124	-----
.714	-.111	-.124	-----
.761	-.107	-.112	-----
.785	-.107	-.104	-----
.809	-.098	-.100	-----
.832	-.100	-.096	-----
.856	-.100	-.092	-----
.880	-.092	-.086	-----
.904	-.082	-.084	-----
.928	-.064	-.072	-----
.951	-.064	-.068	-----
.975	-.060	-.068	-----
.999	-.044	-----	-----
1.000	-.040	-.038	-----



TABLE IV.- PRESSURE COEFFICIENT DATA FOR PARABOLIC BODY  
OF REVOLUTION (RM-10) MOUNTED ON STRAIGHT STING

HALF AXIAL TRANSITION STRIPS - Concluded

(d)  $\alpha = 16.10$

Station, $x/L$	Radial angle, $\phi$ , deg		
	134	224	314
0.024	-0.064	-0.064	0.141
.048	-.066	-.076	.125
.071	-.072	-.080	.143
.095	-.080	-.082	.121
.119	-.090	-.090	.105
.143	-.099	-.097	.095
.167	-.101	-.101	.088
.190	-.101	-.101	.078
.214	-.101	-.101	.078
.238	-.107	-.099	-----
.262	-.105	-.099	-----
.285	-.113	-.101	-----
.333	-.113	-.105	-----
.381	-.113	-.109	-----
.428	-.113	-.113	-----
.476	-.123	-.125	-----
.523	-.125	-.129	-----
.571	-.121	-.141	-----
.618	-.137	-.149	-----
.666	-.145	-.157	-----
.714	-.131	-.137	-----
.761	-.129	-.113	-----
.785	-.123	-.109	-----
.809	-.117	-.107	-----
.832	-.129	-.105	-----
.856	-.129	-.099	-----
.880	-.121	-.093	-----
.904	-.109	-.088	-----
.928	-.090	-.076	-----
.951	-.084	-.076	-----
.975	-.080	-.072	-----
.999	-.058	-----	-----
1.000	-.044	-.040	-----



TABLE V.- PRESSURE COEFFICIENT DATA FOR PARABOLIC BODY  
OF REVOLUTION (RM-10) MOUNTED ON STRAIGHT STING

RADIAL TRANSITION STRIPS LOCATED AT

MAXIMUM THICKNESS  $x/L = 0.614$

(a)  $\alpha = 4.00$

Station, $x/L$	Radial angle, $\phi$ , deg							
	56	86	146	176	236	266	326	356
0.024	0.062	0.042	0.030	0.032	0.038	0.048	0.103	0.105
.048	.060	.042	.032	.030	.028	.042	.084	.094
.071	.050	.034	.026	.024	.020	.028	-----	-----
.095	.048	.032	.016	.016	.020	.030	-----	-----
.119	.050	.030	.016	.012	.016	.024	.060	-----
.143	.042	.026	.010	.008	.008	.020	.060	.074
.167	.040	.022	.012	.010	.008	.014	.060	.072
.190	.038	.018	.008	.008	.008	.012	.052	.066
.214	.034	.016	.004	.004	.004	.010	.052	.064
.238	.026	.008	0	0	-----	.002	-----	-----
.262	.024	.006	.004	.002	.004	.004	-----	-----
.285	.016	0	.006	.004	.006	0	.034	.050
.303	.002	.008	.012	.008	.010	.008	.034	.046
.321	0	.014	.014	.010	.012	.010	.022	.034
.428	.006	.018	.016	.014	.020	.018	.018	.032
.476	.016	.026	.028	.024	.032	.034	.014	.022
.523	.016	.026	.028	.022	.026	.028	.006	.018
.571	.023	.038	.032	.026	.036	.040	.002	.002
.618	.026	.040	.046	.032	.044	.056	.010	.002
.666	.056	.040	.042	.032	.044	.052	.006	.004
.714	.050	.054	.036	.030	.040	.054	.038	.026
.761	.054	.050	-----	-----	.040	.052	.022	.014
.785	.054	.054	.034	.026	.032	.040	.040	.038
.809	.050	.048	.028	.016	.028	.038	.048	.046
.832	.054	.054	.034	.024	.036	.052	.048	.046
.856	.062	.060	.036	.026	.036	.048	-----	-----
.880	.062	.056	.036	.028	.034	.048	-----	-----
.904	.054	.046	.030	.022	.020	.044	-----	-----
.928	.048	.038	.016	.012	.032	.040	.048	.046
.951	.046	.036	.016	.016	.032	.040	.050	.046
.975	.046	.030	.020	.020	.032	.040	.054	.052
.999	.014	.014	.003	.014	-----	.062	.062	.058
1.000	.002	.008	.002	.002	.004	0	.058	.058

NACA

TABLE V.- PRESSURE COEFFICIENT DATA FOR PARABOLIC BODY  
OF REVOLUTION (RM-10) MOUNTED ON STRAIGHT STING

RADIAL TRANSITION STRIPS LOCATED AT MAXIMUM

THICKNESS  $x/L = 0.614$  - Continued

(b)  $\alpha = 8.05$

Station, $x/L$	Radial angle, $\phi$ , deg						
	58	88	148	178	238	268	328
0.024	0.062	0.010	0.006	0.014	0.002	0.018	0.130
.048	.062	.012	.006	.014	-.008	.006	.114
.071	.050	-.002	0	.010	-.012	0	-----
.095	.046	-.006	-.008	.004	-.012	0	-----
.119	.046	-.006	-.008	.002	-.018	-.010	-----
.143	.040	-.012	-.016	-.002	-.022	-.012	.090
.167	.034	-.020	-.018	-.004	-.024	-.018	.086
.190	.034	-.018	-.018	-.002	-.026	-.020	.078
.214	.032	-.020	-.022	-.002	-.028	-.022	.080
.238	.018	-.020	-.030	-.006	-.034	-.034	-----
.262	.016	-.032	-.032	-.006	-.034	-.034	-----
.285	.010	-.038	-.036	-.010	-.038	-.038	.084
.333	.006	-.048	-.036	-.010	-.038	-.038	.080
.381	-.010	-.054	-.034	-.014	-.048	-.050	.076
.428	-.022	-.056	-.034	-.018	-.054	-.056	.064
.476	-.034	-.060	-.038	-.024	-.062	-.066	.052
.523	-.038	-.070	-.036	-.020	-.058	-.064	.044
.571	-.048	-.078	-.038	-.026	-.062	-.078	.028
.618	-.082	-.102	-.034	-.040	-.066	-.088	.024
.666	-----	-.046	-.050	-.036	-.062	-.094	.026
.714	-.082	-.096	-.048	-.034	-.056	-.090	-.012
.761	-.086	-.092	-.054	-.030	-.044	-.082	-.006
.785	-.086	-.092	-.046	-.022	-.038	-.074	-.024
.809	-.082	-.086	-.056	-.032	-.046	-.070	-.042
.832	-.086	-.086	-.056	-.036	-.048	-.074	-.042
.856	-.094	-.088	-.056	-.036	-.046	-.070	-----
.880	-.094	-.076	-.054	-.036	-.046	-.062	-----
.904	-.086	-.060	-.044	-.034	-.030	-.056	-.050
.928	-.078	-.052	-.034	-.022	-.040	-.052	-.050
.951	-.072	-.048	-.034	-.024	-.040	-.050	-.056
.975	-.070	-.040	-.038	-.032	-.040	-.050	-.064
.999	-.040	-.044	-.028	-.040	-----	-----	-.074
1.000	-.016	-.044	-.022	-.022	-.014	-.024	-.068

NACA

TABLE V.- PRESSURE COEFFICIENT DATA FOR PARABOLIC BODY  
OF REVOLUTION (RM-10) MOUNTED ON STRAIGHT STING

RADIAL TRANSITION STRIPS LOCATED AT MAXIMUM

THICKNESS  $x/L = 0.614$  - Continued

(c)  $\alpha = 12.05$

Station, $x/L$	Radial angle, $\phi$ , deg		
	58.7	148.7	238.7
0.024	0.048	-0.028	-0.036
.048	.052	-.032	-.044
.071	.034	-.036	-.048
.095	.034	-.040	-.050
.119	.032	-.044	-.056
.143	.024	-.056	-.058
.167	.016	-.058	-.060
.190	.020	-.058	-.058
.214	.016	-.058	-.064
.238	.004	-.068	-.068
.262	0	-.072	-.066
.285	-.014	-.076	-.066
.333	-.020	-.080	-.078
.381	-.036	-.092	-.082
.428	-.044	-.092	-.084
.476	-.058	-.108	-.088
.523	-.064	-.108	-.090
.571	-.080	-.112	-.092
.618	-.108	-.136	-.090
.666	-----	-.116	-.090
.714	-.112	-.106	-.076
.761	-.124	-----	-.016
.785	-.120	-.072	-.014
.809	-.120	-.056	-.056
.832	-.126	-.056	-.052
.856	-.134	-.052	-.064
.880	-.140	-.052	-.068
.904	-.136	-.042	-.064
.928	-.128	-.032	-.036
.951	-.118	-.044	-.054
.975	-.104	-.048	-.050
.999	-.060	-.032	-.052
1.000	-.040	-.028	-.032
			0.170
			.156
			-----
			-----
			-----
			.128
			.124
			.116
			.112
			-----
			-----
			-----
			.092
			.084
			.084
			.072
			.052
			.040
			.024
			.020
			.016
			-.016
			-.014
			-.038
			-.052
			-.048
			-----
			-----
			-.064
			-.068
			-.076
			-.088
			-.088

NACA

TABLE V.- PRESSURE COEFFICIENT DATA FOR PARABOLIC BODY  
OF REVOLUTION (RM-10) MOUNTED ON STRAIGHT STING

RADIAL TRANSITION STRIPS LOCATED AT MAXIMUM

THICKNESS  $x/L = 0.614$  - Concluded

(d)  $\alpha = 16.10$

Station, $x/L$	Radial angle, $\phi$ , deg					
	59	89	149	179	239	269
0.024	0.040	-0.090	-0.072	-0.030	-0.076	-0.080
.048	.062	-.082	-.076	-.016	-.080	-.092
.071	.036	-.098	-.078	-.012	-.084	-.100
.095	.024	-.110	-.088	-.024	-.088	-.102
.119	.018	-.112	-.102	-.026	-.092	-.108
.143	.012	-.118	-.112	-.032	-.100	-.116
.167	0	-.126	-.112	-.028	-.104	-.120
.190	.004	-.122	-.112	-.032	-.104	-.120
.214	-.008	-.122	-.116	-.032	-.104	-.120
.238	-.012	-.130	-.126	-.038	-.102	-.116
.262	-.020	-.134	-.124	-.036	-.102	-.116
.285	-.030	-.138	-.128	-.040	-.104	-.118
.308	-.044	-.136	-.134	-.044	-.112	-.124
.331	-.054	-.130	-.140	-.050	-.116	-.128
.354	-.068	-.130	-.142	-.060	-.124	-.128
.376	-.080	-.136	-.152	-.072	-.134	-.136
.399	-.094	-.136	-.150	-.072	-.132	-.126
.421	-.108	-.136	-.144	-.076	-.132	-.124
.444	-.134	-.158	-.156	-.101	-.142	-.126
.466	-.106	-.106	-.148	-.099	-.116	-.128
.489	-.148	-.142	-.124	-.070	-.084	-.104
.511	-.162	-.134	-.124	-.068	-.068	-.088
.534	-.168	-.130	-.076	-.068	-.068	-.084
.556	-.166	-.126	-.064	-.068	-.076	-.082
.579	-.174	-.130	-.076	-.072	-.084	-.092
.601	-.184	-.126	-.082	-.076	-.076	-.092
.624	-.188	-.114	-.086	-.072	-.068	-.088
.646	-.188	-.102	-.084	-.064	-.040	-.078
.669	-.188	-.094	-.076	-.060	-.060	-.072
.691	-.184	-.082	-.080	-.062	-.060	-.064
.714	-.144	-.072	-.080	-.076	-.060	-.060
.736	-.064	-.074	-.040	-.074	-.040	-.060
.759	-.040	-.074	-.036	-.044	-.040	-.072
.781						
.804						
.826						
.849						
.871						
.894						
.916						
.939						
.961						
.984						
1.000						

NACA

TABLE VI.-- PRESSURE COEFFICIENT DATA FOR PARABOLIC BODY  
OF REVOLUTION (RM-10) MOUNTED ON STRAIGHT STING

RADIAL TRANSITION STRIPS LOCATED

AT  $x/L = 0.834$

(a)  $\alpha = 4.00$

Station, $x/L$	Radial angle, $\phi$ , deg							
	56	86	146	176	236	266	326	356
0.024	0.074	0.044	0.032	0.032	0.040	0.048	0.096	0.106
.048	.072	.042	.032	.032	.030	.042	.086	.098
.071	.060	.034	.028	.024	.022	.030	-----	-----
.095	.058	.032	.022	.020	.022	.032	-----	-----
.119	.058	.032	.016	.016	.016	.024	-----	-----
.143	.052	.026	.012	.008	.012	.020	.064	.074
.167	.048	.022	.012	.012	.008	.016	.064	.074
.190	.048	.018	.008	.008	.008	.016	.056	.066
.214	.044	.018	.006	.008	.006	.012	.056	.066
.238	.024	.008	0	0	0	.004	-----	-----
.262	.024	.006	0	0	-.002	.004	-----	-----
.285	.016	0	-.004	-.004	-.002	0	.044	.050
.333	.004	-.008	-.008	-.008	-.008	-.004	.042	.046
.381	0	-.010	-.012	-.008	-.012	-.008	.026	.036
.428	-.006	-.018	-.016	-.012	-.018	-.016	.024	.034
.476	-.016	-.026	-.024	-.024	-.028	-.032	.016	.022
.523	-.016	-.024	-.028	-.020	-.024	-.028	.006	.018
.571	-.028	-.038	-.036	-.024	-.036	-.038	-.004	.002
.618	-.038	-.046	-.040	-.032	-.042	-.046	-.008	.002
.666	-----	-----	-.040	-.032	-.042	-.048	-.004	.004
.714	-.052	-.050	-.040	-.032	-.042	-.054	-.028	-.020
.761	-.056	-.052	-----	-----	-.040	-.054	-.028	-.024
.785	-.056	-.052	-.034	-.032	-.030	-.048	-.048	-.038
.809	-.054	-.048	-.028	-.020	-.034	-.046	-.052	-.046
.832	-.028	-.046	.036	0	.086	0	-.052	-.046
.856	-.068	-.062	-.036	-.028	-.040	-.056	-----	-----
.880	-.064	-.062	-.034	-.024	-.034	-.056	-----	-----
.904	-.060	-.058	-.028	-.016	.010	.022	-----	-----
.928	-.054	-.046	-.016	-.008	-.024	-.036	-.044	-.038
.951	-.050	-.034	-.012	-.008	-.028	-.036	-.048	-.046
.975	-.044	-.026	-.016	-.008	-.028	-.036	-.052	-.050
.999	-.022	-.026	-.012	-.026	-----	-----	-.060	-.058
1.000	.002	-.022	-.008	-.012	.002	-.012	-.056	-.060



TABLE VI.-- PRESSURE COEFFICIENT DATA FOR PARABOLIC BODY  
OF REVOLUTION (RM-10) MOUNTED ON STRAIGHT STING

RADIAL TRANSITION STRIPS LOCATED

AT  $x/L = 0.834$  - Continued

(b)  $\alpha = 8.05$

Station, $x/L$	Radial angle, $\phi$ , deg							
	58	88	148	178	238	268	328	358
0.024	0.064	0.014	0.010	0.012	0.006	0.016	0.132	0.159
.048	.068	.014	.006	.014	-.002	.004	.114	.145
.071	.054	0	.002	.010	-.006	0	-----	-----
.095	.048	-.006	-.006	.004	-.008	0	-----	-----
.119	.048	-.002	-.006	.002	-.014	-.008	-----	-----
.143	.044	-.010	-.014	0	-.018	-.012	.094	.119
.167	.032	-.016	-.014	-.004	-.022	-.020	.088	.115
.190	.036	-.016	-.016	0	-.022	-.020	.078	.105
.214	.032	-.016	-.018	-.004	-.022	-.024	.082	.105
.238	.020	-.026	-.026	-.006	-.030	-.032	-----	-----
.262	.016	-.030	-.030	-.006	-.030	-.032	-----	-----
.285	.008	-.038	-.032	-.008	-.030	-.032	.060	.090
.333	-.004	-.046	-.032	-.012	-.036	-.038	.056	.086
.381	-.010	-.050	-.030	-.012	-.044	-.048	.054	.078
.428	-.020	-.056	-.032	-.020	-.050	-.056	.046	.066
.476	-.032	-.066	-.034	-.026	-.058	-.068	.032	.056
.523	-.034	-.066	-.034	-.020	-.054	-.064	.022	.046
.571	-.048	-.076	-.040	-.024	-.060	-.076	.008	.034
.618	-.064	-.082	-.046	-.036	-.062	-.080	0	.026
.666	-----	-----	-.046	-.036	-.062	-.080	.004	.026
.714	-.080	-.086	-.048	-.036	-.058	-.080	-.024	-.002
.761	-.082	-.082	-----	-----	-.056	-.076	-.028	-.006
.785	-.082	-.078	-.050	-.030	-.052	-.068	-.048	-.024
.809	-.076	-.074	-.050	-.024	-.056	-.064	-.056	-.038
.832	-.044	-.070	-.012	.048	.042	-.068	-.056	-.038
.856	-.084	-.082	-.070	-.036	-.062	-.072	-----	-----
.880	-.076	-.078	-.070	-.044	-.062	-.072	-----	-----
.904	-.072	-.062	-.062	-.034	-.052	.010	-----	-----
.928	-.066	-.046	-.054	-.026	-.054	-.048	-.052	-.038
.951	-.068	-.040	-.056	-.024	-.050	-.052	-.060	-.042
.975	-.058	-.034	-.062	-.032	-.046	-.052	-.064	-.048
.999	-.046	-.056	-.040	-.048	-----	-----	-.074	-.058
1.000	-.032	-.054	-.024	-.036	-.028	-.036	-.072	-.062

NACA



TABLE VI.- PRESSURE COEFFICIENT DATA FOR PARABOLIC BODY  
OF REVOLUTION (RM-10) MOUNTED ON STRAIGHT STING

RADIAL TRANSITION STRIPS LOCATED

AT  $x/L = 0.834$  - Continued

(c)  $\alpha = 12.05$

Station, $x/L$	Radial angle, $\phi$ , deg							
	58.7	88.7	148.7	178.7	238.7	268.7	328.7	358.7
0.024	0.054	-0.036	-0.028	-0.006	-0.034	-.036	0.167	0.219
.048	.056	-.036	-.030	-.004	-.040	-.044	.151	.207
.071	.038	-.052	-.036	-.006	-.046	-.048	-----	-----
.095	.038	-.048	-.040	-.008	-.048	-.054	-----	-----
.119	.034	-.054	-.044	-.010	-.052	-.060	-----	-----
.143	.026	-.062	-.052	-.016	-.056	-.064	.123	.171
.167	.018	-.070	-.056	-.014	-.056	-.068	.123	.171
.190	.022	-.064	-.056	-.014	-.060	-.072	.111	.159
.214	.016	-.068	-.058	-.012	-.060	-.072	.111	.163
.238	.002	-.076	-.068	-.020	-.064	-.080	-----	-----
.262	0	-.080	-.068	-.020	-.064	-.076	-----	-----
.285	.014	-.088	-.076	-.020	-.062	-.078	.090	.143
.333	-.018	-.092	-.076	-.020	-.076	-.088	.088	.139
.381	-.034	-.094	-.092	-.032	-.080	-.096	.086	.135
.428	-.042	-.094	-.090	-.030	-.084	-.092	.074	.115
.476	-.056	-.096	-.103	-.038	-.086	-.094	.054	.105
.523	-.062	-.094	-.107	-.036	-.086	-.092	.042	.092
.571	-.076	-.094	-.109	-.044	-.092	-.094	.024	.076
.618	-.088	-.096	-.119	-.060	-.092	-.094	.022	.068
.666	-----	-----	-.115	-.062	-.096	-.096	.018	.064
.714	-.101	-.096	-.115	-.074	-.096	-.096	-.014	.032
.761	-.103	-.092	-----	-----	-.086	-.086	-.016	.024
.785	-.101	-.092	-.107	-.068	-.080	-.084	-.038	.004
.809	-.096	-.084	-.096	-.062	-.084	-.078	-.046	-.008
.832	-.062	-.076	-.076	-.012	.042	-.024	-.042	-.012
.856	-.097	-.090	-.107	-.080	-.076	-.086	-----	-----
.880	-.094	-.084	-.088	-.080	-.076	-.076	-----	-----
.904	-.086	-.062	-.078	-.080	-.014	.018	-----	-----
.928	-.088	-.050	-.068	-.076	-.056	-.052	-.050	-.018
.951	-.082	-.066	-.056	-.054	-.060	-.054	-.056	-.024
.975	-.074	-.060	-.058	-.060	-.056	-.056	-.064	-.032
.999	-.050	-.056	-.048	-.060	-----	-----	-.074	-.046
1.000	-.046	-.054	-.040	-.030	-.040	-.048	-.074	-.050



TABLE VI.- PRESSURE COEFFICIENT DATA FOR PARABOLIC BODY  
OF REVOLUTION (RM-10) MOUNTED ON STRAIGHT STING

RADIAL TRANSITION STRIPS LOCATED

AT  $x/L = 0.834$  - Concluded

(d)  $\alpha = 16.10$

Station, $x/L$	Radial angle, $\phi$ , deg							
	59	89	149	179	239	269	329	359
0.024	0.044	-0.090	-0.068	-0.030	-0.068	-0.086	0.218	0.294
.048	.054	-.088	-.072	-.016	-.076	-.096	.204	.287
.071	.036	-.101	-.076	-.014	-.080	-.097	-----	-----
.095	.026	-.109	-.084	-.022	-.084	-.107	-----	-----
.119	.020	-.111	-.100	-.026	-.088	-.111	-----	-----
.143	.016	-.119	-.108	-.032	-.096	-.119	.170	.243
.167	.002	-.127	-.108	-.028	-.100	-.119	.164	.235
.190	.004	-.123	-.108	-.032	-.100	-.119	.152	.223
.214	-.002	-.123	-.112	-.032	-.100	-.123	.154	.223
.238	-.010	-.131	-.120	-.036	-.100	-.119	-----	-----
.262	-.016	-.133	-.120	-.036	-.100	-.117	-----	-----
.285	-.032	-.137	-.124	-.038	-.100	-.119	.130	.207
.333	-.042	-.135	-.128	-.044	-.108	-.127	.130	.199
.381	-.054	-.127	-.134	-.048	-.116	-.127	.122	.193
.428	-.066	-.131	-.136	-.060	-.120	-.131	.112	.183
.476	-.080	-.135	-.148	-.072	-.128	-.135	.094	.163
.523	-.094	-.135	-.146	-.072	-.124	-.127	.078	.151
.571	-.106	-.135	-.142	-.076	-.128	-.123	.052	.123
.618	-.126	-.139	-.152	-.094	-.124	-.123	.038	.115
.666	-----	-----	-.152	-.092	-.124	-.125	.038	.105
.714	-.138	-.129	-.140	-.082	-.116	-.117	.006	.076
.761	-.132	-.119	-----	-----	-.100	-.099	-.006	.060
.785	-.128	-.111	-.136	-.076	-.094	-.094	-.020	.040
.809	-.118	-.107	-.124	-.076	-.100	-.088	-.028	.036
.832	-.078	-.092	-.110	-.020	.022	-.026	-.022	.034
.856	-.122	-.107	-.136	-.092	-.096	-.094	-----	-----
.880	-.122	-.107	-.116	-.096	-.084	-.084	-----	-----
.904	-.126	-.094	-.100	-.088	-.014	-.016	-----	-----
.928	-.130	-.107	-.086	-.084	-.062	-.056	-.038	.012
.951	-.138	-.096	-.080	-.056	-.060	-.060	-.044	.006
.975	-.134	-.076	-.068	-.076	-.052	-.060	-.054	0
.999	-.064	-.068	-.040	-.078	-----	-----	-.070	-.020
1.000	-.038	-.068	-.036	-.040	-.044	-.070	-.074	-.028



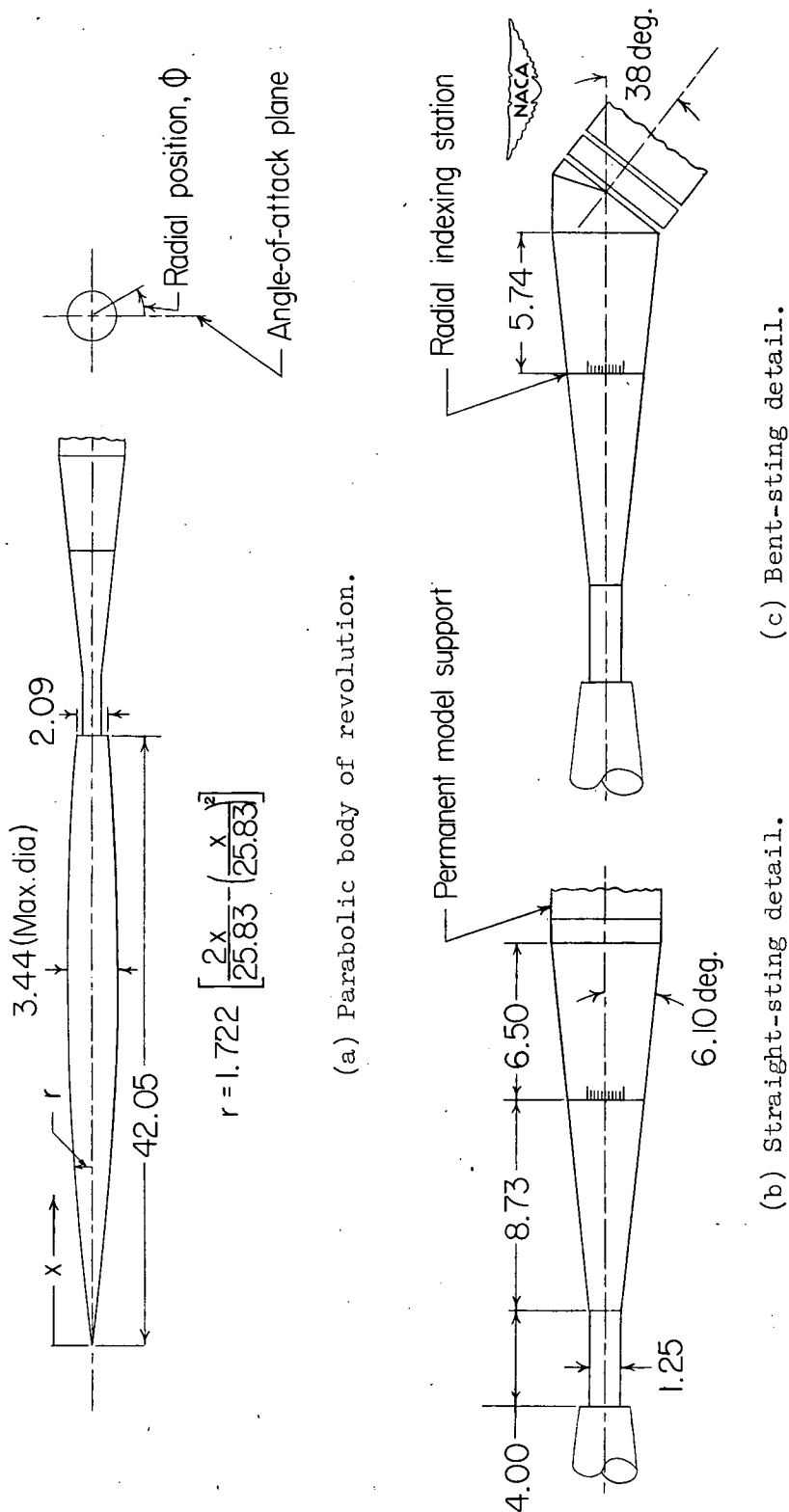
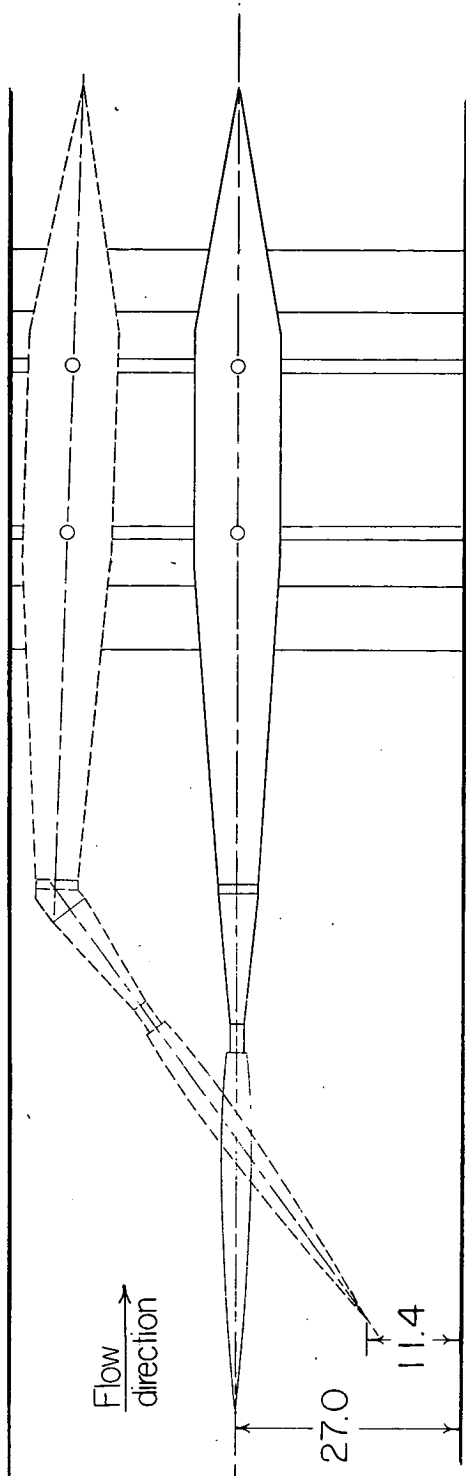
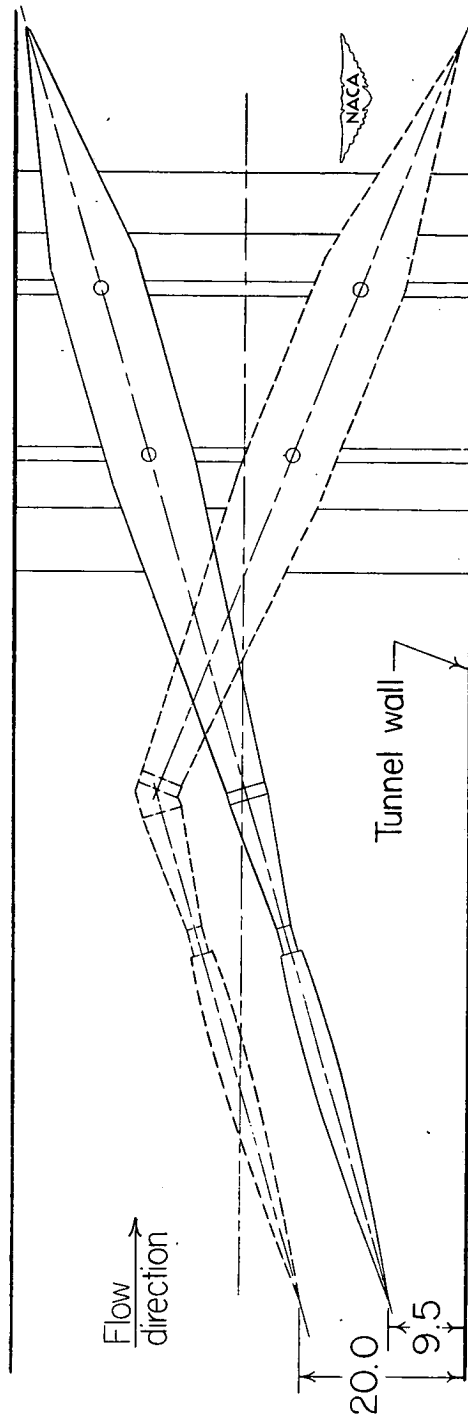


Figure 1.- Schematic layout of a parabolic body of revolution and sting mounting details. All dimensions in inches unless otherwise specified.

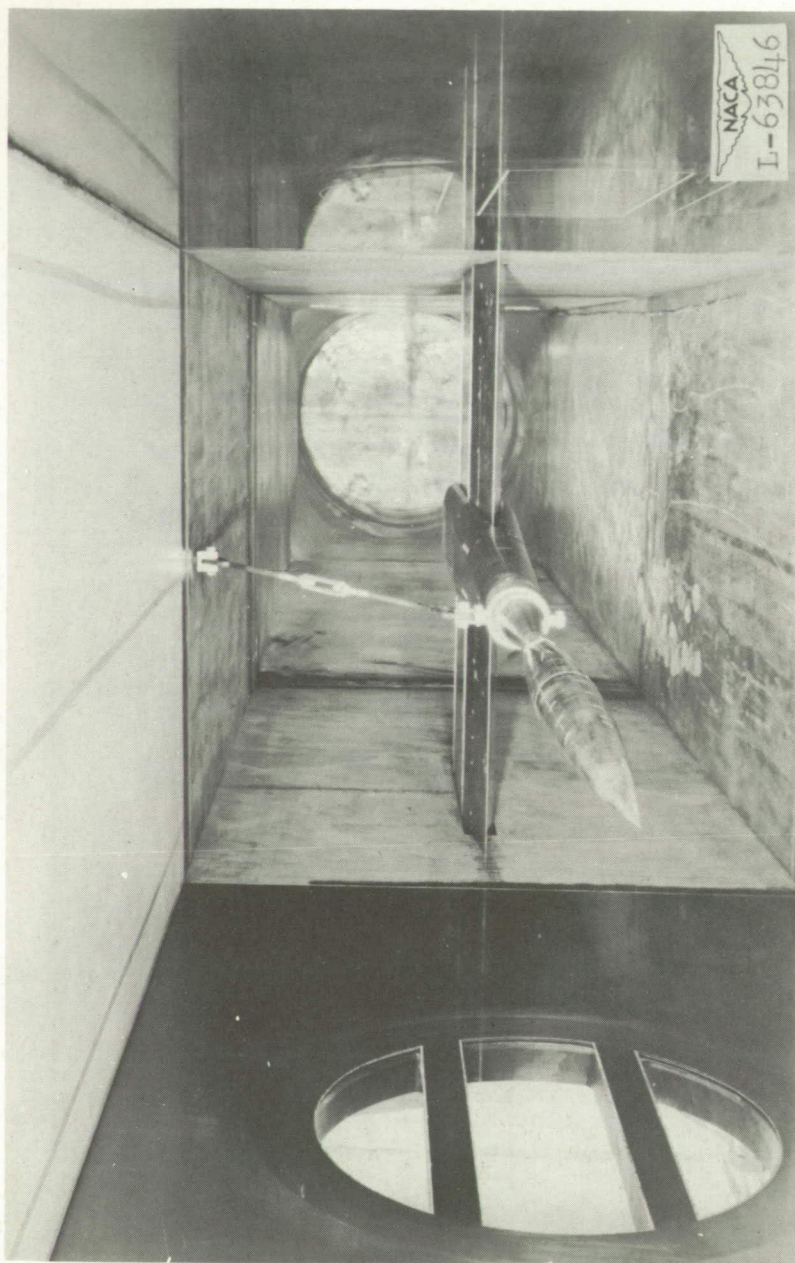


(a) Model installation,  $\alpha = 0^\circ$  and  $36^\circ$ .



(b) Model installation,  $\alpha = 16^\circ$ .

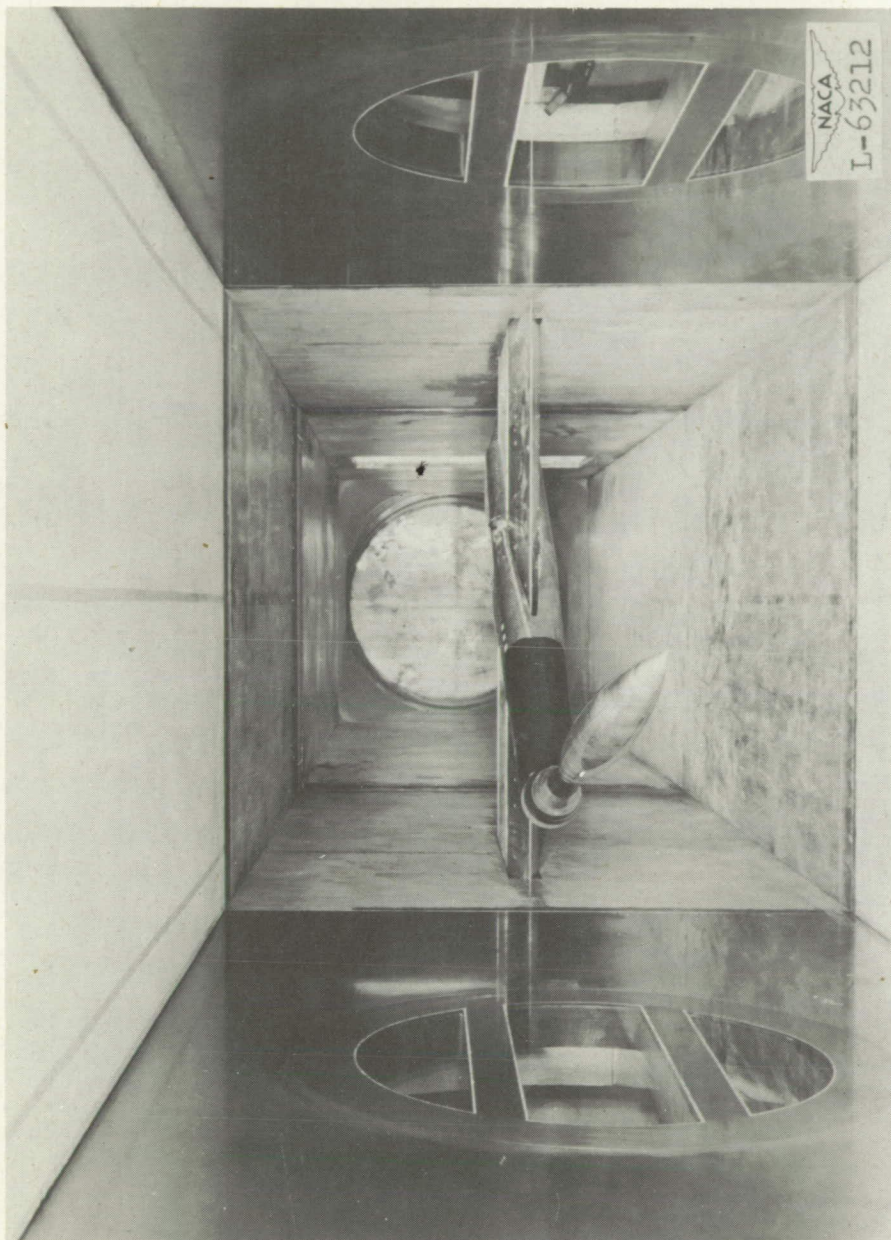
Figure 2.- Schematic arrangement of model mounted on straight and bent stings in the Langley 4- by 4-foot supersonic tunnel for extreme angular positions. All dimensions in inches unless otherwise specified.



(a) Straight sting.

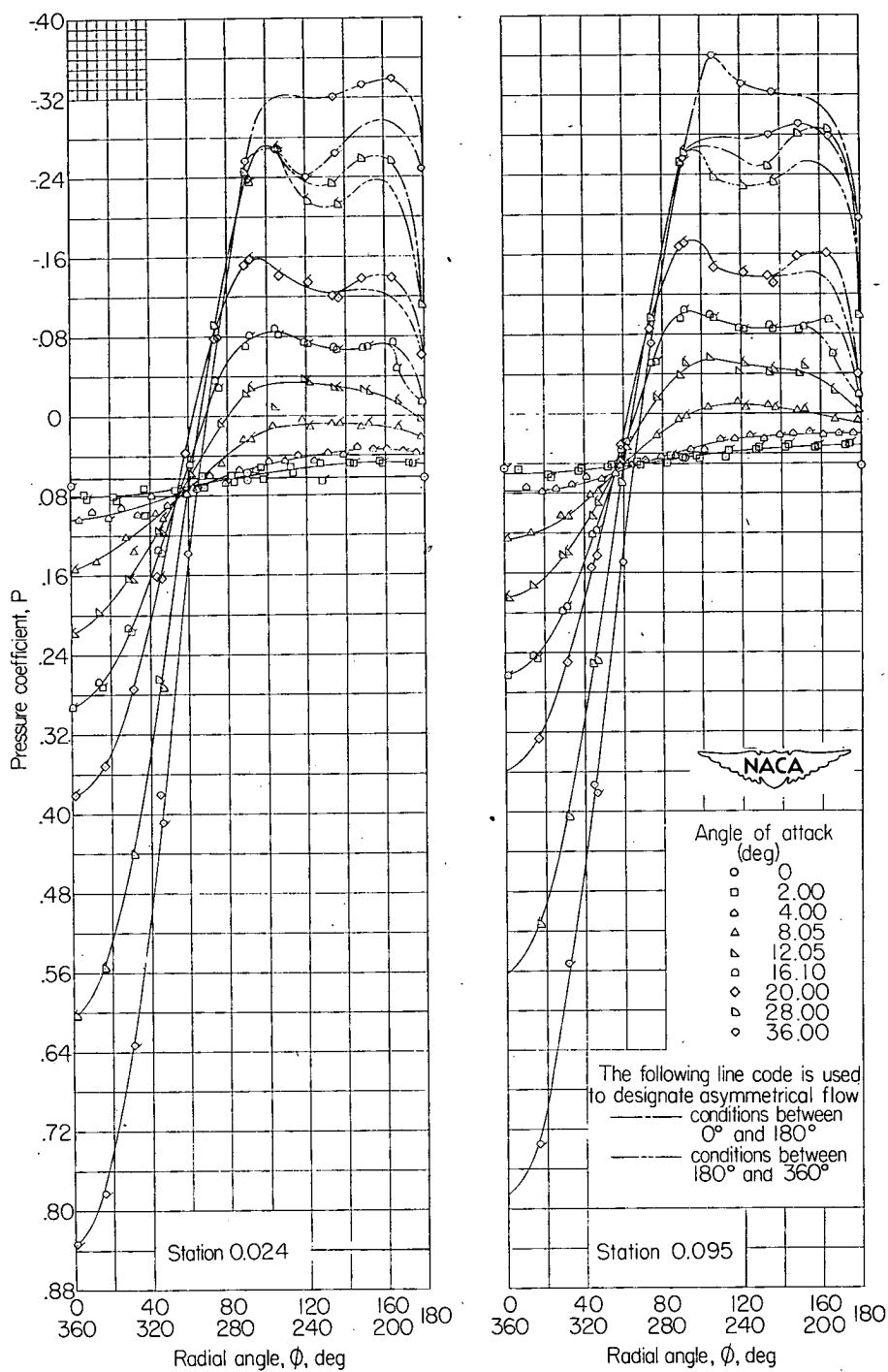
Figure 3.- Downstream view of test model mounted on the straight and the  
38° bent stings in the Langley 4- by 4-foot supersonic tunnel.





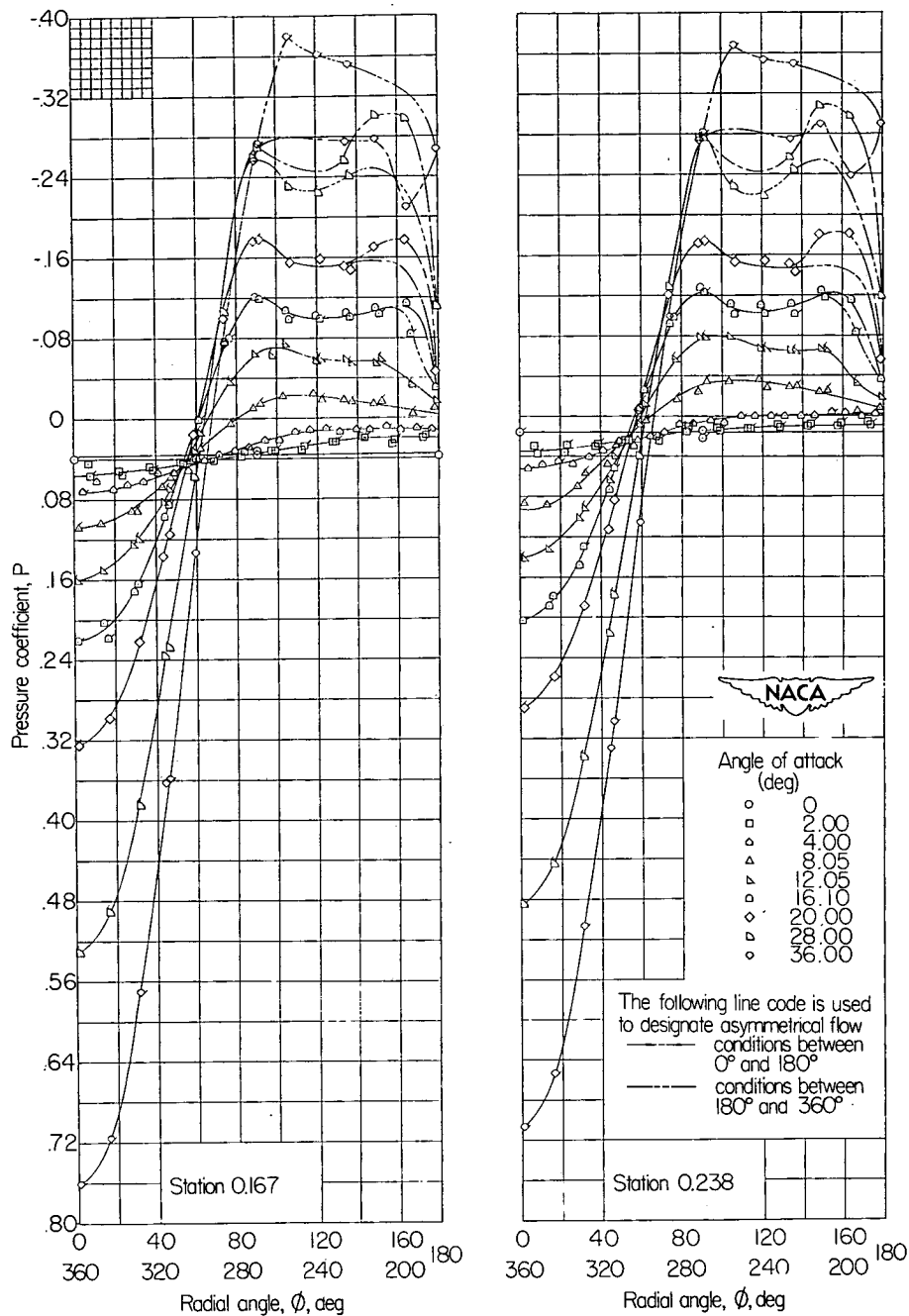
(b) 38° bent sting.

Figure 3.- Concluded.



(a) Stations 0.024 and 0.095.

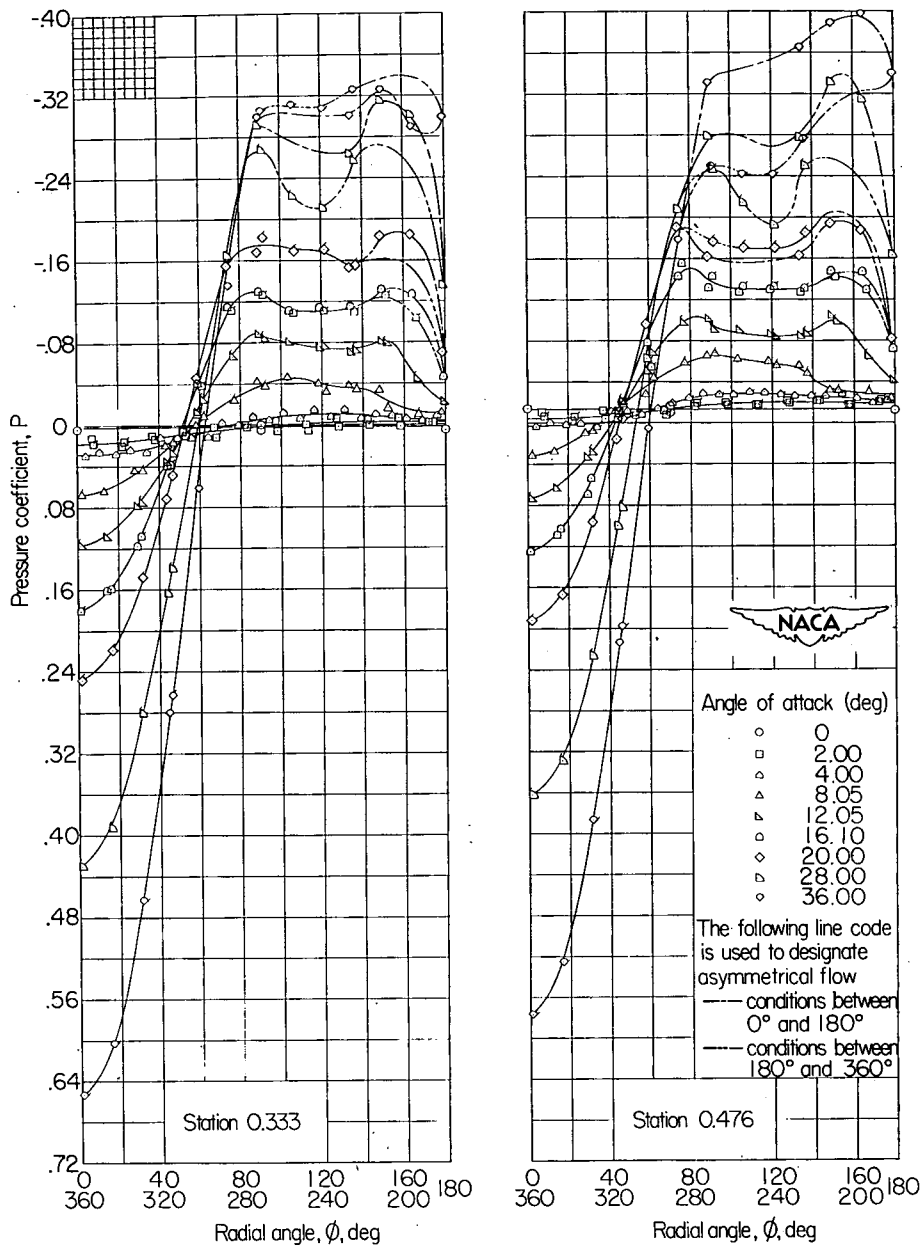
Figure 4.- Pressure-coefficient variation with radial position for 12 representative stations along the body. (Flagged symbols indicate test points between  $180^\circ$  and  $360^\circ$ .)



(b) Stations 0.167 and 0.238.

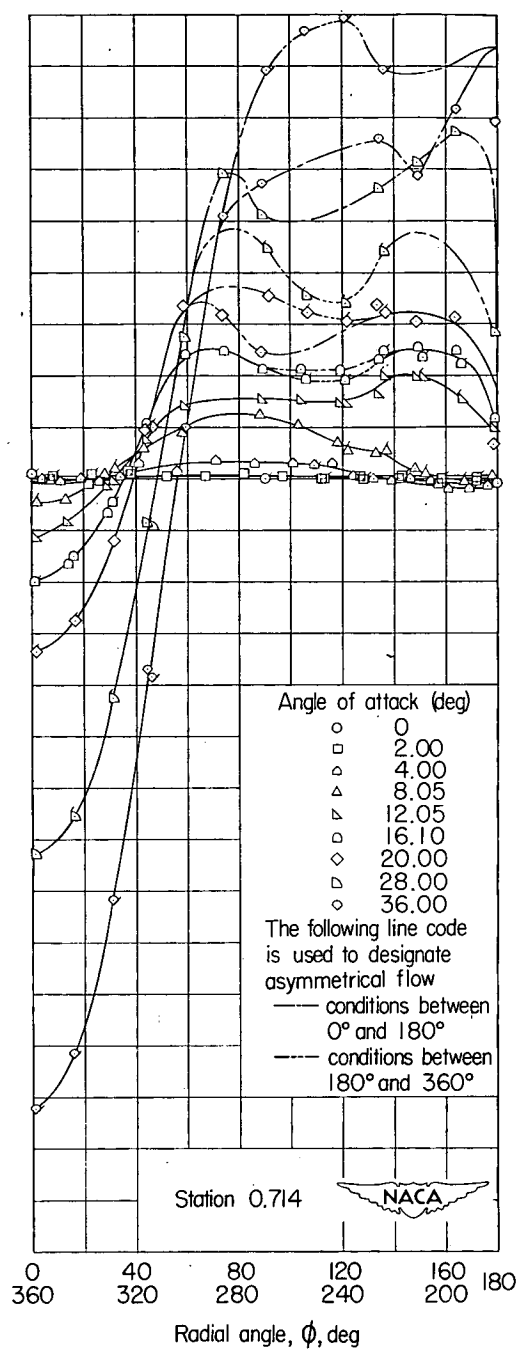
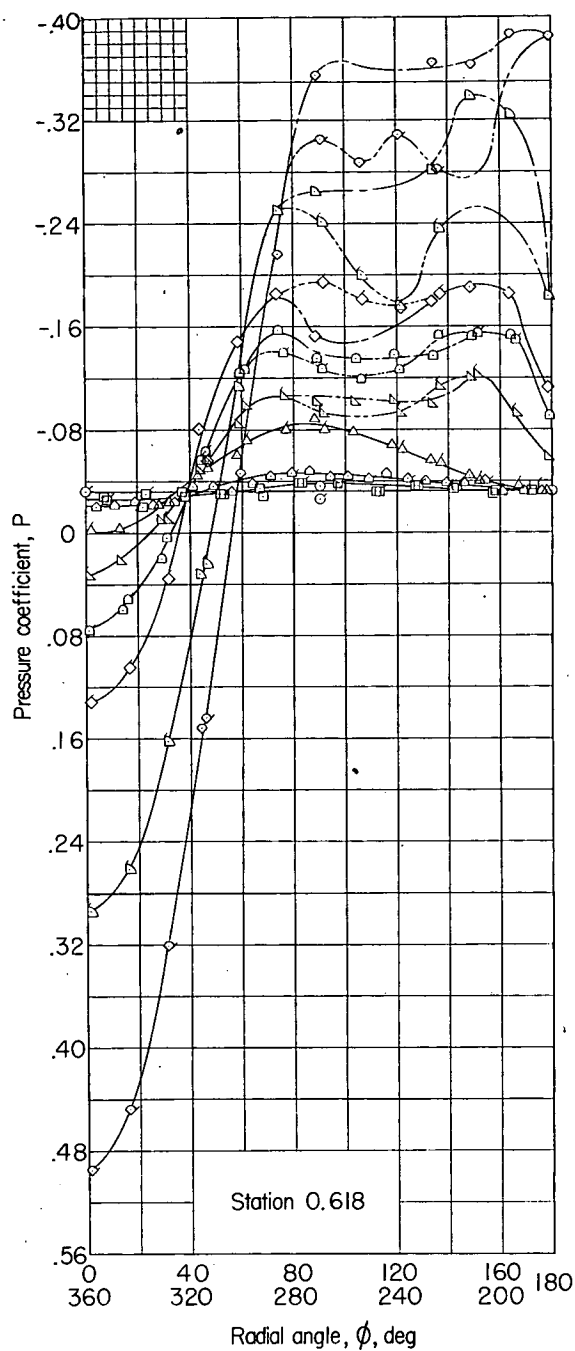
Figure 4.- Continued.





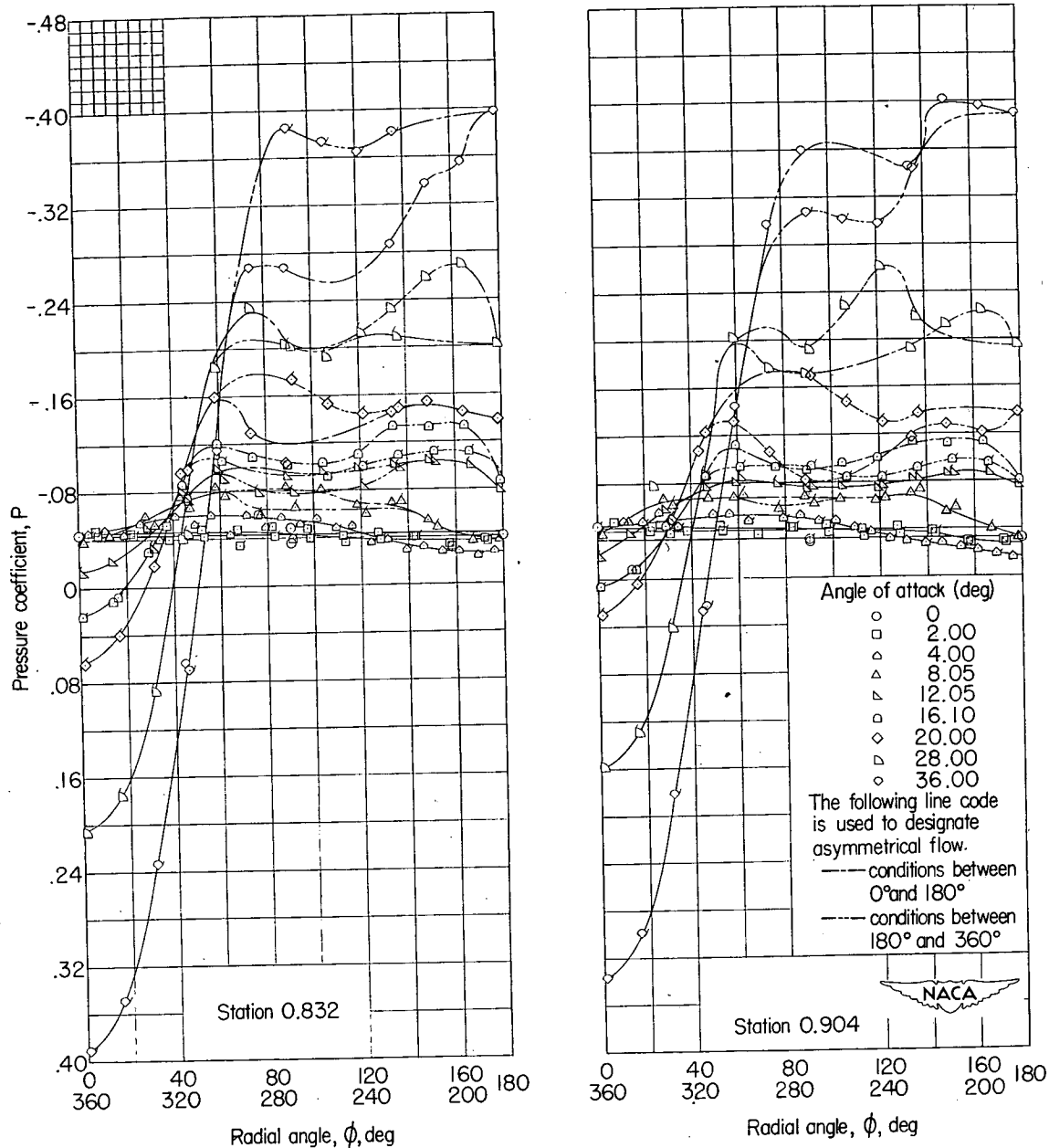
(c) Stations 0.333 and 0.476.

Figure 4.- Continued.



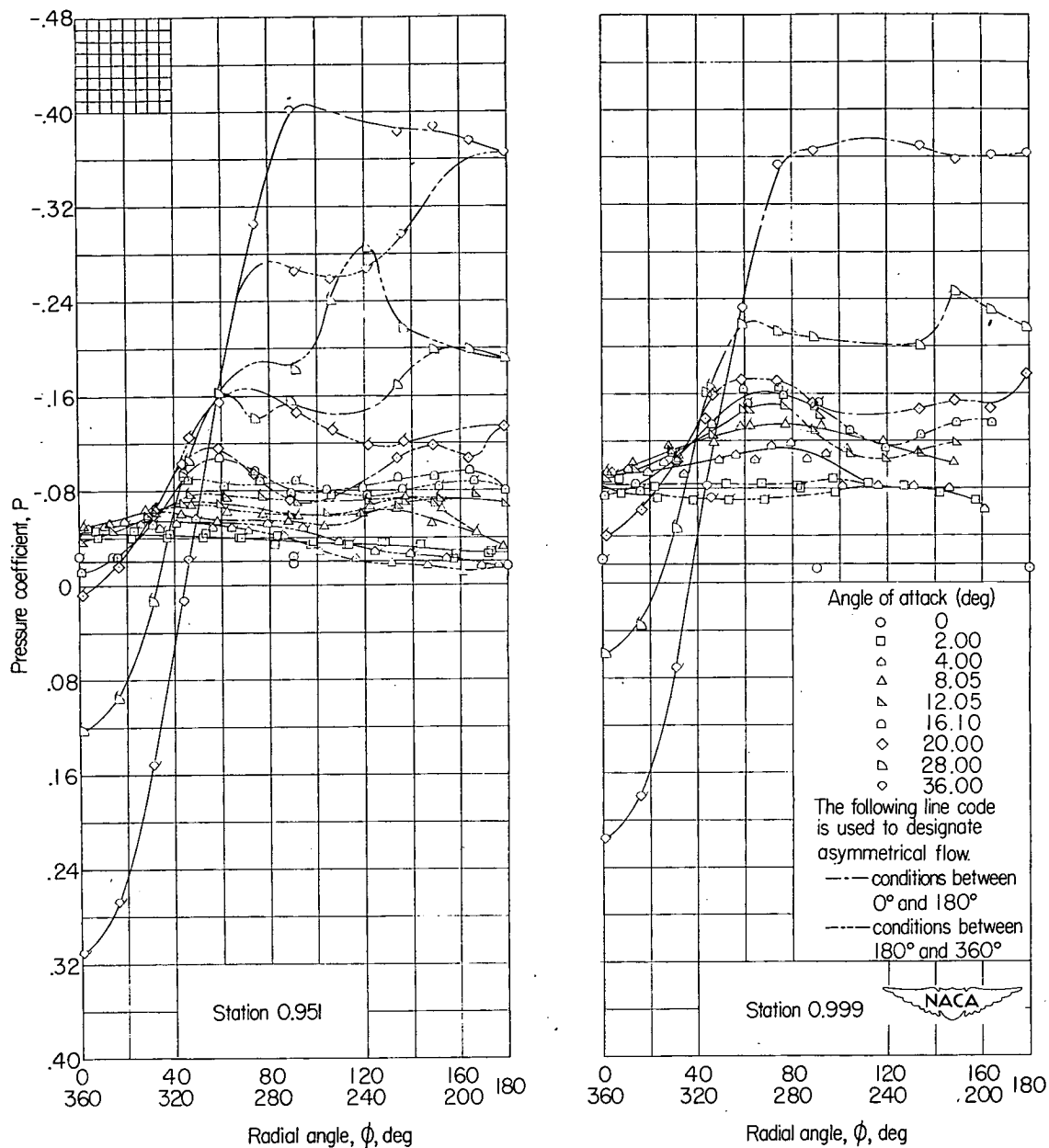
(d) Stations 0.618 and 0.714.

Figure 4.- Continued.



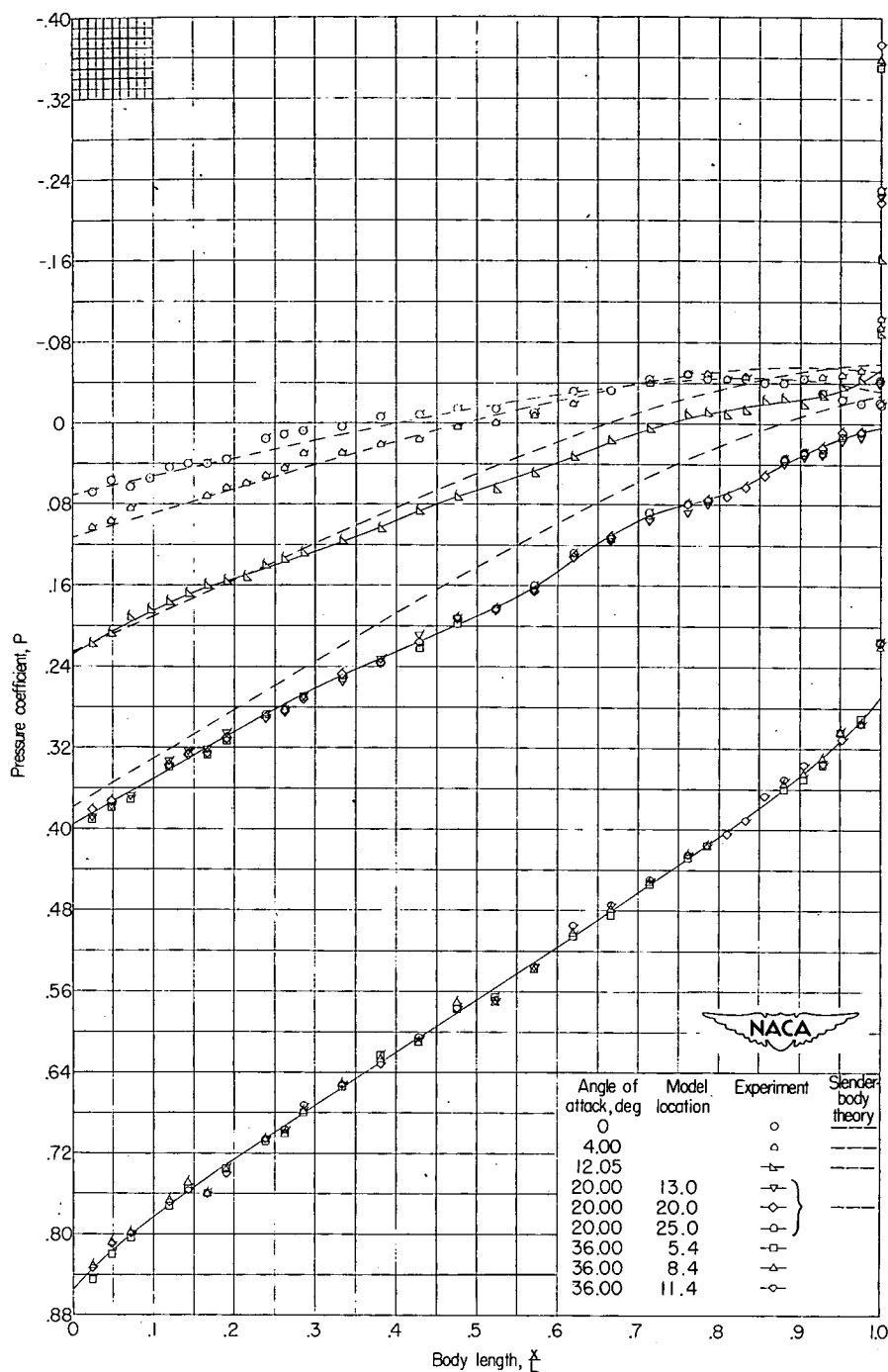
(e) Stations 0.832 and 0.904.

Figure 4.- Continued.



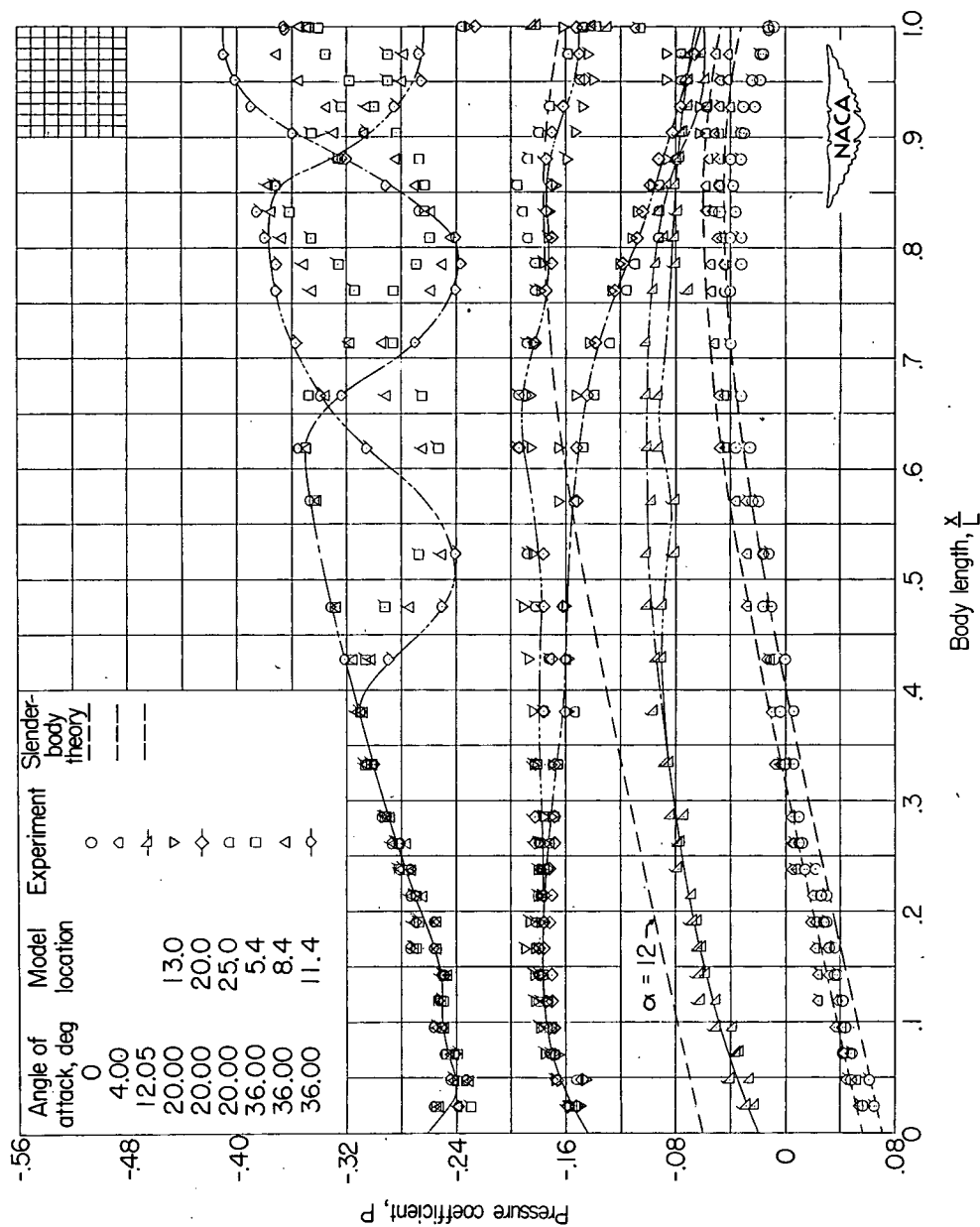
(f) Stations 0.951 and 0.999.

Figure 4.- Concluded.



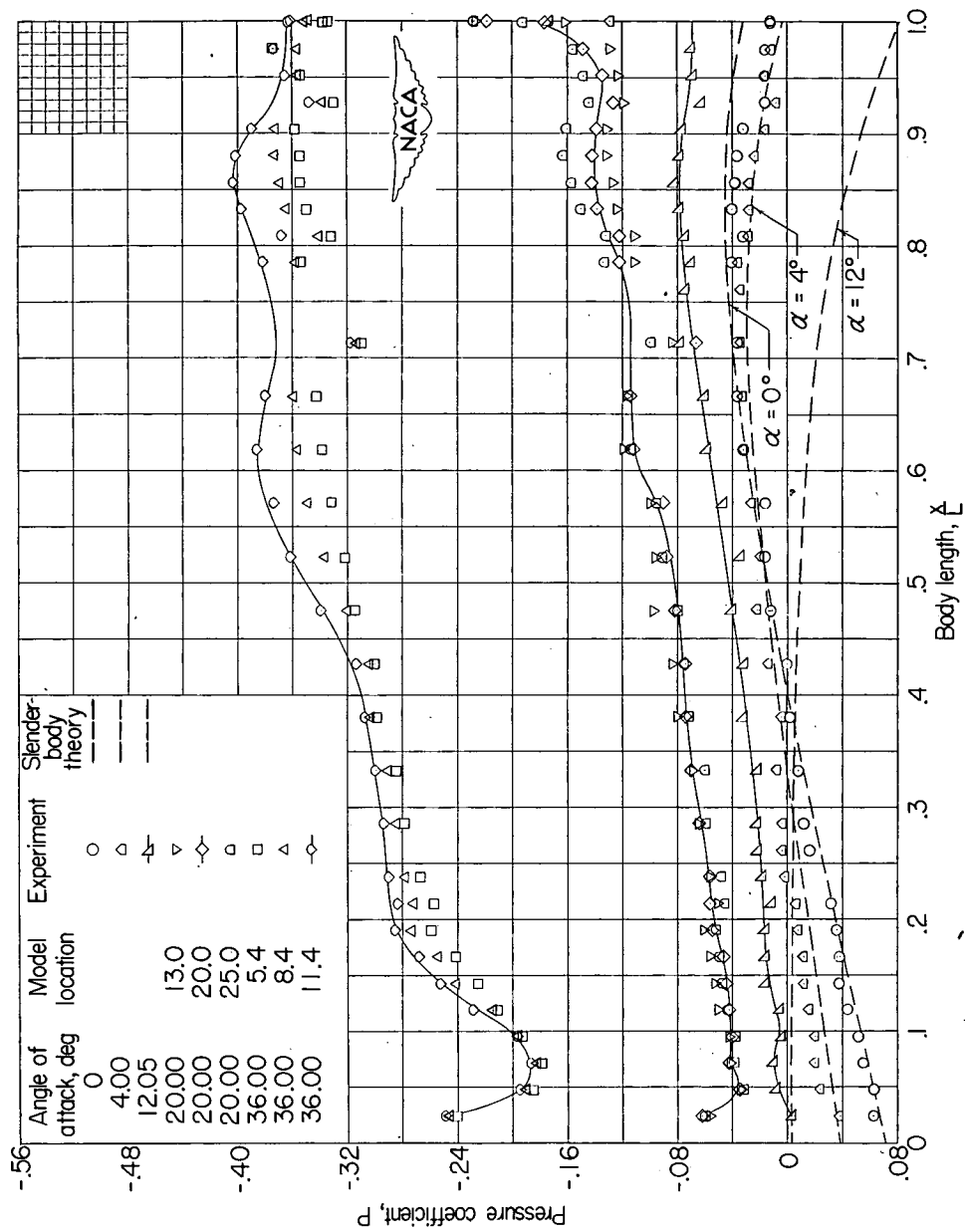
(a)  $\phi = 0^\circ, 360^\circ$ .

Figure 5.- Axial pressure distributions on a parabolic body of revolution for several radial locations.. (Flagged symbols indicate test points between  $180^\circ$  and  $360^\circ$ .) Model location refers to distance of model nose from tunnel wall.



(b)  $\phi = 90^\circ, 270^\circ$ .

Figure 5.- Continued.



(c)  $\phi = 180^\circ$ .

Figure 5.- Concluded.

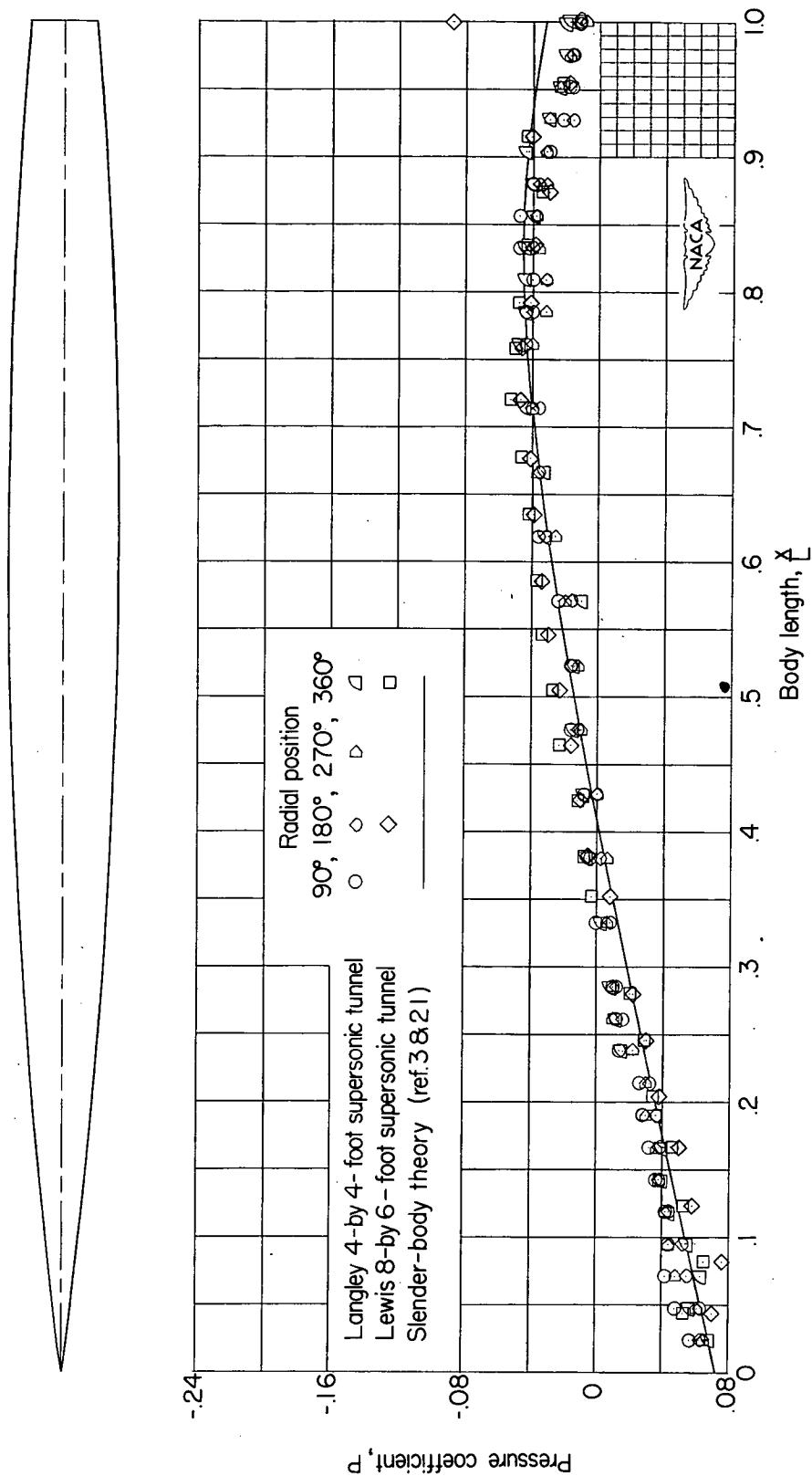


Figure 6.- Comparison of experimental and theoretical pressures on a parabolic body of revolution for an angle of attack of 0° and a Mach number of 1.59.



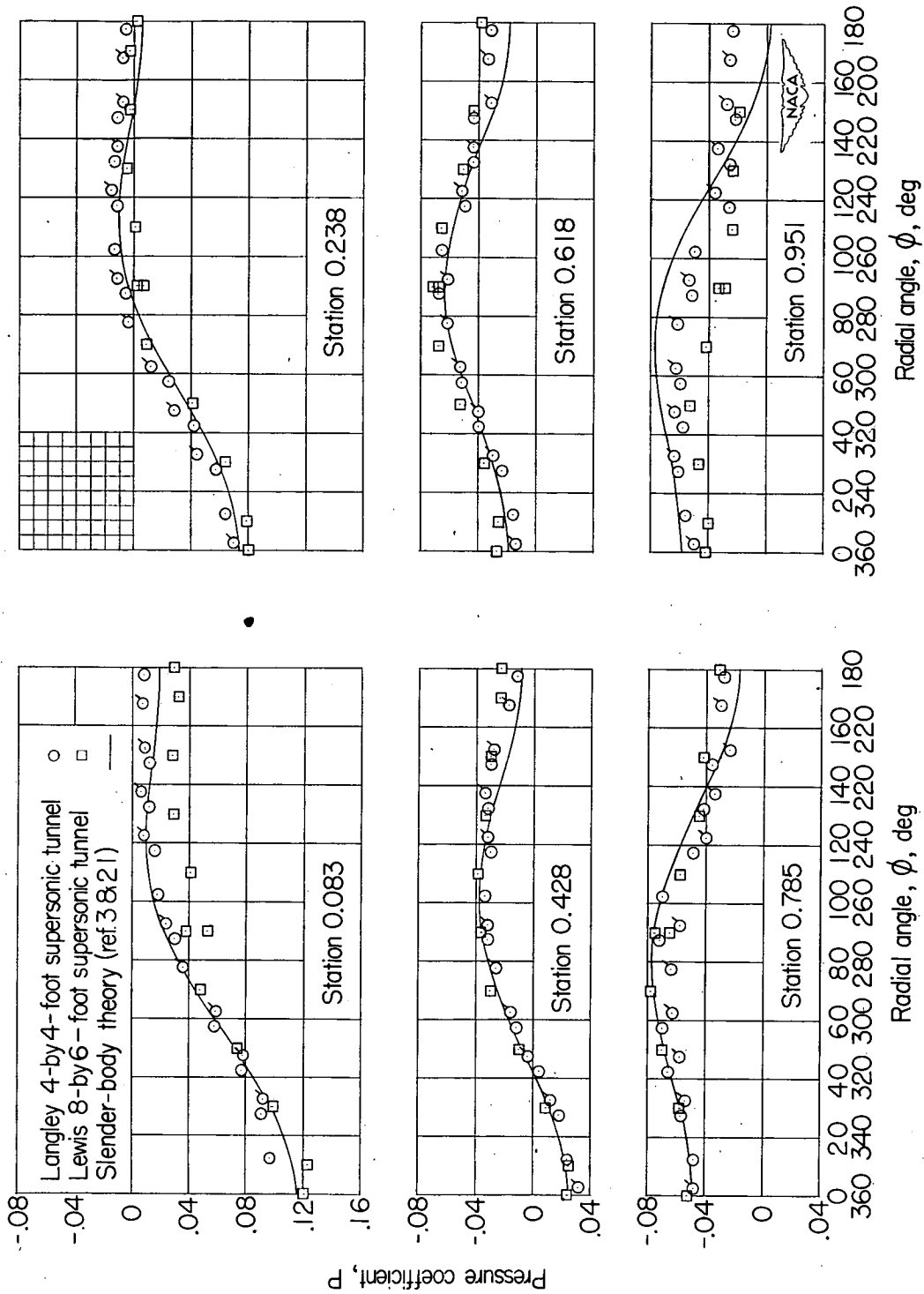


Figure 7.- Comparison of experimental and theoretical pressures on a parabolic body of revolution for an angle of attack of  $6^\circ$  and a Mach number of 1.59. (Flagged symbols indicate test points between  $180^\circ$  and  $360^\circ$ .)

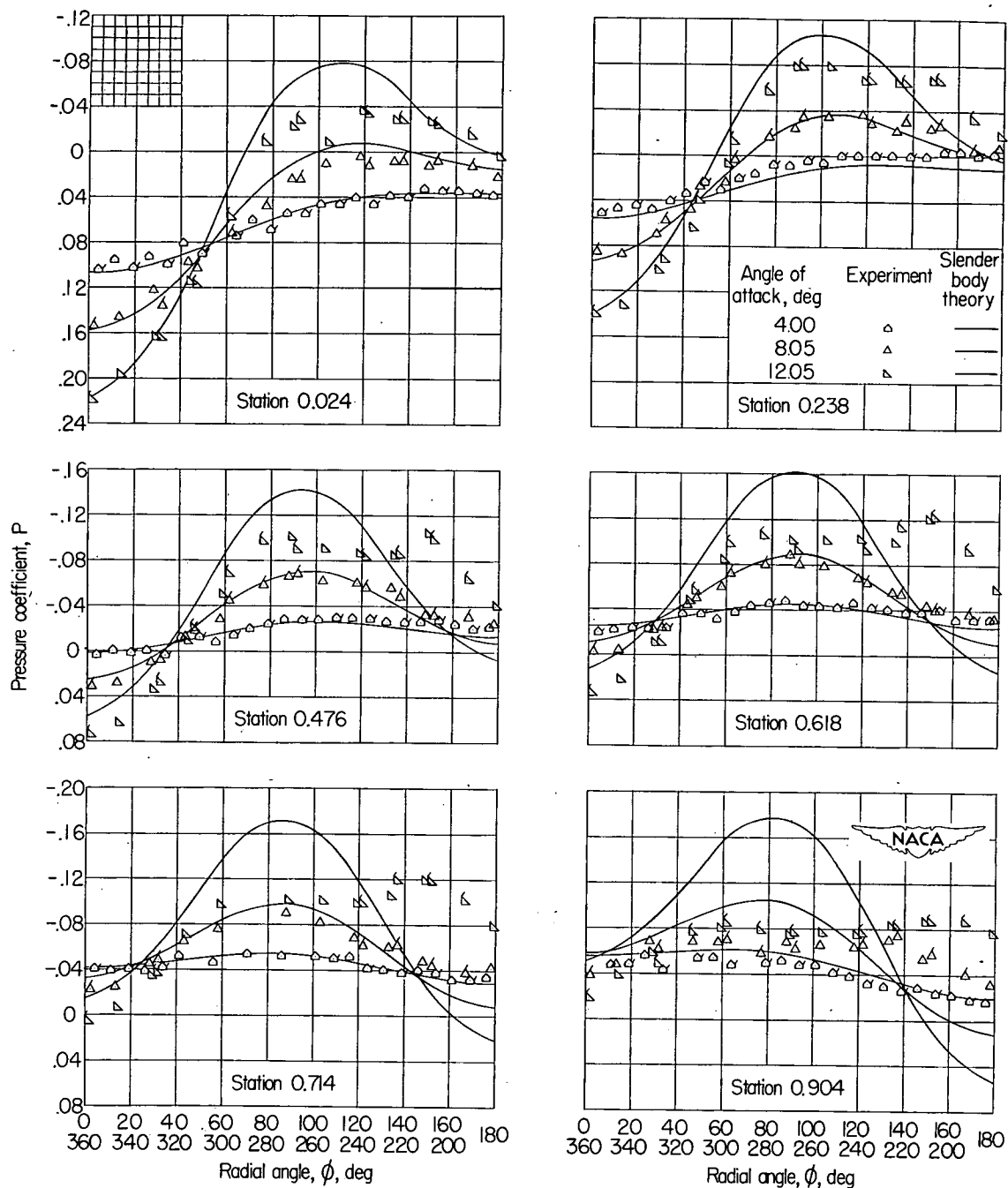
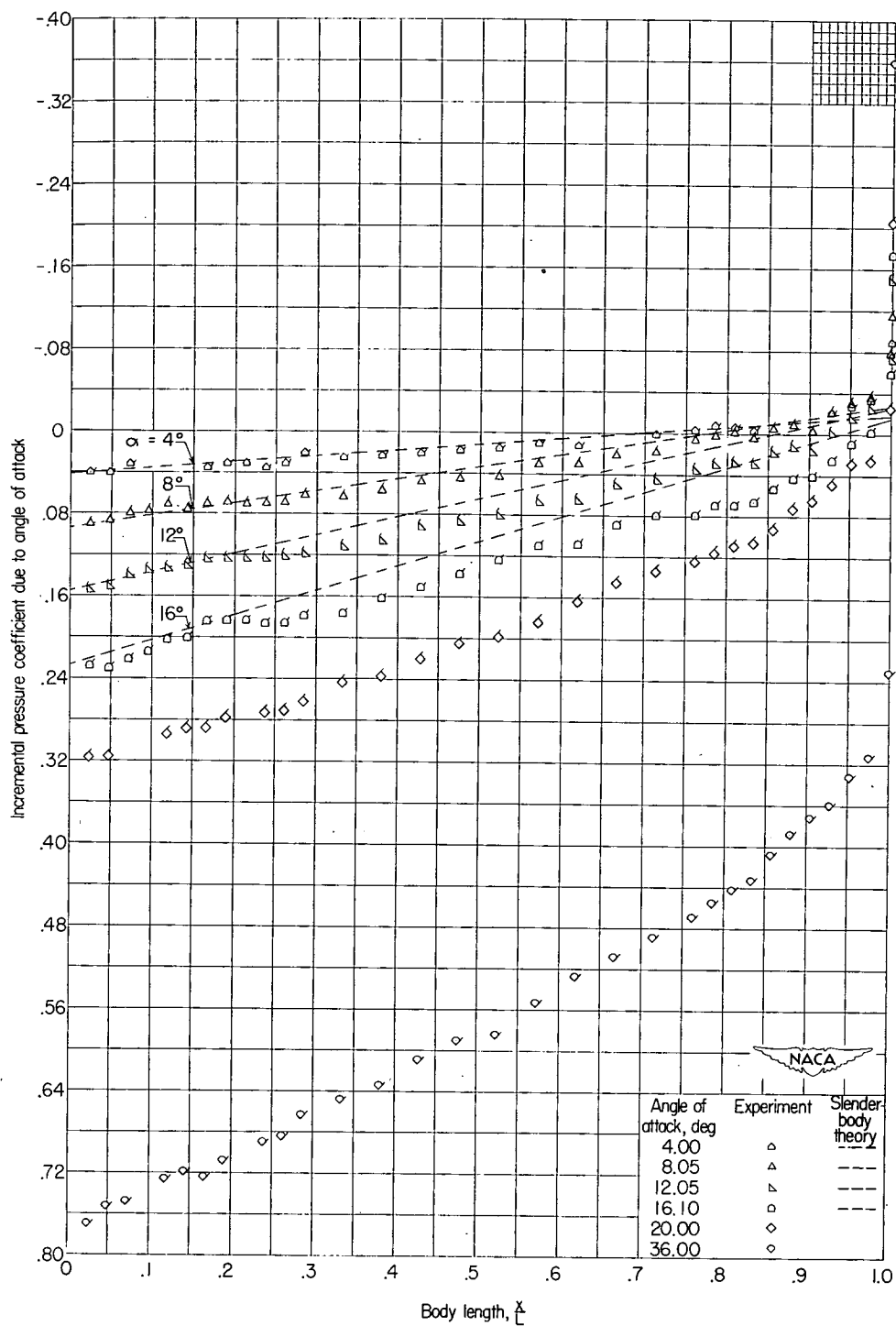
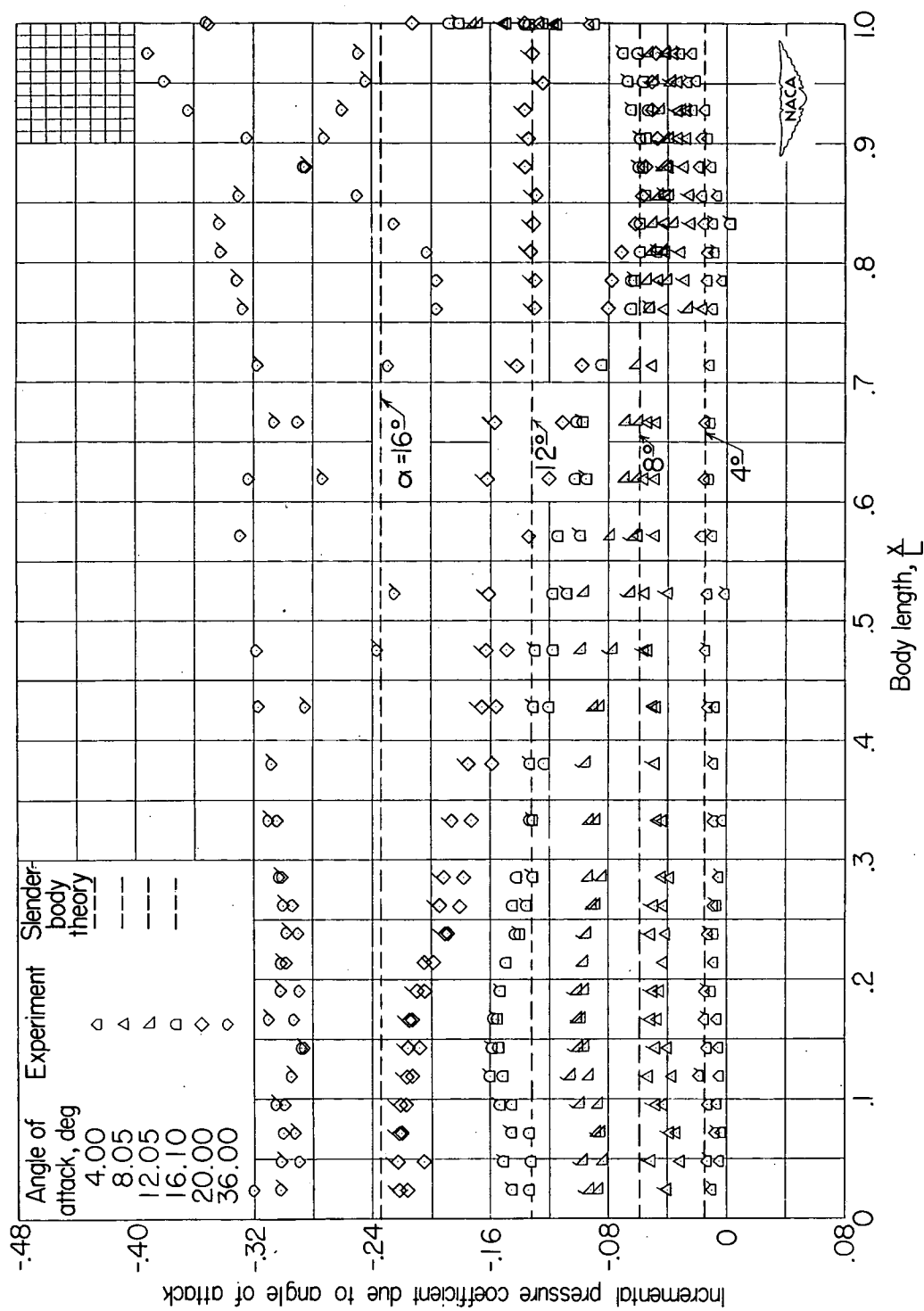


Figure 8.- Comparison of experimental and theoretical pressures on a parabolic body of revolution for six axial stations. (Flagged symbols indicate test points between  $180^\circ$  and  $360^\circ$ .)



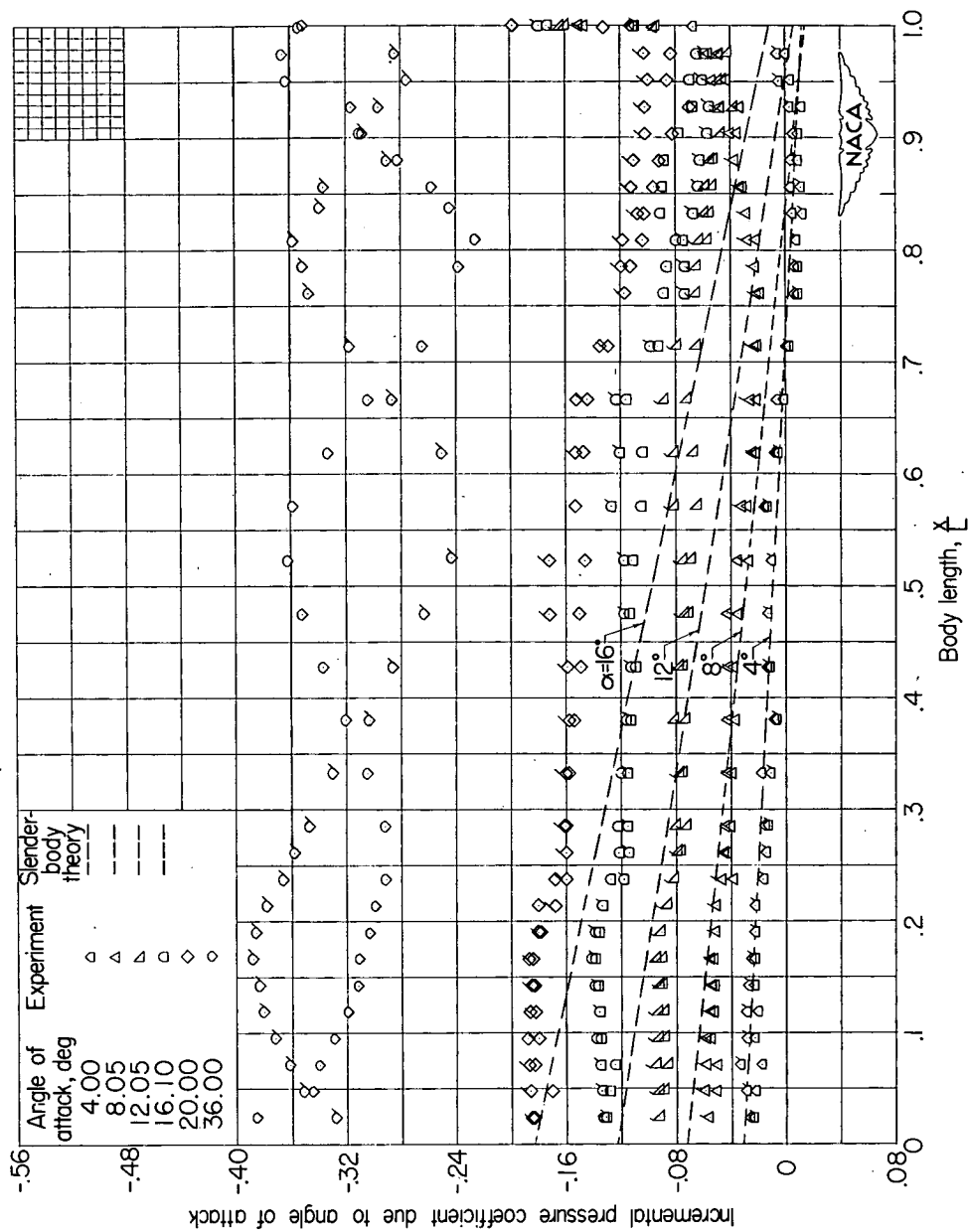
(a)  $\phi = 0^\circ, 360^\circ$ .

Figure 9.- Incremental pressure coefficient due to angle of attack as a function of axial position. (Flagged symbols indicate test points between  $180^\circ$  and  $360^\circ$ .)



(b)  $\phi = 90^\circ, 270^\circ$ .

Figure 9.- Continued.



(c)  $\phi = 135^\circ, 225^\circ$ .

Figure 9.- Continued.

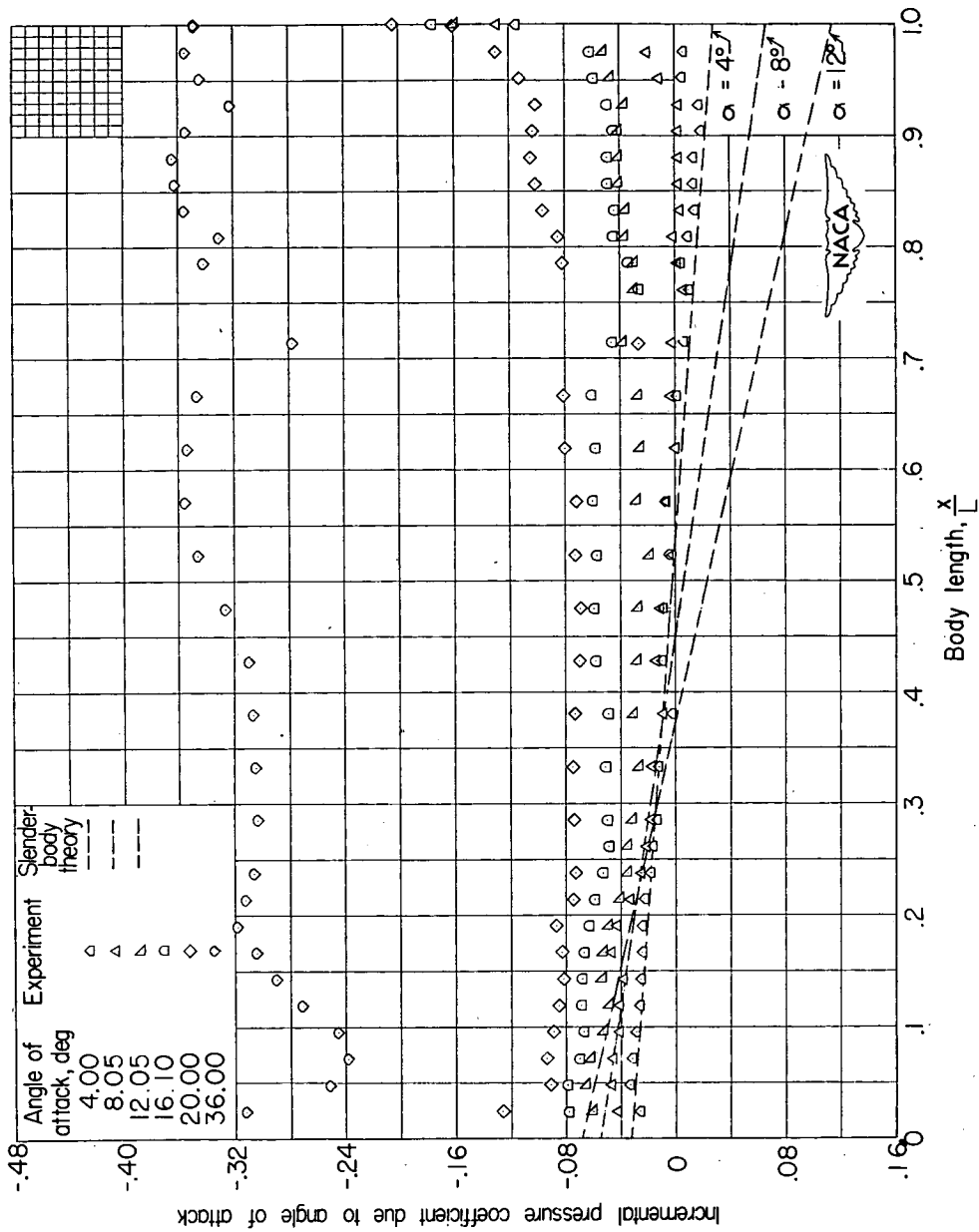
(a)  $\phi = 180^\circ$ .

Figure 9.- Concluded.

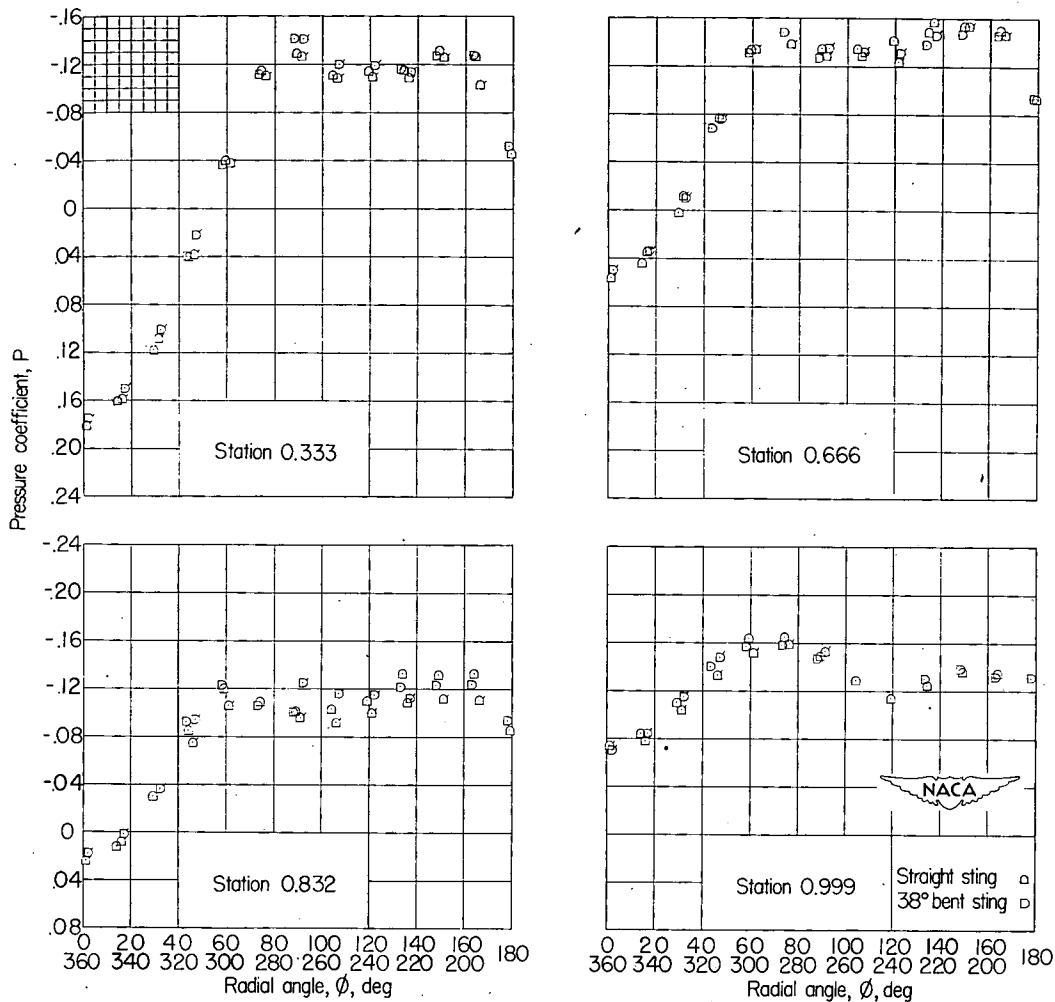
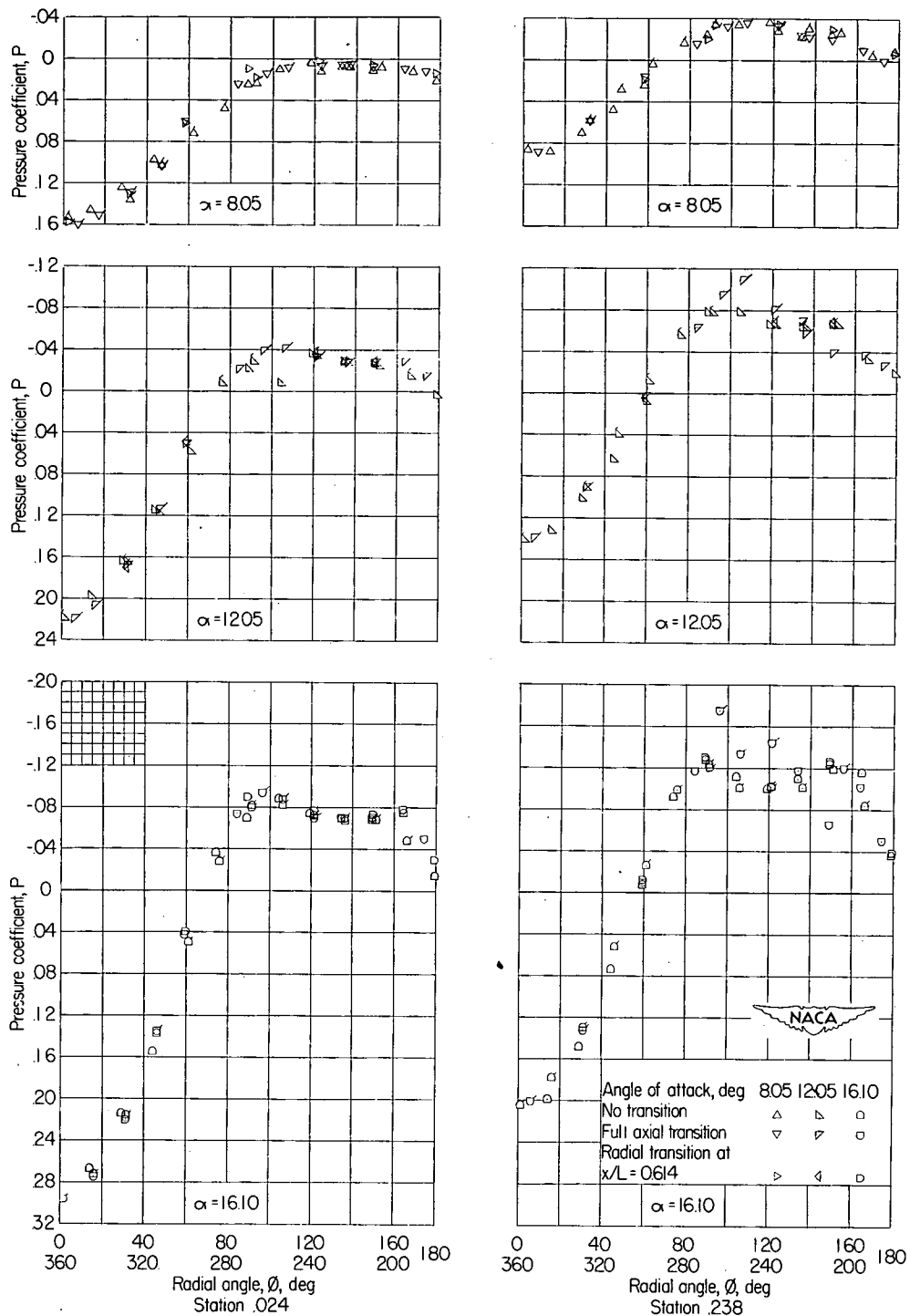


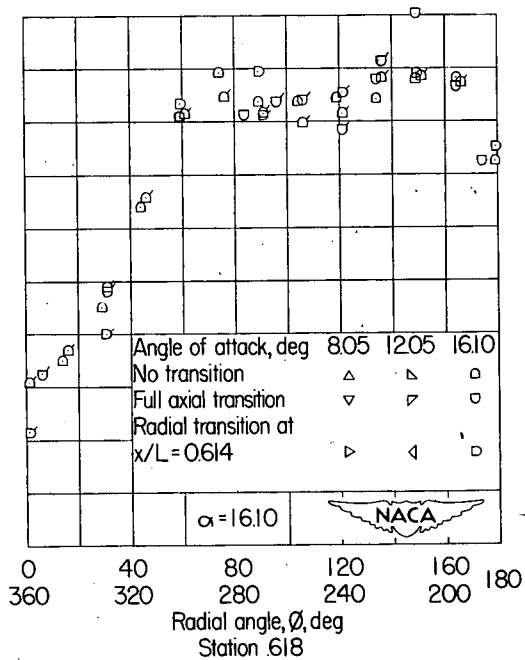
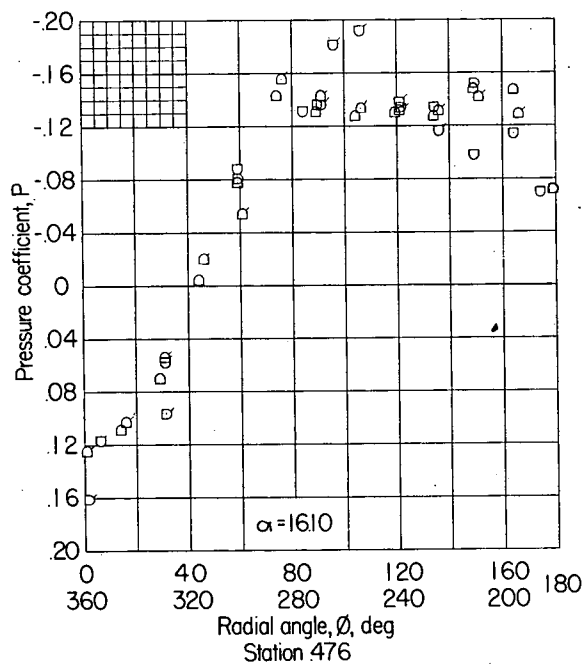
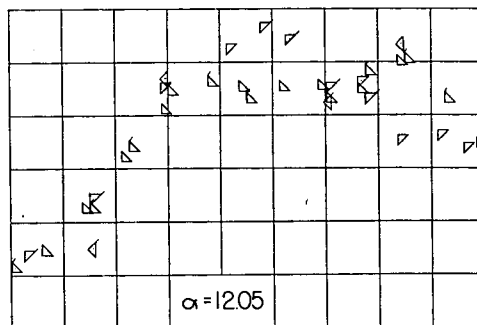
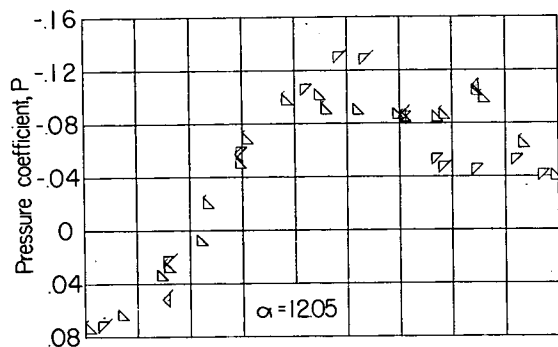
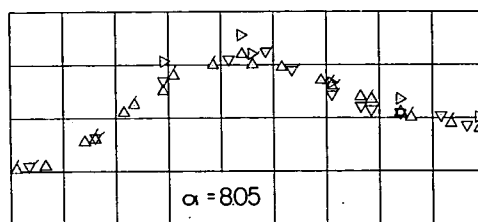
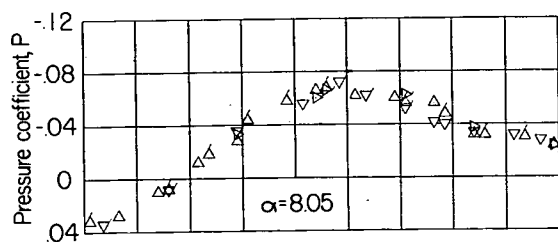
Figure 10.- Pressure-coefficient variation with radial position for the parabolic body of revolution mounted on the straight and the 38° bent stings.  $\alpha = 16.10^\circ$ . (Flagged symbols indicate test points between  $180^\circ$  and  $360^\circ$ .)



(a) Stations 0.024 and 0.238.

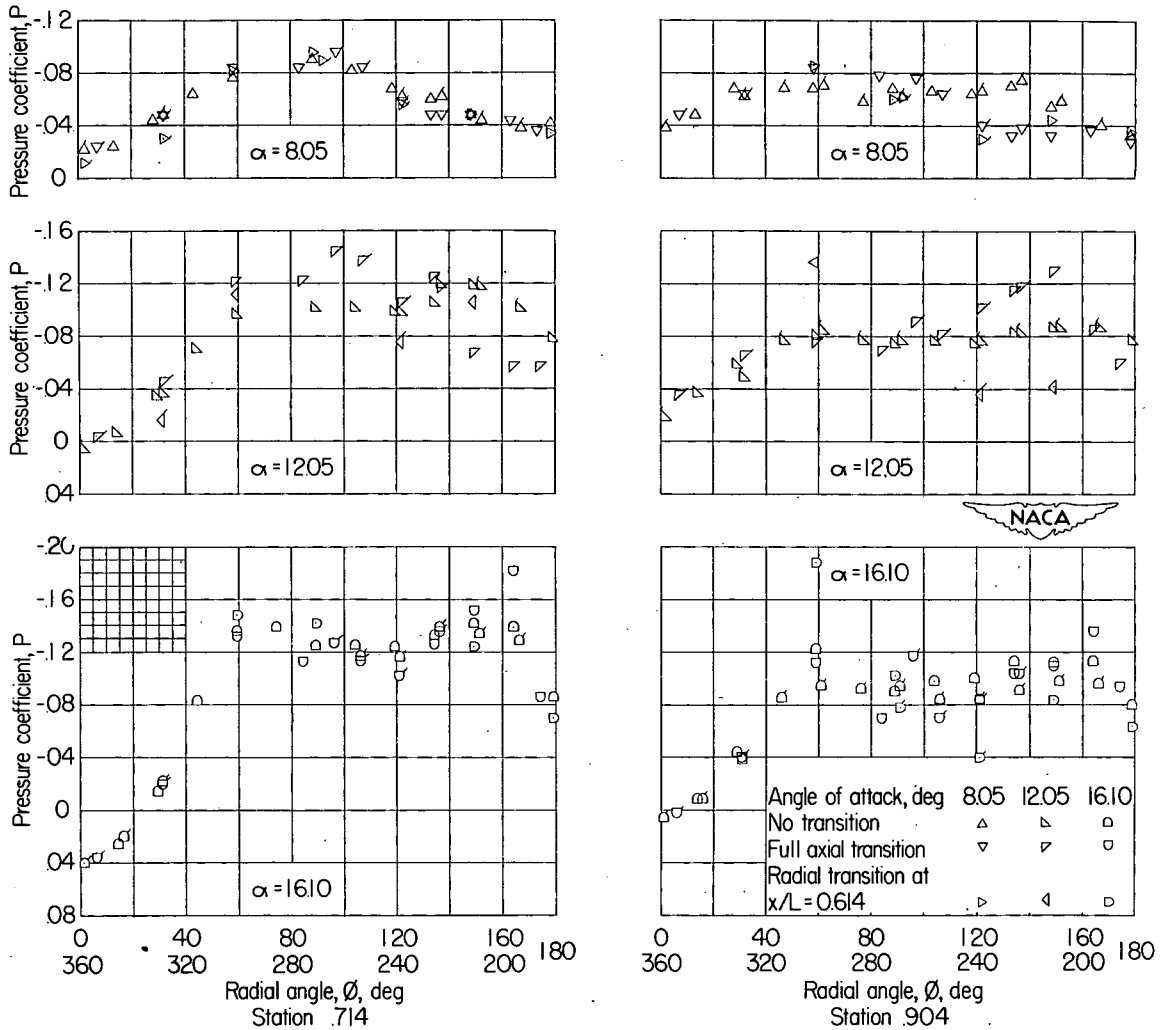
Figure 11.- Comparison of radial pressure distributions at six axial stations with and without transition strips. (Flagged symbols indicate test points between  $180^\circ$  and  $360^\circ$ .)





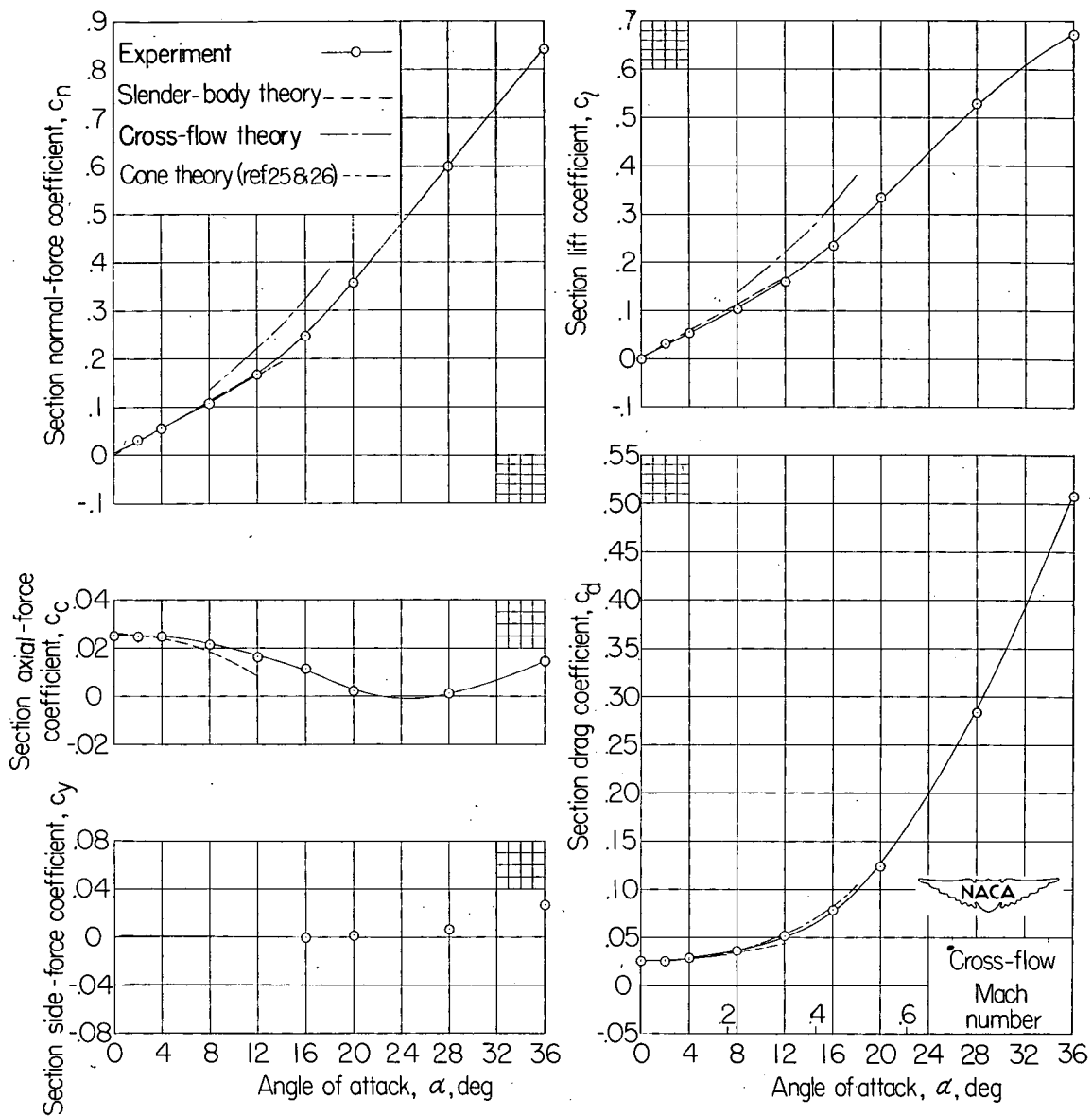
(b) Stations 0.476 and 0.618.

Figure 11.- Continued.



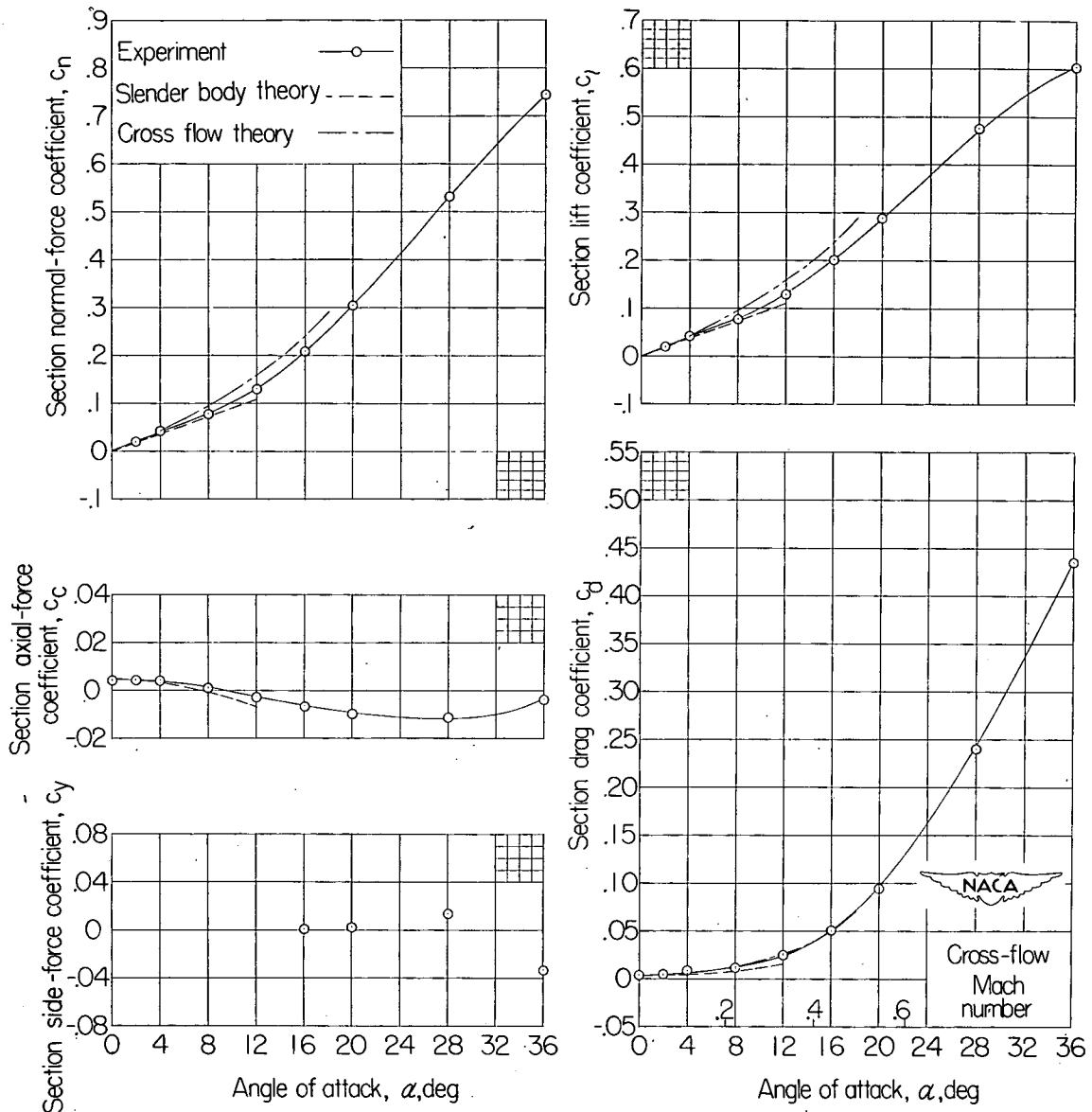
(c) Stations 0.714 and 0.904.

Figure 11.- Concluded.



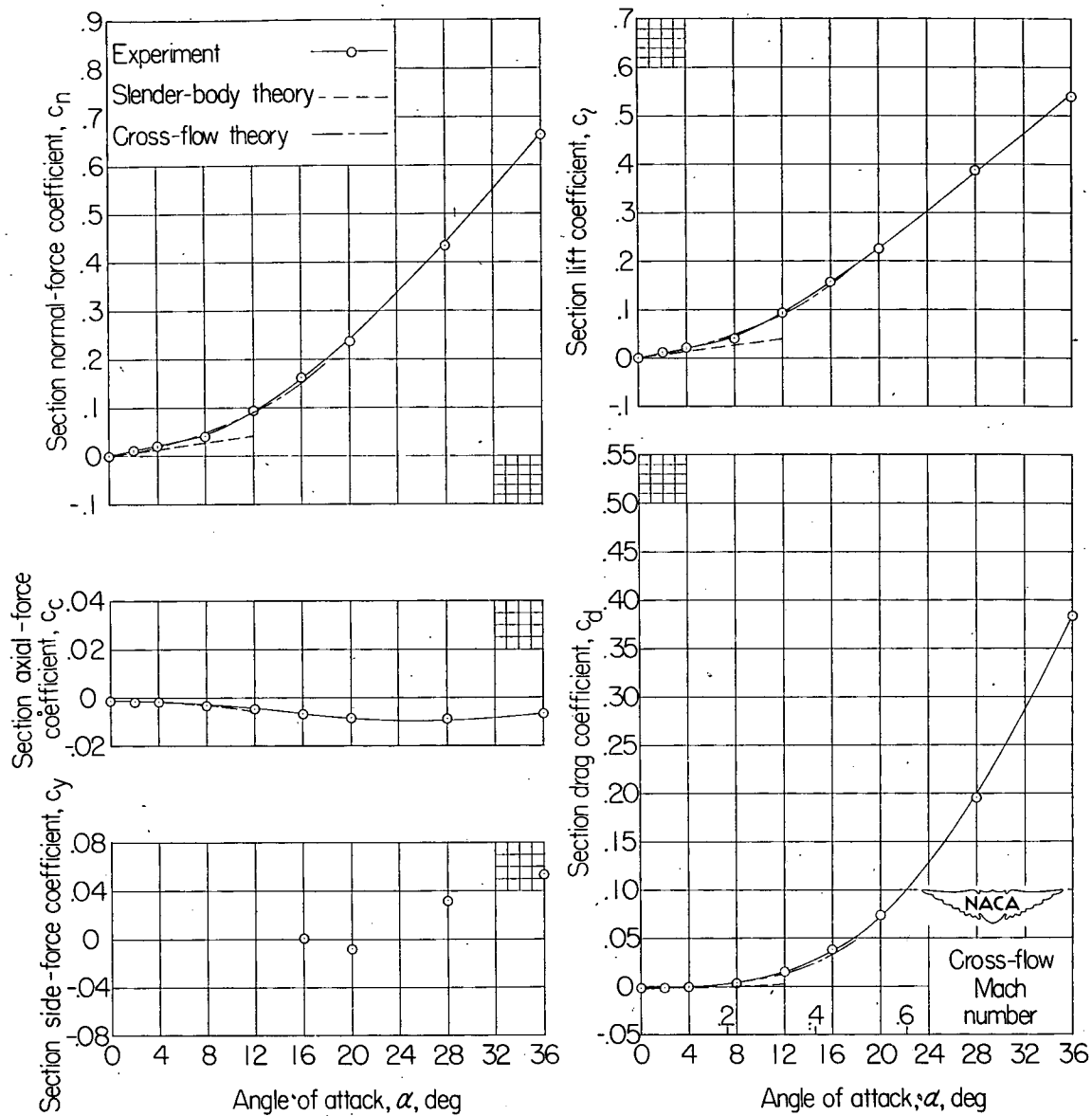
(a) Station 0.024.

Figure 12.- Section aerodynamic characteristics on a parabolic body of revolution at six axial stations.  $M = 1.59$ .



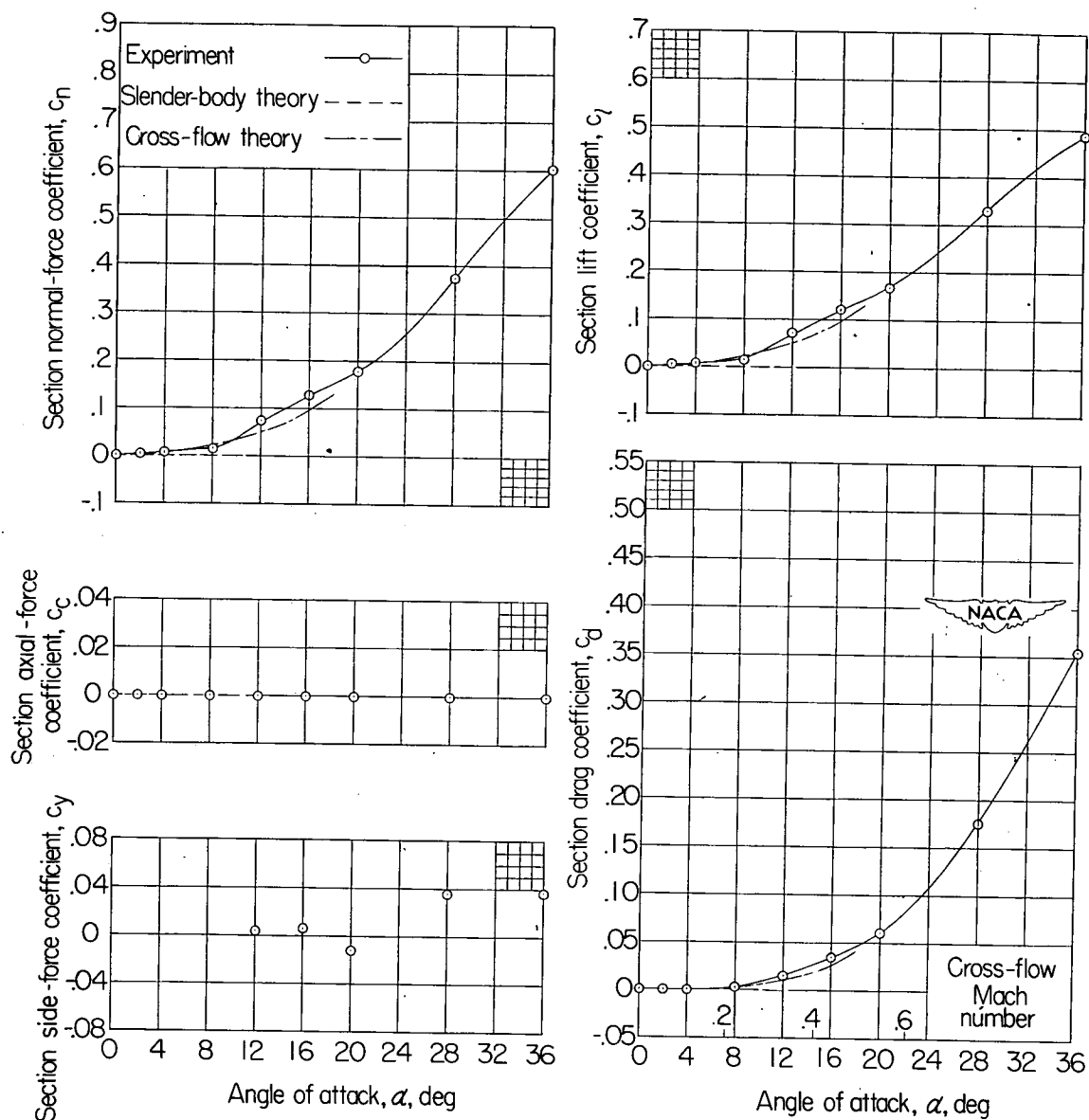
(b) Station 0.238.

Figure 12.- Continued.



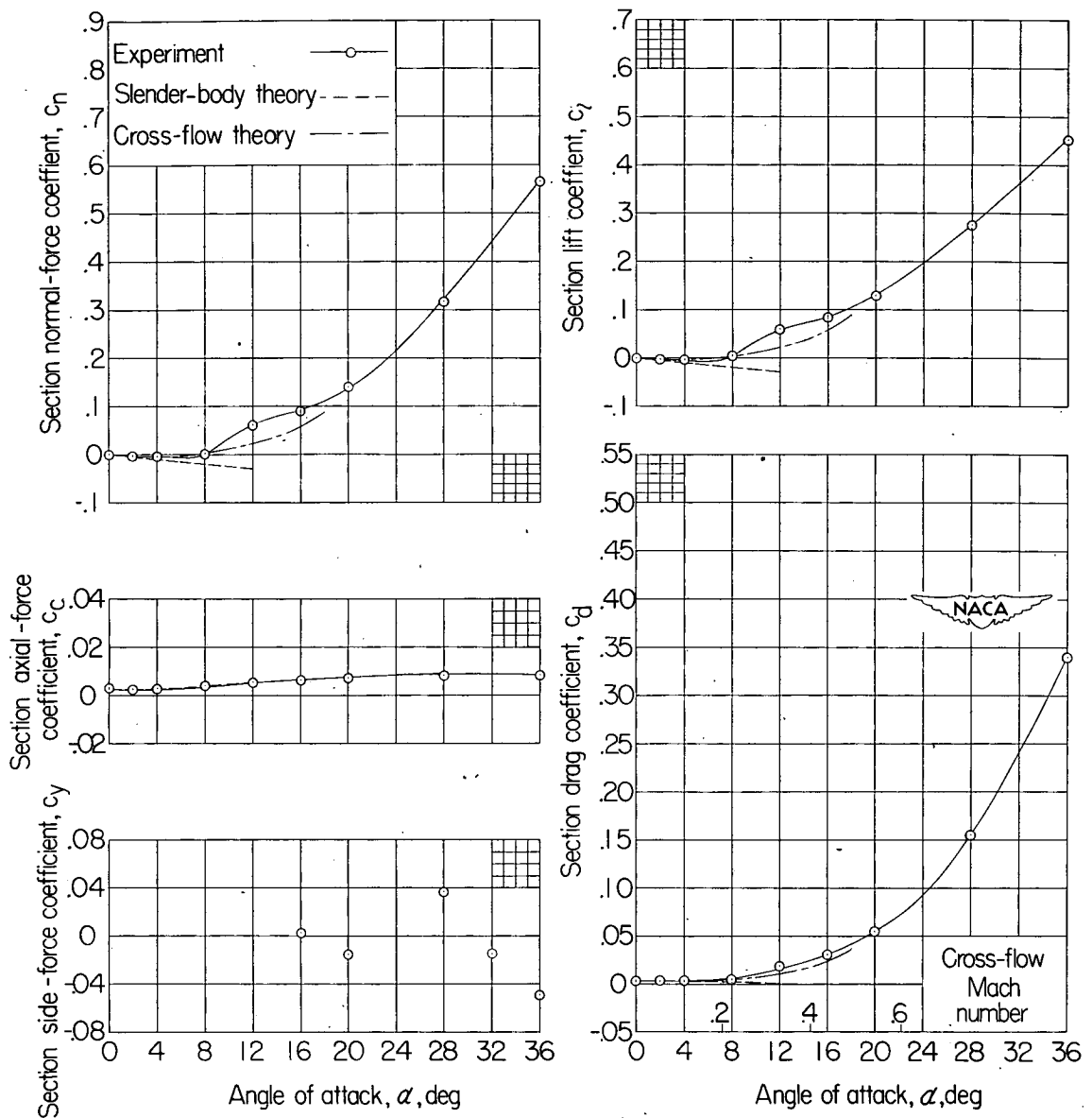
(c) Station 0.476.

Figure 12.- Continued.



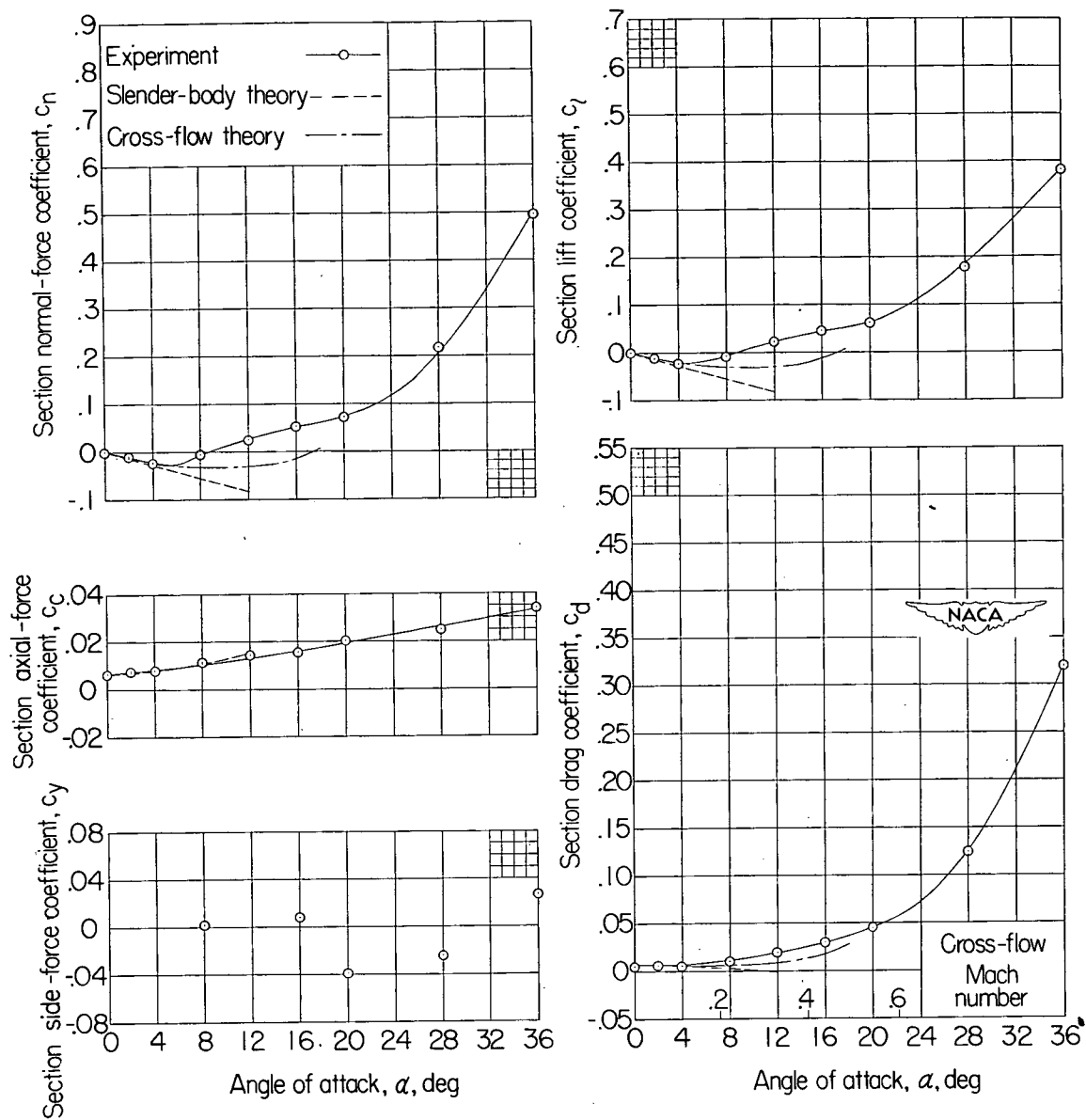
(d) Station 0.618.

Figure 12.- Continued.



(e) Station 0.714.

Figure 12.- Continued.



(f) Station 0.904.

Figure 12.- Concluded.



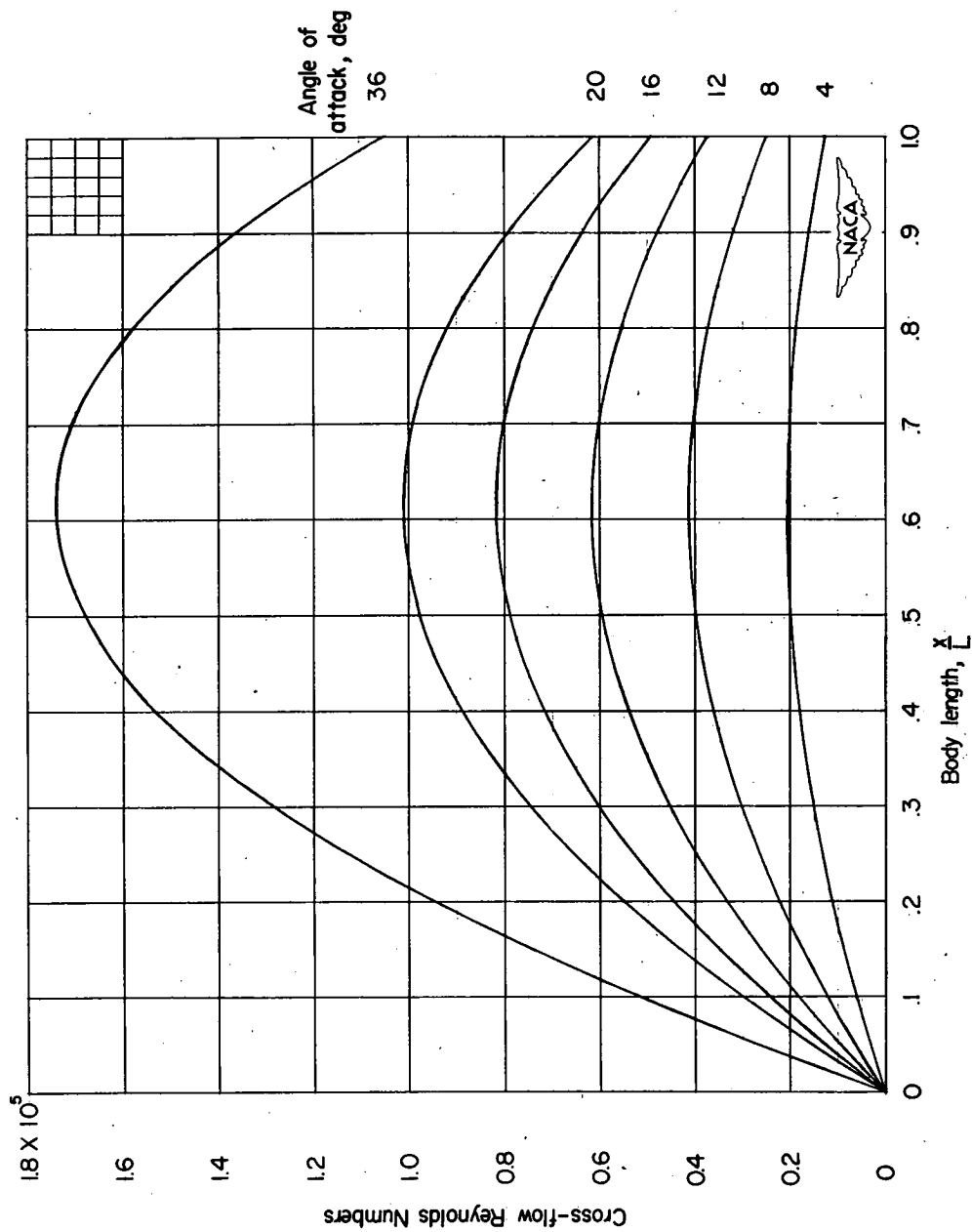


Figure 13.- Cross-flow Reynolds numbers for a series of representative angles of attack  $M = 1.59$ .

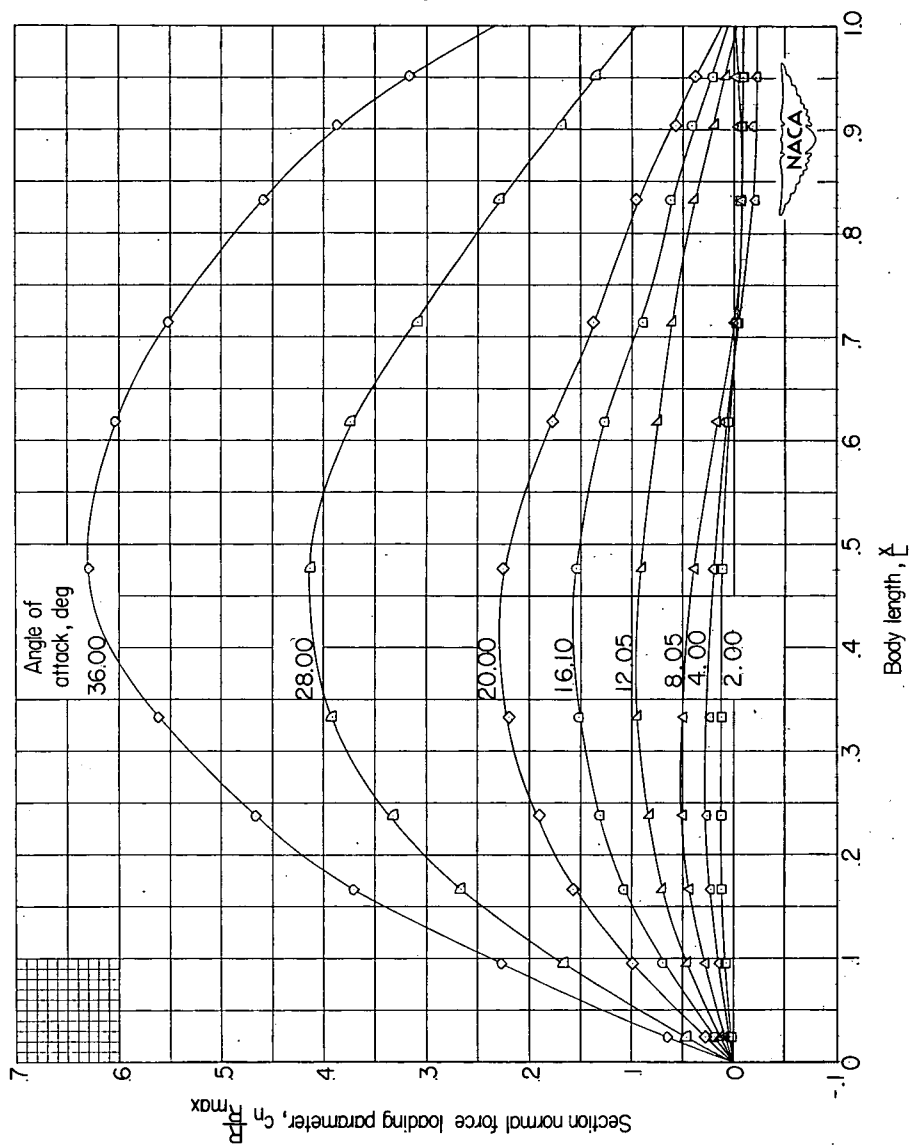


Figure 14.- Normal-force loading distribution on parabolic body of revolution.  $M = 1.59$ .

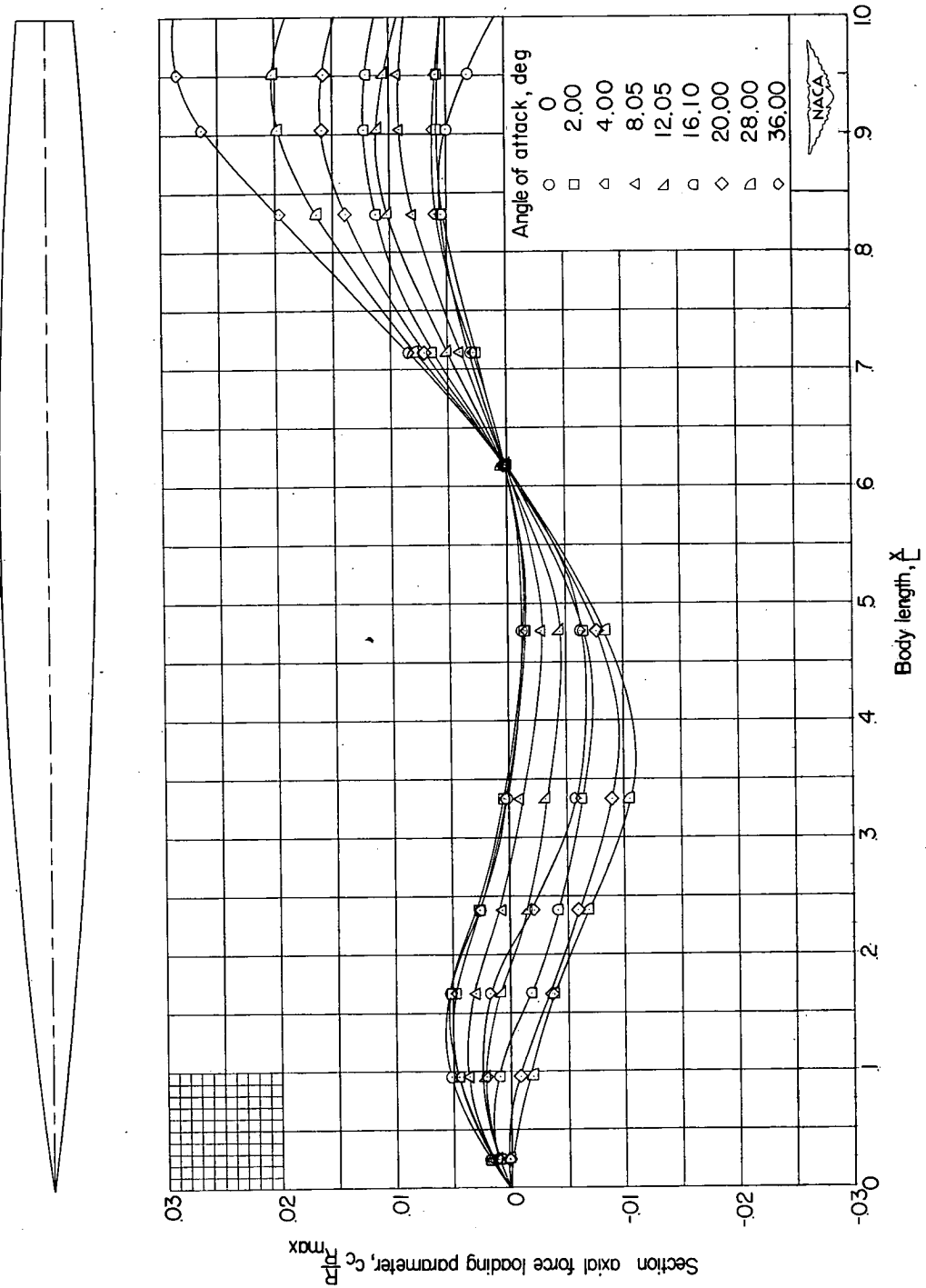


Figure 15.- Axial-force loading distribution on parabolic body of revolution.  $M = 1.59$ .

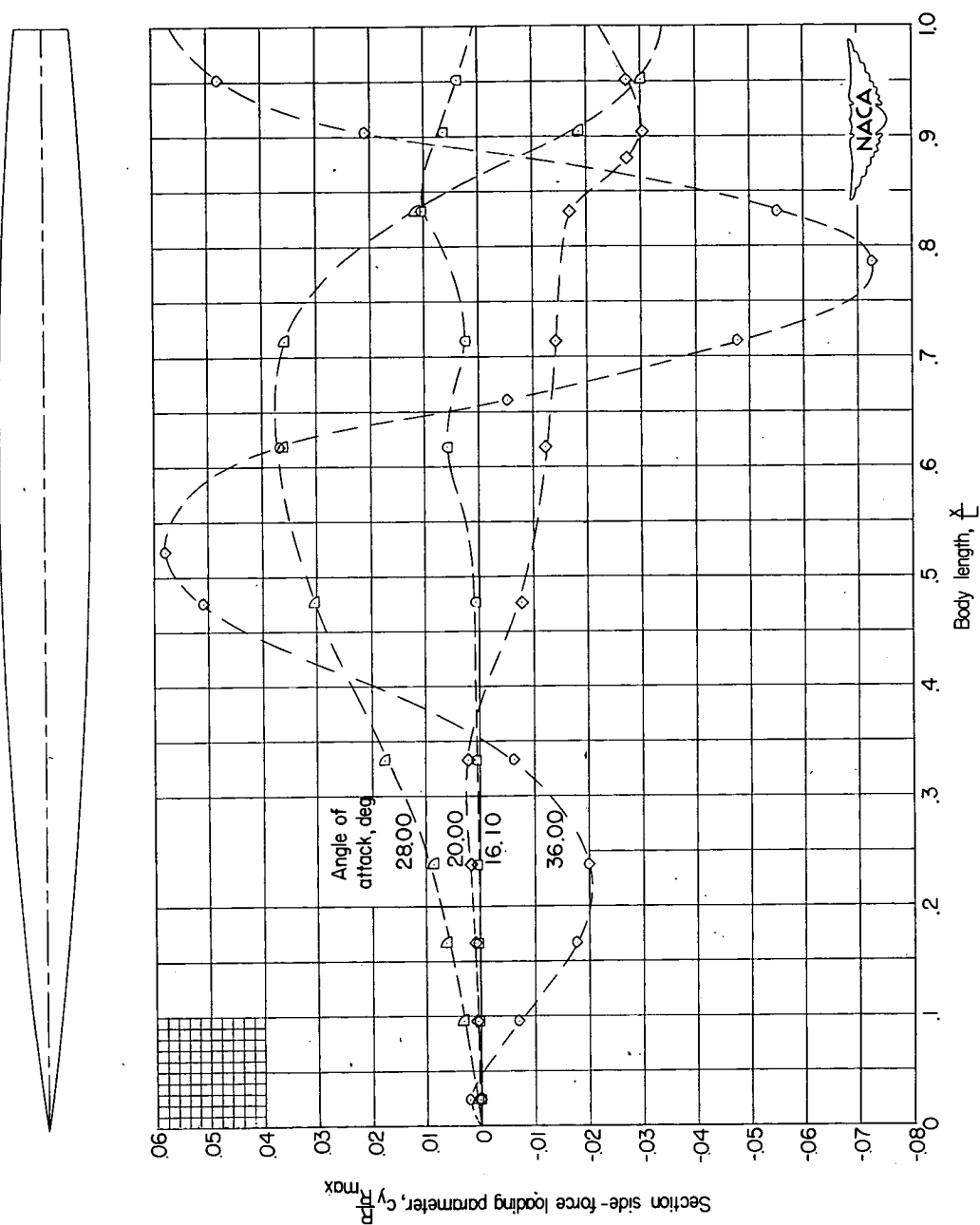


Figure 16.- Side-force loading distribution on parabolic body of revolution.  $M = 1.59$ .

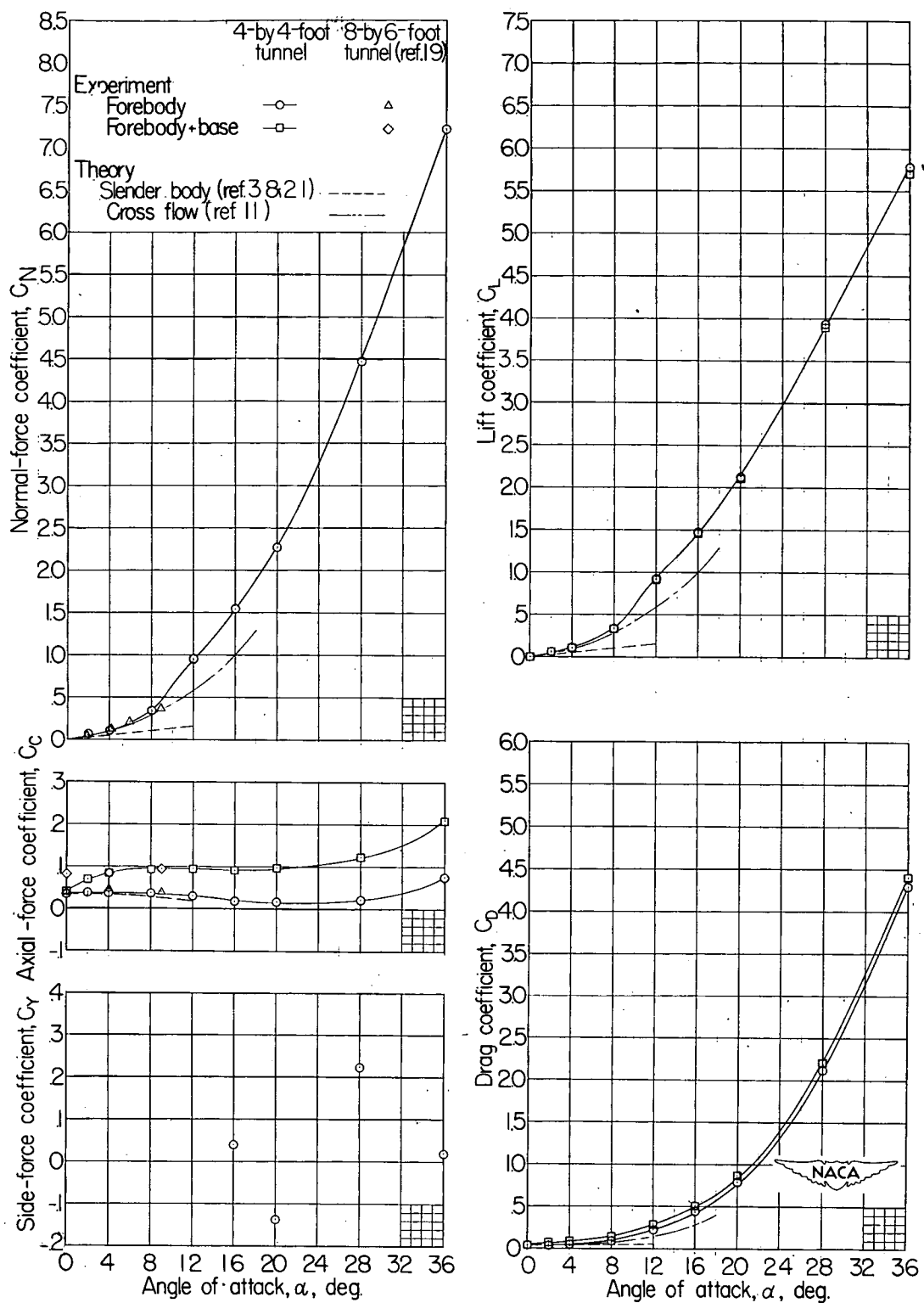


Figure 17.- Aerodynamic characteristics of parabolic body of revolution.  
 $M = 1.59$ .

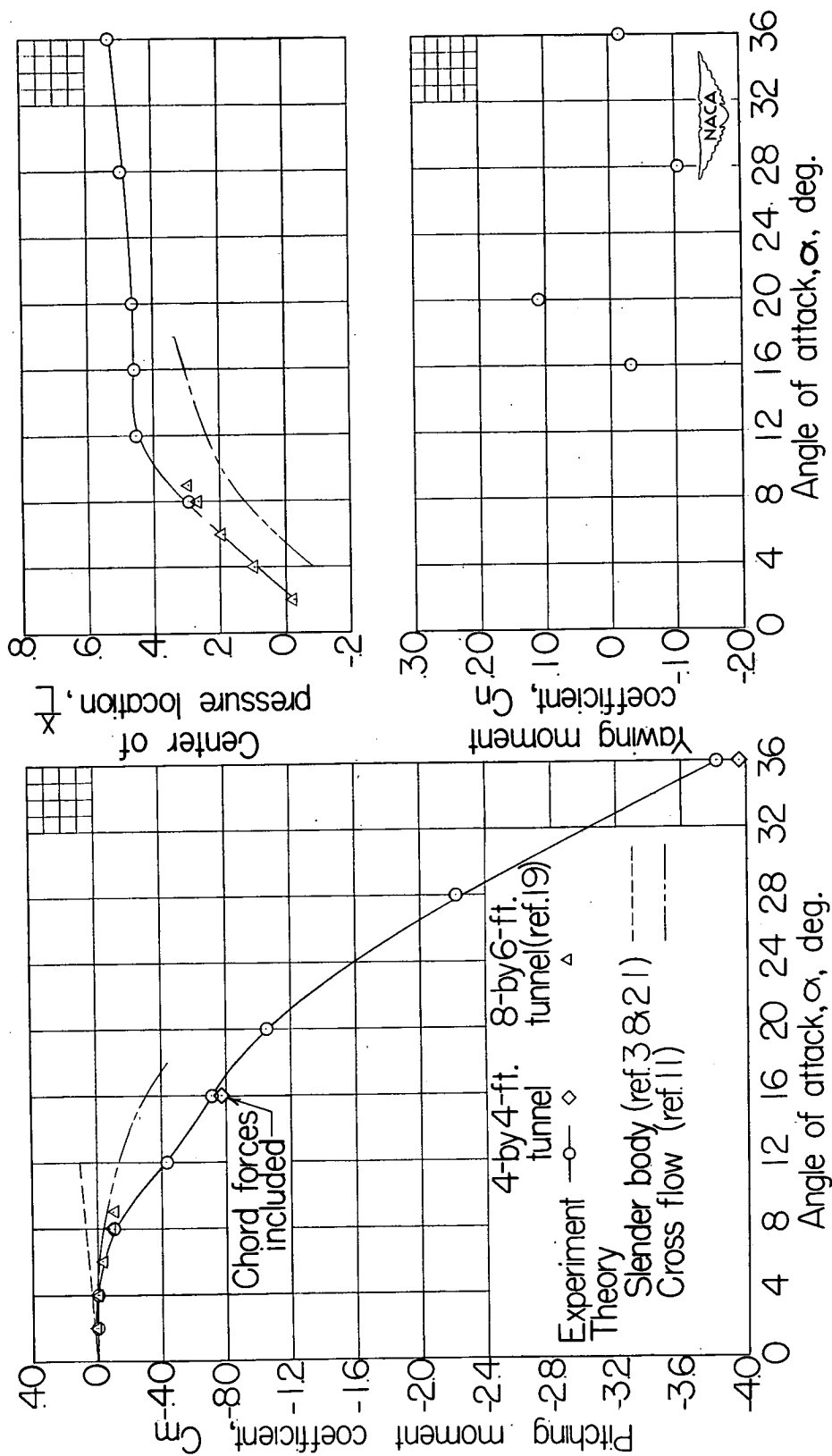


Figure 17.- Concluded.

# SECURITY INFORMATION

[REDACTED]

~~CONFIDENTIAL~~